

**EXPANSION AND CHARACTERIZATION OF HUMAN BREAST
CIRCULATING CANCER CELLS**

KHOO BEE LUAN

(B.Sc. (Hons), NTU, 2011)

A THESIS SUBMITTED
FOR THE DEGREE OF DOCTOR OF PHILOSOPHY
MECHANOBIOLOGY INSTITUTE
NATIONAL UNIVERSITY OF SINGAPORE

2015

DECLARATION

I hereby declare that this thesis is my original work and it has been written by me in its entirety. I have duly acknowledged all the sources of information which have been used in this thesis.

This thesis has also not been submitted for any degree in any university previously.



Bee Luan Khoo (add signature)

25th May 2015

Acknowledgements

This thesis would not have been possible without the guidance and support of several individuals, who in one way or another contributed and had been instrumental in the preparation and completion of this study.

First and foremost, the author would like to extend the deepest gratitude to her advisers, Professor Lim Chwee Teck and Professor Jean Paul Thiery, for the support throughout her doctoral work via their invaluable comments, guidance and enthusiasm. Their broad expertise enabled her to work under a variety of research fields, ranging from clinical biology to engineering aspects. This thesis would not have been successful without their knowledge and support.

Next, the author would like to express her sincere thanks to all healthy volunteers, cancer patients, clinicians (including Dr. Lee Soo Chin, Dr. Ruby Huang, Dr. Darren Lim and Dr. Daniel Tan) and staff from National University Hospital of Singapore (NUHS), National Cancer Centre (NCCS), Cancer Science Institute (CSI), Ministry of Health (MOH) and Singapore General Hospital (SGH) who participated in these clinical studies, without whom these projects will never achieve clinical relevance.

The author is extremely grateful to the members of Singapore MIT Alliance for Research and Technology (SMART) BioSyM IRG, especially Professor Jongyoon Han, Dr. Majid Ebrahimi Warkiani, Dr. Hou Han Wei and Dr. Ali Asgar Bhagat as well as other staff, graduate and undergraduate students, including Dr. Narayanan Balasubramanian, Teng Yang, Bena Lim and Andy Tay for their assistance and support. Further thanks to Dr.

Gianluca Greci, Parthiv Kant Chaudhuri, Chua Ai Leng, Cheng Sor Yan and the members from Mechanobiology Institute (MBI) for their constructive comments and assistance in administrative issues or other projects. The author is also extremely grateful to the members of Institute of Molecular and Cell Biology (IMCB), A*STAR, especially Prashant Kumar, Sayantani Nandi and Joanne Ong for going all the way to accommodate her projects. She would also like to extend her thanks to Clearbridge Biomedics for providing technical support.

The author will like to give special thanks to the author's thesis advisory committee (TAC) chair, Professor Evelyn Lim, as well as other professors who have provided valuable guidance along the journey. Further thanks to the examiners, for their careful review and insightful comments which have greatly improved the quality of the thesis.

The author wants to thank Chua Song Lin, and all colleagues in the Nanobiomechanics Laboratory under the NUS Division of Biomedical Engineering for their kindness and happy moments.

Finally, the author would like to acknowledge MBI for the Research Scholarship and the financial support of National Research Foundation (NRF) Singapore and Ministry of Education through the MBI research programme for the study.

25th May 2015

Contents

| | |
|---|------|
| Acknowledgements..... | III |
| Contents | V |
| Summary | VII |
| List of Tables..... | IX |
| List of Figures | X |
| List of Symbols and Acronyms..... | XIII |
| List of Publications, Patents and Conferences abstracts | XVII |

Chapter 1: Introduction1

| | |
|---|----|
| 1.1 Background on cancer..... | 1 |
| 1.1.1 Cancer heterogeneity and mortality | 1 |
| 1.1.2 Cancer metastasis..... | 2 |
| 1.2 Circulating Tumor cells (CTCs)..... | 4 |
| 1.2.1 Breast Cancer CTCs and statistics | 7 |
| 1.2.2 Clinical significance of CTCs | 9 |
| 1.3 Current literature on CTC enrichment | 11 |
| 1.3.1 Label-dependent techniques..... | 14 |
| 1.3.2 Physical methods based on cell size and deformability..... | 17 |
| 1.3.3 Techniques based on proliferative capability | 17 |
| 1.4 CTC biology and limitations of existing techniques..... | 21 |
| 1.4.2 Variation in morphology, size and other physical properties | 24 |
| 1.4.3 CTCs may be associated to other cell types in blood | 25 |
| 1.4.4 CTC release and life cycle in circulation | 26 |
| 1.5 Prospects of expanding CTCs for clinical utility | 26 |
| 1.6 Hypotheses and project proposal | 27 |

Chapter 2: Materials and Methods30

| | |
|---|----|
| 2.1 Preparation of culture assay | 30 |
| 2.2 Characterization of biochemical changes of patterned dishes | 30 |
| 2.3 Blood collection | 31 |
| 2.4 Maintenance of cancer cell lines..... | 31 |
| 2.5 Cancer cell line cultures for optimization of assay parameters | 32 |
| 2.6 Preparation of blood samples for culture | 33 |
| 2.7 Primary human CTC culture | 33 |
| 2.8 Cluster formation, imaging and diameter measurements | 34 |
| 2.9 Flow cytometry to determine proportion of viable cells..... | 35 |
| 2.10 Histological staining of size-sorted cultured cells | 35 |
| 2.11 Enumeration of putative CTCs..... | 36 |
| 2.12 Immunophenotyping of cell clusters..... | 37 |
| 2.13 Characterization of putative CTCs via immunophenotyping of cytosots | 39 |
| 2.15 DNA FISH | 43 |
| 2.16 RNA FISH..... | 44 |
| 2.17 Validating presence of residual macrophages with a phagocytosis assay..... | 45 |
| 2.18 Establishment of spheroids from cultured CTCs | 45 |

| | |
|---|------------|
| 2.19 Invadopodia assay and phalloidin staining | 46 |
| 2.20 Western blot | 46 |
| 2.21 Cell cycle analysis..... | 47 |
| 2.22 Statistical analysis..... | 47 |
| Chapter 3: Microwell-based Culture and Expansion of Viable CTCs..... | 49 |
| 3.1 Optimization of culture conditions | 49 |
| 3.1.1 Microwell dimensions and surface treatment | 49 |
| 3.1.2 Characterization of microwell surface chemistry | 53 |
| 3.1.3 Culture preparation and maintenance | 55 |
| Section 3.1.4 Section Summary and Discussion..... | 64 |
| 3.2 Overview of resultant cultures of clinical samples | 66 |
| 3.2.1 Cell viability..... | 69 |
| 3.2.2 Size heterogeneity of clusters and individual cells | 70 |
| 3.2.2 Detection of residual blood cells..... | 76 |
| 3.2.3 Amplification of CK+ cells in culture..... | 82 |
| 3.3 Chapter summary | 87 |
| Chapter 4: Characterization of Cultured CTCs | 89 |
| 4.1 Detection of cultured CTCs with genetic alterations | 89 |
| 4.1.1 DNA FISH | 89 |
| 4.2 EMT phenotypes | 95 |
| 4.2.1 Pooled sample analysis with qRT-PCR..... | 96 |
| 4.2.2 Single cell characterization with immunostaining | 97 |
| 4.2.3 RNA FISH..... | 100 |
| 4.2.4 Cancer stem cells (CSCs)..... | 103 |
| 4.3 Functional characteristics and mechanisms of cultured CTCs | 108 |
| 4.4 Chapter summary | 113 |
| Chapter 5 Clinical Utility of CTC cultures..... | 115 |
| 5.1 Sample cohort | 115 |
| 5.2 Evaluation and tabulating of results..... | 117 |
| 5.2.1 Metastatic cohort (CTB) | 117 |
| 5.2.2 Locally advanced patients (PCL and P2A/B cohorts) | 120 |
| 5.2.3 Cluster formation in early-stage cancer samples (CES cohort) | 122 |
| 5.3 Chapter Summary | 124 |
| Chapter 6: Conclusions and Future Work..... | 126 |
| 6.1 Conclusions..... | 126 |
| 6.2 Future Work | 129 |
| 6.2.1 Bench to bedside applications..... | 130 |
| 6.2.2 Insights on metastatic cascade | 130 |
| 6.2.3 CTC profiling..... | 131 |
| References | 133 |
| Appendices..... | 154 |

Summary

Cancer metastasis often leads to patient mortality. Recent advancements in technology have reinvigorated cancer research by enabling the detection of circulating tumor cells (CTCs) in the peripheral blood circulation, which may participate in cancer metastasis. Increased CTC counts in blood have been found to correlate with worsened patient prognosis. However, CTCs are rare events, and are phenotypically and genetically heterogeneous. These render isolation and subsequent characterization extremely challenging, and hinders the exhaustive profiling of CTCs and detection of positive blood samples with low cancer cell counts. Recently, the generation of CTC cell lines had been reported, opening new possibilities in the characterization of CTCs and screening for anti-cancer drugs. Though promising, these techniques have low efficiency (<20% rate in formation of cultures), require lengthy procedures and additional pre-enrichment techniques.

This study presents a label-free technique using microwells for the culture of CTCs from patients at different stages of breast cancer. Clusters comprising of putative CTCs were established directly from the nucleated cell fraction after red blood cell (RBC) lysis. Healthy blood samples, serving as controls, led to cellular debris or a monolayer of residual blood cells. This protocol allowed unbiased enrichment of a wide range of heterogeneous cancer cells, leading to a higher detection efficiency (62.2%, n=391) in contrast to conventional enrichment techniques (<50%). A minimal sample input of 2.5 ml of patient's blood was required and results could be obtained rapidly after short-term culturing of 2 weeks.

Resultant multilayered clusters comprised Small putative CTCs ($\leq 25 \mu\text{m}$; high nuclear to cytoplasmic (N/C) ratio; CD45-) and larger blood cells ($>25 \mu\text{m}$; low N/C ratio; either macrophages (CD68+) or natural killer cells (CD56+)). Relative proportion of putative CTCs increased with the depletion of most leukocytes. Characterization of the cultures revealed cellular heterogeneity via histological staining, protein and gene expression analyses. Cultured CTCs presented a range of epithelial–mesenchymal transition (EMT) phenotypes. Among these, a subset of CTCs were identified that expressed markers correlating to breast cancer stem cells (CSC), another rare subpopulation of carcinoma cells with reported drug resistance/tolerance and stem cell-like properties. The combination of hypoxia and tapered microwell topography led to the highest proportion of CSC-like cells. Characterization with invadopodia assays suggested the presence of more invasive cancer cells. Intriguingly, a large proportion of cultured cells appeared to be arrested in G1/S phase of the cell cycle, a likely protective mechanism, but could be induced into spheroids upon passaging into fresh 3D matrix or non-adherent well dishes.

From a clinical perspective, the ability to form clusters correlated with patient overall survival (OS), and was reduced in samples obtained at later treatment time points. A portion of samples from patients with early-stage cancer also lead to positive cultures, even a year after treatment, which may hint at an increased risk of relapse. Overall, the microwell CTC culture assay can potentially serve as a valuable tool for rapid monitoring of patient prognosis and expansion of the CTC cohort, which may enable CTC profiling and insights on tumor biology and metastasis.

List of Tables

| | |
|---|--|
| Table 1.1 List of notable CTC enrichment techniques. | |
| Table 1.2 List of markers utilized for CTC enrichment via positive selection using epithelial, mRNAs, tumor-related or organ-related markers..... | |
| Table 1.3 Reported methods on the culture of CTCs..... | |
| Table 1.4 CTC counts ml^{-1} as reported by notable CTC enrichment methods (non-culture-based) | |
| Table 2.1 List of primary antibodies targeting MSC-derived cell types, WBCs and endothelial cells | |
| Table 2.2 List of primary antibodies targeting antigens expressed by a variety of stem cells or epithelial cells or mesenchymal cells, including an antibody to decorate actin microfilaments and another for cell proliferation status..... | |
| Table 2.3 List of PCR probes..... | |
| Table 2.4 List of DNA FISH probes..... | |
| Table 2.5 List of RNA FISH probes..... | |
| Table 3.1 Demographics for healthy volunteers (n=17)..... | |
| Table 5.1 Demographic details of patients (n=60) with locally advanced or metastatic breast cancer | |
| Table 5.2 List of 14 post-treatment samples from patients with refractory cancer computed for survival statistics in Figure 5B..... | |
| Table 5.3 CK+ CTC cell count ml^{-1} of blood..... | |

List of Figures

| | |
|--------------------|--|
| Figure 1.1 | Schematic summarizing the major steps of the metastatic cascade..... |
| Figure 2.1 | Fabrication of microwell assay via laser ablation..... |
| Figure 2.2 | Preparatory procedures before culture..... |
| Figure 2.3 | Measurement of average diameter for clusters and single cells..... |
| Figure 3.1 | Optimization of microwell fabrication..... |
| Figure 3.2 | Optimization of assay parameters with SKBR3 breast cancer cell line..... |
| Figure 3.3 | Characterization of laser-ablated surfaces to determine changes in surface chemistry..... |
| Figure 3.4 | Determining time point for culture characterization..... |
| Figure 3.5 | Optimization of pre-processing procedure to obtain nucleated cells for culture |
| Figure 3.6 | Determination of media and incubator conditions for CTC culture..... |
| Figure 3.7 | Estimation of the minimal sample volume required for clinical sample culture |
| Figure 3.8 | Schematics of the optimization procedures..... |
| Figure 3.9 | Fabrication of microwell assay via laser ablation..... |
| Figure 3.10 | Workflow for culture of clinical samples..... |
| Figure 3.11 | Schematic illustrating the series of downstream experiments done on cells obtained from established putative CTC cultures..... |
| Figure 3.12 | Determination of the proportion of apoptotic or senescent cells in established putative CTC cultures..... |
| Figure 3.13 | Cultures obtained from clinical samples vary from those generated with healthy blood..... |
| Figure 3.14 | Phenotyping Large cells of cultures from clinical samples..... |

Figure 3.15 Immunostaining of cultures at different time points with antibodies targeting haematopoietic precursors and leukocytes.....

Figure 3.16 Immunostaining of cultures at different time points with antibodies targeting monocytes and macrophages.....

Figure 3.17 Immunostaining of cultures at different time points with antibodies targeting other blood components.....

Figure 3.18 Characterizing putative CTCs (Small CK+ cells) in culture.....

Figure 3.19 Immunostaining of cultures at different time points with antibodies targeting MSCs or MSC- derivatives.....

Figure 4.1 DNA FISH of cultured cells and controls (1 probe to 1 sample).....

Figure 4.2 Quantification of the percentage of cells with ≥ 3 red signals after DNA FISH (1 probe to 1 sample).....

Figure 4.3 Combined DNA FISH (6 probes to 1 sample) for cultured cells.....

Figure 4.4 Gene expression profiles of EMT associated genes via qRT-PCR.....

Figure 4.5 Immunostaining of epithelial and mesenchymal markers for Day 14 cultures....

Figure 4.6 RNA FISH with probes targeting EMT markers.....

Figure 4.7 Proportion of putative breast CSCs (CD44+/CD24-) in cultures.....

Figure 4.8 Immunostaining of cultured cells from different sample time points with antibodies targeting ESC-associated markers.....

Figure 4.9 Formation of spheroids in 3D Geltrex or low adhesive substrates.....

Figure 4.10 Gene or protein expression analyses to suggest mechanisms for CTC proliferation.....

Figure 4.11 Invasiveness and migratory aspects of cultured CTCs.....

Figure 5.1 Graphical representation of the Kaplan–Meier survival analysis.....

Figure 5.2 Clinical correlation of cluster formation with patient survival.....

List of Symbols and Acronyms

| | |
|---|---------------|
| Alpha-Fetoprotein | AFP |
| American Joint Committee on Cancer | AJCC |
| American Type Culture Collection | ATCC |
| Analysis Of Variance | ANOVA |
| Atomic Force Microscopy | AFM |
| Biomedical Microelectromechanical Systems | Bio-MEMS |
| Cancer Stem Cells | CSCs |
| Carcinoembryonic Antigen | CEA |
| CD31 gene | <i>PECAMI</i> |
| CD45 gene | <i>PTPRC</i> |
| Circulating Epithelial Cells | CEpC |
| Circulating Tumor cells | CTCs |
| Collagen Adhesion Matrix | CAM |
| Complementary Deoxyribonucleic Acid | cDNA |
| Computer Aided Design | CAD |
| Confidence Interval | CI |
| Cytokeratin | CK |
| Disseminated Tumor Cell | DTC |
| Doxorubicin /Cyclophosphamide | AC |
| Drop-Shape Analysis Profile | ADSA-P |
| Dulbecco's Modified Eagle Medium | DMEM |
| E-cadherin Gene | <i>CDHI</i> |

| | |
|---|---------|
| Embryonic Stem Cells | ESCs |
| Epithelial Cell Adhesion Molecule | EpCAM |
| Epithelial To Mesenchymal Transition | EMT |
| Ethylenediaminetetraacetic | EDTA |
| Fetal Bovine Serum | FBS |
| Fillamentous Actin | F-actin |
| Fluorescein Isothiocyanate | FITC |
| Fluorescence <i>In situ</i> Hybridization | FISH |
| Fluorescence-Activated Cell Sorting | FACS |
| Food And Drug Administration | FDA |
| Herringbone-Chip | HB-chip |
| High-Definition | HD |
| Hours | Hrs |
| Human Epidermal Growth Factor Receptor 2 | HER2 |
| Human Telomerase Reverse Transcriptase | hTERT |
| Hypoxia | H |
| Immunoglobulin G | IgG |
| Institute Of Molecular And Cell Biology | IMCB |
| Invasive Lobular Carcinoma | ILC |
| Isolation By Size Of Epithelial Carcinoma cells | ISSET |
| Leukocytes White Blood Cell | WBC |
| Macrophage Inhibiting Factor | MIF |
| Magnetic Resonance Imaging | MRI |

| | |
|--|-----------|
| Mesenchymal Stem Cells | MSCs |
| Mesenchymal to Epithelial Transition | MET |
| Messenger Ribonucleic Acid | mRNA |
| Microwell | W |
| Milliliter | ml |
| Millimetre | mm |
| Minute | Mins |
| Natural Killer Cell | NK cell |
| Nuclear/Cytoplasmic Ratio | N/C ratio |
| Overall Survival | OS |
| Paclitaxel+Carboplatin+Lapatinib | PCL |
| Papanicolaou | PAP |
| Paraformaldehyde | PFA |
| Penicillin G And Streptomycin | Pen Strep |
| Phosphate Buffered Saline | PBS |
| Polydimethylsiloxane | PDMS |
| Positron Emission Tomography | PET |
| Progression Free Survival | PFS |
| Propidium Iodide | PI |
| Prostate Specific Antigen | PSA |
| Prostate-Specific Membrane Antigen | PSMA |
| Real-Time Quantitative Reverse Transcription Polymerase Chain Reaction | qRT-PCR |

| | |
|--|-----------------|
| Red Blood Cell | RBC |
| Roswell Park Memorial Institute | RPMI |
| Saline Sodium Citrate | SCC |
| Scanning Electron Microscope | SEM |
| Senescence-Associated Beta Galactosidase | SA β -gal |
| Squamous-Cell Carcinoma Antigen | SCCA |
| Sunitinib | Sutent |
| Tetramethylrhodamine | TRITC |
| The Cancer Genome Atlas | TCGA |
| Three-Dimensional | 3D |
| Transforming Growth Factor Beta | TGFB |
| Vimentin Gene | <i>VIM</i> |
| Von Willebrand Factor | vWF |
| World Health Organization | WHO |
| X-Ray Computed Tomography | X-ray CT |

List of Publications, Patents and Conferences abstracts

Publications

1. Warkiani, M.E., Bhagat, A.A.S., **Khoo, B.L.**, Han, J., Lim, C.T., Gong, H.Q., Fane, A.G. Isoporous micro/Nanoengineered membranes. ACS nano 7: 1882-1904, 2013
2. Hou, H.W., Warkiani, M.E.*, **Khoo, B.L.***, Li, Z.R., Soo, R.A., Tan, D.S.W., Lim, W.T., Han, J., Bhagat, A.A.S., Lim, C.T. Isolation and retrieval of circulating tumor cells using centrifugal forces. Scientific reports, 3, 2013 (Co-2nd author)(*These authors contributed equally to the manuscript.)
3. Warkiani, M.E.*, Guan, G.F.*, **Khoo, B.L.***, Lee, W.C., Bhagat, A.A., Chaudhuri, P.K., Tan, D.S., Lim, W.T., Lee, S.C., Chen, P.C., Lim, C.T., Han, J. Slanted spiral microfluidics for the ultra-fast, label-free isolation of circulating tumor cells. Lab on a Chip 14:128-137, 2014 (Co-1st author)(*These authors contributed equally to the manuscript.)
4. **Khoo, B.L.***, Warkiani, M.E.*, Guan, G.F., Tan, D.S., Lim, A.S.T., Lim, W.T., Yap, Y.S., Lee, S.C., Soo, R.A., Han, J., Lim, C.T. Ultra-High Throughput Enrichment of Viable Circulating Tumor Cells. The 15th International Conference on Biomedical Engineering, 1-4, 2014
5. Warkiani, M.E.*, **Khoo, B.L.***, Tan, D.S.W., Bhagat, A.A., Lim, W.T., Yap, Y.S., Lee, S.C., Soo, R.A., Han, J., Lim, C.T. An ultra-high-throughput spiral microfluidic biochip for the enrichment of circulating tumor cells. Analyst. 139 (13): 3245-3255, 2014. (Co-1st author)(*These authors contributed equally to the manuscript.)

6. **Khoo, B.L.***, Warkiani, M.E.*, Tan, D.S.W.*, Bhagat, A.A., Irwin, D., Lau, D.P., Lim, A.S.T., Lim, K.H., Krisna, S.S., Lim, W.T., Yap, Y.S., Lee, S.C., Soo, R.A., Han, J., Lim, C.T. Clinical validation of an ultra-high-throughput spiral microfluidics for the detection and enrichment of viable circulating tumor cells. *PloS one*. 9 (7): e99409
7. Warkiani, M.E.*, Tay, A.K.P.*, **Khoo, B.L.**, Xu, X., Han, J., Lim, C.T. Malaria detection using inertial microfluidics. *Lab on a Chip*, 2015
8. **Khoo, B. L.***, S. C. Lee*, P. Kumar, T. Z. Tan, M. E. Warkiani, S. G. Ow, S. Nandi, C. T. Lim and J. P. Thiery (2015). "Short-term expansion of breast circulating cancer cells predicts response to anti-cancer therapy." *Oncotarget* **6**(17): 15578-15593.
9. Warkiani, M.E., **Khoo, B.L.**, Wu, L., Tay, A.K.P., Bhagat, A.A., Han, J., Lim, C.T. Ultra-fast, label-free isolation of circulating tumor cells from blood using spiral microfluidics. *Nature Protocols* (accepted), 2015
10. **Khoo, B.L.**, Chaudhuri, P.K., Ramalingam, N., Lim, C.T., Warkiani, M.E. Rising above the crowd: Single-cell profiling approaches to cancer heterogeneity. *International Journal of Cancer* (in review), 2015

Book Chapter

1. **Khoo, B.L.**, Kumar, P.*, Thiery, J.P. Circulating Tumor cells: Genesis of Circulating Tumor Cells (CTCs) through Epithelial-Mesenchymal Transition as a mechanism for distant dissemination (Eds Cote and Ram). Springer, New York. 2015 (Accepted)
2. Tay, K.P., **Khoo, B.L.**, Warkiani, M.E. The Role of Microfluidics in Infectious Diseases Diagnostics. Springer, New York. 2015 (In review)

Patent

Khoo, B. L. and Lim, C. T., UK Patent Application No. 1421342.5, Title: Cell Culture,

ILO Ref: 12351N-UK/PRV2

Conferences attended (since 2010)

2015 World Congress on Bioengineering (WACBE)

Oral Presentation, Session Chair

2014 6th annual DUNES Symposium (Duke-NUS)

Poster Presentation

2014 Advances in Circulating Tumor Cells (ACTC)

Poster Presentation

2014 Asian Pacific Organization of Cell Biology (APOCB)

Poster Presentation, Full sponsorship

2013 The 15th International Conference on Biomedical Engineering (ICBME)

Oral Presentation

Chapter 1: Introduction

1.1 Background on cancer

1.1.1 Cancer heterogeneity and mortality

Cancer research has undergone tremendous boost over the past few years, spurred on by the validation that cancer phenotypes can be induced from both somatic and germ line mutations. These mutations act together to affect multiple signaling pathways, resulting in a vast degree of tumor heterogeneity (Stratton et al. 2009).

The extent of tumor heterogeneity presents a problem during targeted therapeutics, and is one of the main reasons why cancer often leads to morbidity and fatality worldwide. According to the World Health Organization (WHO), 14 million new cancer cases were reported in the year 2012, and cancer-related deaths amounted to more than 8 million people (Stewart and Wild 2014).

Another major factor contributing to cancer fatality is the lack of early intervention, which often results in the patient developing metastases (Chambers et al. 2002). In fact, most clinical cases were only detected after cells from the primary tumor had migrated to other parts of the body (Nguyen et al. 2009). Due to the current lack of treatment strategies, it is generally accepted that the core treatment objective is to achieve secondary prevention with the aid of more sensitive detection methods, enabling early intervention before further spread of disease. Hence, an advancement in technologies to detect or characterize cancer will bring vast benefits to both tumor biology and healthcare (Spinney 2006).

1.1.2 Cancer metastasis

Metastasis is a complex, multistep process (Steeg 2006, Nguyen et al. 2009) (**Figure 1.1**). These processes are mediated by stimulation from the microenvironment, as described in the ‘seed and soil hypothesis’ established in 1989 (Paget 1989, Talmadge and Fidler 2010). Paget described the occurrence of metastasis as a result between the interactions of metastatic tumor cells (‘seed’) and its microenvironment (‘soil’), a hypothesis which has since been confirmed by various experimental data. Occurrence of metastasis is highly correlated to worsened patient prognosis.

Metastasis is regulated by genetic, environmental, physical and mechanical factors present in the microenvironment. Although detailed mechanisms of the metastatic cascade remains an enigma, recent investigations are starting to map the pieces together (Gupta and Massague 2006).

The primary tumor is established when normal epithelial cells undergo cellular aberration after long-term exposure to mutagens. In most cases, this leads to the formation of an adenoma (cells with a loss of apico-basal polarity and growth control) and subsequent transition to carcinoma *in situ*. Vascularisation occurs to supply the growing tumor with nutrients, a process termed as angiogenesis (Carmeliet and Jain 2011), while the tumor remains confined within the basement membrane. At this point of time, the tumor already presents genetic or physical heterogeneity, and is associated with several other cell types, including macrophages, white blood cells, cancer-associated fibroblasts (myofibroblasts), all of which are gathered in close proximity within extracellular matrix (ECM). The combination of all these cell types constituting the stromal niche provides various stimuli

for cells, triggering epithelial to mesenchymal transition (EMT) (Kalluri and Weinberg 2009, Thiery and Lim 2013) as carcinoma cells migrate from the stromal niche (Barcellos-Hoff et al. 2013) to the blood vessel. This is followed by the hematogeneous dissemination in the bloodstream, and these dissociated cells are termed circulating tumor cells (CTCs). Although it is now known that these cells are technically cancer cells (not tumor cells, which comprise of both malignant and non-malignant cells), the term CTC will be preserved in the thesis to allow further reference. Metastatic carcinoma cells are highly deformable (Hur et al. 2011) and may extravasate as single cells or clusters (microemboli), the latter which are often associated with platelets (Labelle et al. 2011). Carcinoma cells undergo mesenchymal to epithelial transition (MET) after arrest at a distant secondary site.

The two major processes leading to metastasis, namely intravasation and extravasation, are likely to be driven by EMT and MET, as initially proposed by Thiery in 2002 (Thiery and Sleeman 2006, Chaffer and Weinberg 2011). These processes promote the loss or gain of cell-cell adhesion respectively, and may also be regulated by the expression of various chemokines in the primary tumor (Kang et al. 2003, Minn et al. 2005).

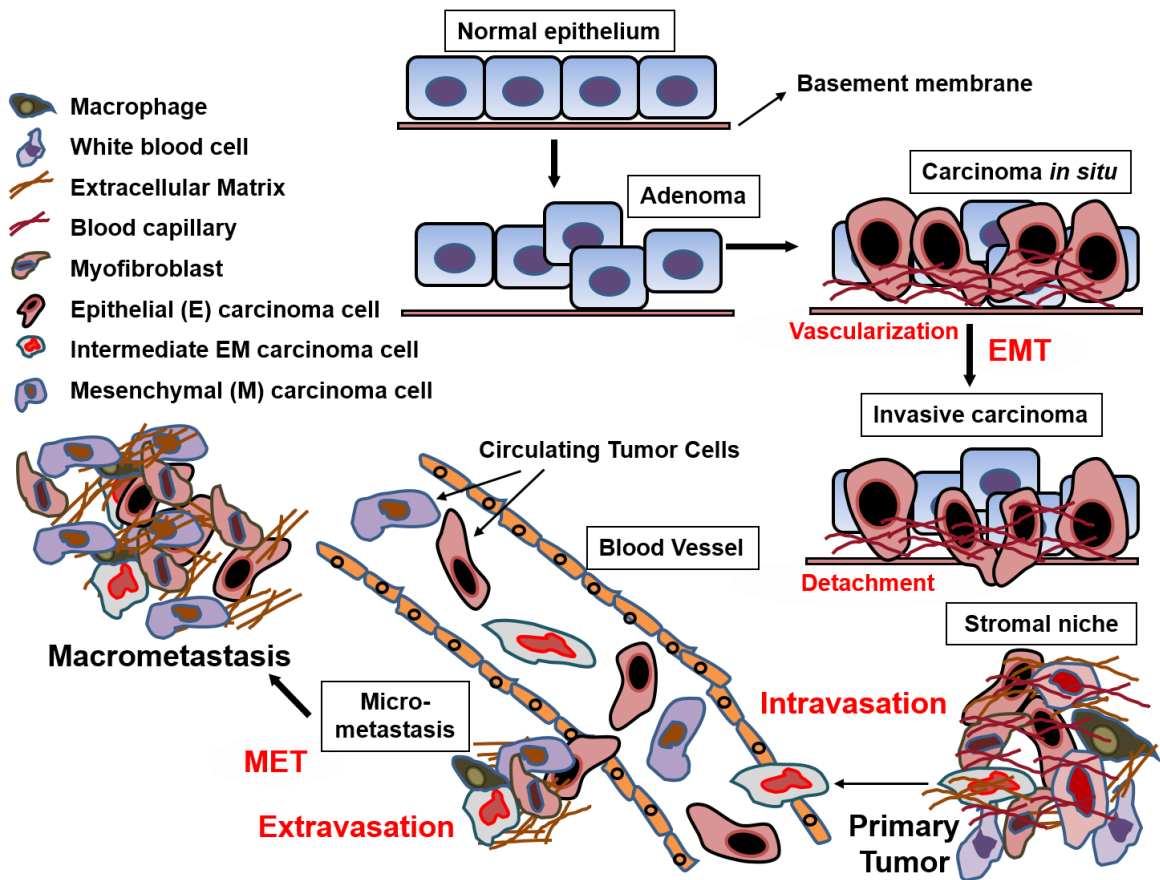


Figure 1.1 Schematic summarizing the major steps of the metastatic cascade. Normal epithelial cells undergo cellular aberration, forming adenoma and subsequently carcinoma *in situ*. Capillaries are formed to supply nutrients to the growing primary tumor. In the stromal niche, other cell types, such as macrophages, white blood cells, myofibroblast are also present, all of which are bundled in close proximity with the carcinoma cells by the extracellular matrix. The carcinoma cells undergo EMT, detach from the stromal niche and penetrate into the blood vessel, in a process known as intravasation. Carcinoma cells that enter the peripheral bloodstream are termed as CTCs, which are then disseminated through the body via the bloodstream. Some carcinoma cells undergo MET. Under suitable environmental stimuli, single or a cluster of carcinoma cells of various epithelial (E), mesenchymal (M) or intermediate EM phenotypes may be arrested within the endothelial cell lining of the blood vessel, eventually migrating into the surrounding local tissue (extravasation). Extravasated cells may generate micrometastasis and subsequent macrometastasis. Major steps are indicated in red.

1.2 Circulating Tumor cells (CTCs)

Metastasis results in the shedding of CTCs into the peripheral bloodstream. The metastatic cascade has been investigated mainly with the use of animal models, such as

the mouse (Kienast et al. 2010, Zlotnik et al. 2011), and was previously thought to occur only at advanced disease stages. However in recent years, technological advancements enabled scientists to detect CTCs in patients with early stage cancer (Nagrath et al. 2007, Husemann et al. 2008), implying the possible application of CTC detection in early cancer diagnosis.

Although documented in the 1800s (Ashworth 1869), the presence of CTCs remained as a hypothesis till technological breakthroughs in the past decade, which allowed for the isolation of CTCs from patients with metastatic cancer (Allard et al. 2004, Nagrath et al. 2007, Gascoyne et al. 2009, Stott et al. 2010, Hou et al. 2013). CTCs can now be routinely detected from blood samples (liquid biopsies), which is a less stressful and invasive procedure as compared to conventional tumor biopsies (Loeb et al. 2013). Preliminary studies correlate high CTC counts in blood of metastatic patients with lower overall survival (Cristofanilli et al. 2004, Cristofanilli et al. 2005, de Bono et al. 2008), rendering it as a potential indicator for prognosis. CTC counts also correlate with disease progression (Nole et al. 2008) and treatment efficacy (Reuben et al. 2008).

Current consensus defines CTCs as nucleated cells with high nuclear to cytoplasmic (N/C) ratio, and which express epithelial markers (e.g. cytokeratin (CK) and Epithelial Cell Adhesion Molecule (EpCAM)), but not leukocyte markers (e.g. CD45). This definition was adopted from the standard used for disseminated tumor cell (DTC) detection in the 1990s (Borgen et al. 1999). DTCs are cancer cells found in the bone marrow, and also originate from tumors.

However, it is now known that this definition is inadequate for cancer cell identification.

Subpopulations of CTCs may undergo EMT (Thiery 2002), leading to varied phenotypes which could be conferred with protective traits to avoid anoikis (programmed cell death) (Howard et al. 2008) or senescence (Ansieau et al. 2008). Some cells may even acquire stem cell-like properties (Singh et al. 2003, Clevers 2011). In fact, cancer cells often exist as a range of either full-blown or intermediate EMT phenotypes, to provide favoring characteristics at each stage of the metastatic cascade (Jordan et al. 2011, Davidson et al. 2012, Huang et al. 2013, Yu et al. 2013).

The exact frequency of CTCs in blood has been under debate, partly due to the varied detection sensitivity and recovery efficiency present with each enrichment assay. Previous experiments using mouse models with highly metastatic disease estimate the amount of shed carcinoma cells per day to be around 10k (Fidler 1970). A later study even suggested this number to be a million per day for each gram of tumor (Butler and Gullino 1975). The frequency of CTCs also varies with disease stage and presence of treatment or surgical procedures that may evoke heightened release of CTCs (Fidler 1970).

Exact mapping of the timeline for CTC occupancy in blood is still unknown, but vaguely estimated to be several hours or days. Most of these cells are believed to have brief periods in circulation (Riethdorf and Pantel 2009, Coumans et al. 2013). When cancer cells were injected into mouse, only 1% of cells were left circulating in blood after 24 hrs. The high loss of CTCs is mainly attributed to damage induced by the fluid shear flow or host immune response (Chambers et al. 2002), since single CTCs are vulnerable in the absence of its stromal niche. Thus, the process of metastasis is not an efficient process (Weiss 1990, Brodland and Zitelli 1992), and is also further impeded by the fact that only

few CTCs have metastatic potential.

Cancer cells which remain in circulation are likely to remain viable. However, most of these persisting CTCs may undergo dormancy (Chambers et al. 2002, Coumans et al. 2013). Dormant cancer cells are likely to proliferate again under the right circumstances. Ability of a CTC to generate micrometastases *in vivo* may be heightened by a myriad of factors, such as encounters with fenestrated blood vessels that encourage extravasation, or suitable microenvironmental stimuli (chemical secretions, topography and other forms of interactions) provided by the premetastatic niche (Nguyen et al. 2009, Barcellos-Hoff et al. 2013).

1.2.1 Breast Cancer CTCs and statistics

CTCs of various cancer types have now been isolated from blood of patients, including but not limited to, breast, prostate and lung cancer (Farace et al. 2011). Clinical trials of patients with breast cancer, one of the most common cancer types in women, were the focus in this study.

There is a great necessity to improve the prospects of overall survival (OS) and progression free survival (PFS) in breast cancer patients, which vary due to a range of demographic factors such as age, tumor status, stage and grade. Patients with PFS do not experience deterioration in their condition during or after treatment, while the OS reflects the percentage of patients who survived with respect to time after treatment. According to the data from American Cancer Society's Cancer Facts and Figures 2014 report, 40,000 out of 232670 women (17.1%) diagnosed with breast cancer died from the disease. A

portion of treated patients also remains vulnerable to the relapse of the disease, which obscures recovery, both physically and mentally. Patients with postoperative recurrence usually have poorer prognosis, which made monitoring of disease even more critical. In Singapore, the estimated relapse frequency for patients with early stage breast cancers is 10-20% for stage I, 30-40% for stage II and 50-70% for stage III cancer (Saxena et al. 2012).

The main factor for mortality of cancer patients is the presence of metastatic lesions (Gupta and Massague 2006). Logically, the presence of CTCs is inversely correlated to patient response to therapy (Farace et al. 2011), a parameter usually determined by the shrinkage of tumor mass (Therasse et al. 2000). CTC counts may even correspond better than tumor size measurement (Foulkes et al. 2009). Although a recent study did not achieve any correlation between CTC counts with tumor status and location (Rack et al. 2010), CTCs may still serve as a superior method when compared to conventional means of evaluation (e.g. biopsy).

The current methods utilized in clinical settings for tumor detection, which affect subsequent treatment evaluation, are highly limited by the device's sensitivity limit, thus preventing observation of tumors smaller than 5 mm or the monitoring of minute changes in tumor size (Erten et al. 2010). In fact, a high percentage of patients initially classified with large operable (localized) tumors, were later found to have metastasized cancer, which often result in death due to the lack of prompt treatment (Coen et al. 2002, Riethdorf et al. 2008). Hence, the generation of novel and sensitive assays to separate blood components, enabling CTC enrichment, is a highly desirable approach (Vona et al.

2000, Loberg et al. 2004, Toner and Irimia 2005, Nagrath et al. 2007, Gascoyne et al. 2009, Stott et al. 2010, Yu et al. 2011, Warkiani et al. 2014a). This may allow better prospects for the cancer patients via the prompt and accurate establishment of suitable clinical trials.

1.2.2 Clinical significance of CTCs

Scientists and clinicians have rekindled the ‘seed and soil’ theory (Paget 1989), and anticipate that CTCs will be of clinical utility (Paget 1989, Cristofanilli et al. 2004). Characterization of CTCs may fill many knowledge gaps in tumor biology, especially in the process of metastasis (Pantel and Alix-Panabieres 2007, Pantel et al. 2008).

TCs can be detected in patients with early stage cancer, and CTC counts may even correlate better to disease status as compared to current detection methods such as X-ray computed tomography, or positron emission tomography (PET) scan techniques (Weissleder 2002). The presence of CTCs in patients with early stage cancers also contradicts previous notion that cancer cell dissemination only occurs late in the disease progression (Loberg et al. 2004, Riethdorf et al. 2008).

CTCs are heterogeneous and may recapitulate the tumor phenotypes better than tumor biopsies. Phenotyping of enriched CTCs reveals that another subpopulation of tumorigenic carcinoma cells are present within the CTCs (Clevers 2011). These tumorigenic cells, termed as ‘cancer stem cells (CSCs)’, also originate from tumors and may present tolerance (Kang and Kang 2007, Eyler and Rich 2008, Sharma et al. 2010) or resistance (Li et al. 2008, Singh and Settleman 2010) to certain chemotherapeutic drugs.

These subpopulations of cancer cells with favorable traits for survival may be valuable drug targets for novel therapies.

The extent of CTC heterogeneity is far from being understood, as seen in terms of morphology, proteomic or genomic profiling (Pantel and Brakenhoff 2004). Some of these CTCs may be conferred with favorable characteristics for propagation and survival, such as the expression of human epidermal growth factor receptor 2 (HER2), which render them more susceptible to complete the metastatic cascade. Due to this variation, scientists have not been able to capture a complete spectrum of CTCs to accurately profile and confirm their clinical utility, leading to a certain amount of controversy (Alix-Panabieres and Pantel 2014). In fact, not all patients detected with CTCs may suffer from observable symptoms or progression in disease (Braun et al. 2005). Despite these findings, the presence of persisting CTCs correlates well with an increased risk of disease relapse (Pantel and Brakenhoff 2004).

Models of metastasis in mice demonstrate that the majority of CTCs have short half-lives, a small portion of which remains viable but dormant (Chambers et al. 2002, Meng et al. 2004). The dormancy of CTCs and the process of triggering them into proliferation are not well investigated, although long term studies of patients under relapse suggest that cancer cells may exit dormancy due to accumulation of new mutations or a change in the microenvironment (Aguirre-Ghiso 2007). To achieve better functional studies and clinical utility, novel techniques are required to detect or enrich significant proportions of CTCs, even via culture of these rare cells, to achieve reliable detection and characterization.

1.3 Current literature on CTC enrichment

Detection of a heterogeneous cell population is a technically challenging process. Cells are small entities in the range of microns, and hence require equipment with a high degree of tunability to separate cells under precise control and selectivity (Van Vliet and Bao 2003). Thus, devices attempting to sort cells have to operate at a micro-scale level, usually via microfluidics (Bhagat et al. 2010) or microelectronics (Wei et al. 2014).

The miniaturization of systems allows analysis with low sample input (Bashir 2004, Whitesides 2006), which is favorable for handling rare samples. However, the sheer extent of CTC heterogeneity induces vast difficulty for its enrichment (Pantel et al. 1999). This is further exacerbated by their extremely low abundance (<1000 cells ml^{-1}) in peripheral blood (Zieglschmid et al. 2005), which comprises of other billions of blood cells, including erythrocytes (red blood cell; RBC), leukocytes (white blood cell; WBC) and thrombocytes (platelets) (Anthea et al. 1993, Racila et al. 1998). Challenges and limitations of these techniques will be further discussed in **Section 1.4**.

In the past decade, a surge in the fields of nanomaterials and microfluidics has led to an impressive number of techniques developed to separate blood and small particles. Several methods have been adopted for the detection and enrichment of CTCs, with notable examples summarized in **Table 1.1**.

Table 1.1 List of notable CTC enrichment techniques. These include methods based on antigen-recognition (immunophenotyping), physical characteristics (size and deformability) as well as membrane electrical or invasive properties.

| Types | Term | Enrichment concept | Average blood volume per test/ml | Estimated range of CTCs detected/ml | Purity/% | Reference |
|-------------------|---|--------------------------------|----------------------------------|-------------------------------------|--------------|----------------------------|
| Immunophenotyping | CTC-chip | Antibody-coated micropillars | 2.7 | 5 to 1,281 | 9.2% ± 0.1% | (Nagrath et al. 2007) |
| | Herringbone-chip | | 4 | 12 to 3,167 | 14.0% ± 0.1% | (Stott et al. 2010) |
| | Nanopillars with microfluidic chaotic micromixers | | 1 | 1 to 33 | ND | (Wang et al. 2011) |
| | Geometrically enhanced differential immunocapture microfluidic device | | 1 | 27 ± 4 | 62 ± 2 | (Gleghorn et al. 2010) |
| | Biomedical microelectromechanical systems (Bio-MEMS) | Antibody-coated microchannels | NA | ND | ND | (Du et al. 2007) |
| | Nanoscale oncometer | Antibody-coated nanotubes | NA | ND | ND | (Shao et al. 2008) |
| | MACS cell separation systems | Immunobeads | 5 to 15 | 1 to 571 | ND | (Deng et al. 2008) |
| | CellSearch | Antibody-coupled ferrofluid | 7.5 | 1 to 1491 | ND | (Riethdorf et al. 2007) |
| | MagSweeper | | 9 | 1 ± 3 | 100% | (Talasaz et al. 2009) |
| | CTC-chip Ephesia | | NA | ND | ND | (Saliba et al. 2010) |
| | Fiber-optic array scanning technology cytometer | Flow cytometry | NA | ND | ND | (Krivacic et al. 2004) |
| | Multiphoton intravital flow cytometry | | 0.5 | 1 to 153 | ND | (He et al. 2007) |
| | AdnaTest | Antibody-coupled microbeads | 5 | ND | ND | (Andreopoulou et al. 2012) |
| | Surface-enhanced Raman scattering and high photothermal contrast | Antibody-coupled nanoparticles | 1 | ND | ND | (Nima et al. 2014) |

| | | | | | | |
|---|---|---|-----|------------|---------|-------------------------|
| Size and deformability | 3D microfilter | Filtration | NA | ND | ND | (Zheng et al. 2011) |
| | Isolation by Size of Epithelial Carcinoma cells | | 6 | 1 to 4 | ND | (Vona et al. 2004) |
| | Microcavity array system | | NA | ND | ND | (Hosokawa et al. 2013) |
| | CT biochip | | 5 | ND | 80-90% | (Tan et al. 2010) |
| | Separable Bilayer Microfiltration Device | | 0.1 | ND | ND | (Zhou et al. 2014) |
| | Spiral inertial biochip | Inertial focusing | 7.5 | 5 to 100 | ~10% | (Hou et al. 2013) |
| | Trapezoidal biochip | | 7.5 | 3 to 125 | 0.6-25% | (Warkiani et al. 2014a) |
| | Vortex chip | | 7.5 | 23-317 | 57-94 | (Sollier et al. 2014) |
| | CTC-iChip | Inertial focusing coupled with ferrofluid | 10 | 0.5 to 610 | 7.80% | (Ozkumur et al. 2013) |
| Dielectrophoretic field-flow fractionation | ApoStream | Morphologic and electrical conductivity differences | NA | ND | ND | (Gupta et al. 2012) |
| Invasive properties | Collagen Adhesion Matrix (CAM) assay | Ingestion of fluorescent CAM fragments | 1 | 18-256 | 0.5-35% | (Lu et al. 2010) |

1.3.1 Label-dependent techniques

The first available techniques for CTC detection relied on affinity-based methods. CTCs can be enriched via positive selection with epithelial, tumor- or organ-associated markers, or negative selection via the removal of blood cells (**Table 1.2**). Conventional methods utilize whole blood samples for flow cytometers (He et al. 2007), which are straightforward but of low efficiency.

Currently, CTCs are more often enriched via binding to substrates coated with membrane-specific epithelial antibodies. This step is usually coupled to microfluidics, hence enabling precise processing under controlled laminar conditions. Substrates utilized for this purpose include micropillars (Nagrath et al. 2007, Gleghorn et al. 2010, Stott et al. 2010, Wang et al. 2011), microchannels (Du et al. 2007), nanotubes (Shao et al. 2008), nanoporous surfaces (Mittal et al. 2012), microbeads (Deng et al. 2008), immunomagnetic beads or ferrofluid (Allan et al. 2005, Riethdorf et al. 2007). In these procedures, whole blood or nucleated cells after RBC removal were obtained from patients, followed by incubation with antibody-coated substrates and subsequent separation from blood cells via wash to remove unbound cells. Additional techniques, such as the application of a magnetic field, may be coupled with this method for a more precise enrichment. Other sophisticated techniques, such as the fiber optic array scanning technologies (Krivacic et al. 2004) or Bio-MEMS (Du et al. 2007), are also utilized.

Methods which require cell-substrate interactions usually use EpCAM, a cell surface antigen (Herlyn et al. 1979) associated with stem cell proliferation (Nagao et al. 2009) and regulation of cyclin expression (Munz et al. 2004). Overexpression of EpCAM

leads to epithelial-associated phenotypes (Herlyn et al. 1979).

Enrichment of other epithelial markers has been shown to exceed the sensitivity of assays utilizing only EpCAM. Hence, recent affinity-based CTC detection techniques also target other epithelial markers, messenger ribonucleic acid (mRNAs) of genes over-expressed in cancer cells and tumor- or organ-associated antigens (**Table 1.2**). To achieve better purity of the enriched CTC population, negative selection is sometimes added as a post-processing step to remove contaminating leukocytes expressing CD45 (Allard et al. 2004, Deng et al. 2008). The techniques listed in **Table 1.1**, as well as the markers stated in **Table 1.2**, may be used in combination (e.g. Ikonisys, New Haven, CT) to achieve a sample of higher purity or to increase recovery of CTCs.

Table 1.2 List of markers utilized for CTC enrichment via positive selection using epithelial, mRNAs, tumor-related or organ-related markers.

| Type | Cancer cell target | Marker | Relevance/Specificity for breast cancer | Reference |
|----------------|--------------------|--|---|---------------------------------------|
| Epithelial | All cell types | EpCAM | Specific | (Farace et al. 2011) |
| | | Cytokeratin 8 | | |
| | | Cytokeratin 18 | | |
| | | Cytokeratin 19 | | (Farace et al. 2011, Hou et al. 2013) |
| EGP-2 | | (Molloy et al. 2008) | | |
| mRNAs | | Telomerase | Relevant | (Xu et al. 2010) |
| | | Human telomerase reverse transcriptase (hTERT) | | (Wu et al. 2006) |
| Tumor-related | | Alpha-fetoprotein (AFP) | No | (Hautkappe et al. 2000) |
| | | Carcinoembryonic antigen (CEA) | Relevant | (Wu et al. 2006) |
| | | Squamous-cell carcinoma antigen (SCCA) | | (Kaganoi et al. 2004) |
| Organ-specific | Breast | Mammaglobin | Specific | (Kruger et al. 2001) |
| | | HER2-neu | | (Riethdorf et al. 2010) |
| | | Mucin-1 | | (Mehes et al. 2001) |
| | Prostate | Prostate specific antigen (PSA) | No | (de Bono et al. 2008) |
| | | Prostate-specific membrane antigen (PSMA) | | (Stott et al. 2010) |

Amongst the label-dependent (affinity binding) techniques, CellSearch system (Veridex LLC, Raritan, NJ, USA) is currently the most established and only US Food and Drug Administration (FDA)-approved technique for CTC detection in clinical applications. Despite its potential (Cristofanilli et al. 2004, Farace et al. 2011), CellSearch only demonstrates cancer cell recovery of less than 60% and requires a high minimal input volume for disease detection. The efficiency is further reduced due to its choice of enrichment method using EpCAM-coupled ferrofluids (see **Section 1.4**).

1.3.2 Physical methods based on cell size and deformability

The limitations of affinity-binding enrichment techniques led scientists to generate label-free methods which can recover a larger distribution of CTCs. Common alternatives include filtering whole blood or passing RBC-lysed nucleated cells through a filter membrane. To minimize shear stress and increase recovery, many forms of membranes have been fabricated, including track-etched membranes (Lee et al. 2014) and more recently, three-dimensional (3D) filters (Zheng et al. 2011). Another dominant field of CTC enrichment by size works on the passive focusing of cells by inertial forces within a microfluidic chip (Di Carlo et al. 2007, Kuntaegowdanahalli et al. 2009, Hou et al. 2013, Khoo et al. 2014, Warkiani et al. 2014a, Warkiani et al. 2014b), whereby larger cancer cells can be rapidly separated from the smaller blood cells under continuous flow. Other label-free techniques utilizing physical properties for isolation include density gradient centrifugation (Gertler et al. 2003) or dielectrophoresis (Gascoyne et al. 2009, Gupta et al. 2012).

The obvious advantage of using a label-free system for the detection of a heterogeneous cell population lies in the absence of the need to depend on specific antigens for enrichment. Nonetheless, cells enriched from label-free systems will still require verification by using markers to identify CTCs and contaminating WBCs (**Table 1.2**).

1.3.3 Techniques based on proliferative capability

Most CTCs are believed to have short half-lives, and the rest are thought to be dormant (Chambers et al. 2002). Not surprisingly, previous attempts to culture these cells under conventional methods in ECM-coated culture dishes yielded no positive

results. However, the appeal of expanding CTCs remain definite, since culturing CTCs will overcome the ‘rare cell’ problem and could also be instrumental in utilizing CTCs in actual clinical settings (e.g. drug testing). Expanded CTC populations could also provide enough samples to generate insight on cancer biology via profiling or characterization of cellular processes.

A study in 2007 demonstrated that some CTCs might be active, through the establishment of a protocol that demonstrated active secretion of proteins from enriched CTCs (Alix-Panabieres et al. 2007). In the year 2014, a few techniques claimed (albeit of low efficiency) the establishment of cell lines from long-term culture of CTCs (**Table 1.3**) (Yu et al. 2014) (Yu et al. 2014) (Yu et al. 2014) (Yu et al. 2014) (Yu et al. 2014) (Yu et al. 2014). The reported methods often rely on media supplemented with growth factors, which might serve to promote the switch towards proliferation.

CTCs were not the only rare cell populations that have been cultured. Culture techniques of other rare cancer cell types, such as CSCs of tumor origin, have previously been explored (Heddleston et al. 2009). These protocols were established by mimicking conditions in the tumor microenvironment, such as hypoxia (Casazza et al. 2014). At this point of time, researchers had also been successful in culturing DTCs from the bone marrow of patients with various cancer types, and they reported an inverse correlation of growth potential to patient response (Solakoglu et al. 2002). Some used growth factors (e.g. fibroblast growth factor 2), which might be secreted by cells in their stromal niche, to propagate DTCs (Alix-Panabieres et al. 2007).

Despite the vast interest gained from these current reports, techniques of CTC culture still suffer from many limitations, as will be discussed in **Section 1.4**. Novel methods

of high-throughput, efficiency and reproducibility are required to generate meaningful utilities for CTC expansion. Established protocols of CSC and DTC cultures could be tapped on for the optimization of CTC culture assays.

Table 1.3 Reported methods on the culture of CTCs.

| Pre-enrichment principle | Samples tested | Time points | Efficiency of culture attempts | Culture type | Period of culture | Cancer type | Proposed utility | Reference |
|-----------------------------------|-----------------------|--------------------|---|--|-----------------------------|--------------------|---|------------------------------|
| Affinity binding | 36 | Single | 16.7% | Cell lines, long-term | > 6 months | Breast | Drug susceptibility | (Yu, 2014 #127) |
| Negative selection via FACS | 8 (under FACS) | Single | 37.5% | Colonies (short term), cell lines (long-term) | < 1 month or \geq 1 month | Breast | CTC profiling | Marchetti (Zhang, 2013 #125) |
| Negative selection via RosetteSep | 71 | Single | 2.8% | Cell lines, long-term | > 2 months | Colon | Exploring new drug targets | (Cayrefourcq, 2015 #271) |
| Negative selection via RosetteSep | 17 | Single | ~15-20% | Organoid lines, long-term | > 6 months | Prostate | CTC profiling and drug targets | (Gao, 2014 #126) |
| RBC lysis | 226 | Serial | 61.5 \pm 15.5% overall, varies with treatment duration and type | Primary cultures, short-term (clusters comprise of CTCs and blood cells) | 2-8 weeks | Breast | Correlation with patient survival and prognosis of treatment efficacy | (Khoo, 2015 (in press) #199) |

1.4 CTC biology and limitations of existing techniques

Preliminary findings from conventional CTC detection methods have given us a glimpse into the phenotype of CTCs, which appear to exhibit intra- and inter-patient differences (Vona et al. 2000, Marrinucci et al. 2010, Farace et al. 2011, Navin et al. 2011, Polyak 2011, Gerlinger et al. 2012, Hou et al. 2013, Khoo et al. 2014). This diversity may reflect that of tumors, which are made up with heterogeneous cell populations within a primary tumor (intratumor heterogeneity) or between tumors of different tissues (intertumor heterogeneity).

Due to this variation of biological phenotypes, the current standard for CTC definition (CK+/EpCAM+/CD45- nucleated cells with high N/C ratio; **Section 1.2**) is not sufficient to describe CTCs, and most techniques end up generating an underestimation of the actual CTC frequency in blood. In addition, the reported frequency of CTCs further varies with the different techniques used, due to differences in device sensitivity and selectivity (**Table 1.4**).

Table 1.4 CTC counts ml⁻¹ as reported by notable CTC enrichment methods (non-culture-based).

| Principle | Name | Average CTC counts ml ⁻¹ blood | Specificity | Sensitivity | Reference |
|---------------------|---------------------------------|---|-------------|-------------|-------------------------|
| Antigen recognition | CellSearch | 0-8 (Median: 0) | High | Low | (Riethdorf et al. 2007) |
| Size-based sorting | HB-chip | 12 - 3,167 (Median: 63) | Low | Higher | (Stott et al. 2010) |
| | High-definition (HD)-CTC device | 5-199 (Median: 49.3) | | | (Cho et al. 2012) |
| | Spiral inertial microfluidics | 12-1,275 (Median: 55) | | | (Khoo et al. 2014) |

1.4.1 Low frequency and marker heterogeneity

Due to the heterogeneity of CTCs, conventional enrichment methods by affinity binding can only be made superior if a unique CTC marker is verified. The current use of affinity binding methods for CTC isolation evokes a vicious cycle of incomplete CTC detection, preventing the identification of unique antigens for better CTC detection.

The markers listed in **Table 1.2** for CTC isolation are also expressed by other cell types, thus risking the likelihood of detecting false positives, such as circulating epithelial cells (CEpC) (Ring et al. 2005) or other bone marrow-derived mesenchymal stem cells (MSCs) (Jiang et al. 2002). CEpC are often present in blood of patients harboring proliferative disease or inflammation (Goeminne et al. 2000), and cannot be depleted by further negative selection with antibodies targeting leukocyte markers (Fehm et al. 2005).

False positives can also be incurred by non-specific binding, which is often the result of antibody association with normal WBC expressing Fc receptors (Gadd and Ashman 1983, Riethdorf et al. 2010), or even activated leukocytes expressing EpCAM or

cytokeratin (Jung et al. 1998, Kowalewska et al. 2006). Protocols describing the use of a CTC enrichment device usually utilize healthy blood samples as negative controls to determine the frequency of false positives, and this value has been shown to be present in 0-20% of the enriched cell population (Goeminne et al. 2000, Pantel and Woelfle 2005).

The markers used for CTC detection are not applicable to all its subpopulations (Siewerts et al. 2009), partly due to the process of EMT (Thiery 2002). For example, EpCAM is only expressed on cells with epithelial or intermediate epithelial phenotypes. Hence, techniques which utilize EpCAM as the core antigen for CTC recognition (Farace et al. 2011) suffer from a high rate of false negatives (Pantel and Woelfle 2005, Sun et al. 2011). In addition, EpCAM may not be a reliable marker for epithelial tumors since the association of EpCAM to cellular epithelial state is still unverified.

On the other hand, some cancer cells, such as those from triple negative breast cancer subtype or others characteristic of normal basal epithelial or adipose cells (Siewerts et al. 2009), may even cease to express any of the distinct markers used for CTC identification. It is apparent that only the use of a combination of markers (**Table 1.2**) will be efficient in detecting a wider coverage of CTCs present in blood (Riethdorf et al. 2010, Farace et al. 2011).

In addition to the lack of a definite CTC marker, affinity-based enrichment procedures coupled with microfluidics usually operate at low flow rates and are only optimal at low cell concentrations (to reduce clogging or clotting issues) (Zheng et al. 2011), hence greatly reducing throughput. Viability of the cells is an additional issue, since most of these techniques require long processing hours. Overall, the limitations posed

by affinity dependent techniques are detrimental to enrichment of rare CTCs.

Recent culture techniques suffer from the same drawbacks as affinity-binding methods (**Section 1.4**) as they require pre-enriched cells obtained from affinity-based platforms. Efficiency of these techniques is also low (**Table 1.3**), and require large sample input for culture (8-40 ml whole blood per sample). Hence, a superior and efficient method for culture should be developed without the need for pre-enrichment procedures.

1.4.2 Variation in morphology, size and other physical properties

Isolation of CTCs based on physical properties seems to be a promising method for solving many problems accompanying the use of affinity binding techniques. Samples are usually processed under relatively higher rates, facilitating the speed of which the sample can be processed.

In spite of these benefits, high fluid flow within these devices introduces shear stress, which can still affect cell viability and may even distort cell morphology. Of the label-free techniques, devices capitalizing on sorting by size are the most predominant. However, CTCs are not all larger than the majority of blood cells. Preliminary analysis from various groups reported the observation of Small CTCs within the range of 10-20 μm , which coincides with the leukocyte size range (Alunni-Fabroni and Sandri 2010). Other cells which do not have resemblance to classic cancer phenotypes (e.g. large cells with low N/C ratio present in patients with large cell neuroendocrine carcinoma (Hiroshima, 2006 #264)) may also bare malignant properties, and this heterogeneity will severely limit the usefulness of size-based enrichment methods.

1.4.3 CTCs may be associated to other cell types in blood

CTCs do not only exist as single cells within the circulation, but have been detected as aggregations of 2 or more cells, termed as microemboli. These aggregations could have arisen from the tumors directly or were introduced via intravasation of the neo-vessels (Thiery and Lim 2013). A recent study linked the generation of microemboli with a plakoglobin mechanism which induces cell clustering (Aceto et al. 2014), and associated the presence of microemboli with initiation of metastasis.

However, most CTC enrichment assays are not able to retain these clusters, due to various technical aspects (e.g. high shear rate which breaks up aggregations). Other factors include assay design, such as narrow channels in microfluidics, which also result in significant loss of microemboli. In this aspect, cultures and size-based enrichment techniques can be useful in isolating CTC clusters, which will help verify their roles in systemic spread, collective migration (Friedl and Gilmour 2009) and correlation with disease prognosis (Friedl and Wolf 2003, Wittekind and Neid 2005).

Besides aggregating with their own, CTCs may also associate with platelets to shield themselves from physical fluid shear and immune cells (Kang and Pantel 2013). Platelet coating can induce EMT via the secretion of transforming growth factor beta (TGF β) (Labelle et al. 2011), leading to phenotypes favorable for extravasation and subsequent tumorigenesis. The close proximity of CTCs with other cell types means that these cells are likely to be enriched in the process, leading to contamination that can affect downstream analysis. In addition, CTCs surrounded by the platelet cloak can also evade detection by antibodies in affinity-binding techniques.

1.4.4 CTC release and life cycle in circulation

Most CTCs exist briefly in circulation (Glinsky et al. 2003), with a majority of them being sequestered by narrow vessels within approximately 5 minutes (Luzzi et al. 1998). It is still not fully understood when and why cancer cells were triggered to dissociate from the tumor, but some studies have linked the phenomenon to physical trauma near the tumor site (i.e. iatrogenic procedures) (Liotta et al. 1976, Sugarbaker 1996). Of those CTCs which managed to stay in circulation, some were believed to persist in blood for months (Muller et al. 2005, Stott et al. 2010). Insufficient studies are available to determine if the time of which the liquid biopsy is obtained will affect the correlation of CTC counts to disease parameters.

1.5 Prospects of expanding CTCs for clinical utility

Early detection of disease is inversely correlated to survival rate (Allard et al. 2004, Cristofanilli et al. 2004, Budd et al. 2006). According to the American Cancer Society, one-third of patients who undergo regular checkups receive the wrong evaluation on their disease status, due to the inability of current diagnostic devices to detect small metastases in the body. CTC counts may serve as a valuable and sensitive parameter for cancer detection.

However, due to various technical limitations (**Section 1.4**), there is still no golden standard for CTC detection. A consensus on the selectivity, sensitivity and relevance of existing CTC detection assays has to be reached for actual clinical utility to take place.

CTC cultures are a promising means of amplifying a consistent spectrum of cells potentially pivotal for metastasis and disease relapse. An optimized CTC culture assay

can provide a sensitive and rapid screening method to determine the presence of proliferative cancer cells in patients (Cristofanilli et al. 2004, Hayes et al. 2006, Cohen et al. 2008). This can help to identify cancer in the earlier stages or provide hints of disease relapse. Expansion of a rare cell cohort can also be used to better define the phenotypic and genotypic characteristics without the need for sophisticated single cell analytical (SCA) techniques. In addition, CTC cultures can serve to amplify the sub-populations amongst the heterogeneous CTCs, and identify the ones which would eventually be most important in the process of metastasis. This may help clinicians identify novel drug targets for treatment.

The current methods for CTC cultures face three main issues:

- 1) CTC cell lines are immortalized phenotypes, and cannot represent primary carcinoma cells (Lacroix and Leclercq 2004, van Staveren et al. 2009).
- 2) The long periods required for cell line establishment limits clinical utility, since early detection and treatment is crucial for patient survival.
- 3) Cultures are established at low efficiency and require large sample input. This makes it challenging to monitor patient response over different treatment time points.

1.6 Hypotheses and project proposal

Sensitive CTC enrichment could play a dramatic role in shaping strategies for cancer detection and evaluation of patient prognosis. The development of a novel and rapid assay for the consistent and efficient expansion of primary CTCs is imperative to provide actual clinical value to these rare cells. The hypotheses for this thesis project are as follows:

- Primary CTCs can be expanded efficiently as a short-term culture under suitable conditions.
- Putative CTCs in culture may consist of subpopulations with heightened tumorigenic or metastatic potential.
- Culture phenotypes can correspond to disease severity or patient outcome.

From a mechanobiology purview, the microenvironment of primary cancer cells, such as physical topography, cell-cell or cell-substrate interaction, and other cues from neighboring cells, is crucial for maintaining cancer cell viability and proliferation. Hence, it is expected that CTCs may have to be maintained under an environment similar to its stromal niche *in vivo* to establish culture. Cultured CTCs are likely to be heterogeneous and may comprise subpopulations with higher tumorigenic potential.

The scope and objectives of this study include the design and optimization of a short-term CTC culture relevant to *in vivo* stromal niche conditions, thus achieving a protocol of high efficiency for the proliferation of primary CTCs. The method does not require prior processing with any form of enrichment techniques, which greatly facilitates ease of operation. The lack of pre-processing also reduces cellular damage, thus favoring cell viability and minimizing cell loss. Since an enrichment assay by culture selects for all proliferative CTCs, the protocol is flexible and can be adapted for expanding CTCs of different cancer types.

To achieve this, microwells were proposed as the main feature of the culture assay design. Such topography was previously used to sustain stem cell properties of embryonic stem cells (Moeller et al. 2008), and was also reported to affect the metabolic activities and differentiation of various primary non-cancer cell types (Wang et al. 2009). This project also tested the influence of hypoxia on the

establishment of CTC cultures, since low oxygen levels were known to promote CSC proliferation (Heddleston et al. 2009).

Optimization of the assay was attempted by testing with a range of microwell dimensions and culture conditions, using a breast cancer cell line (SKBR3). Confirmation of culture parameters was then established with actual clinical samples. To validate the presence of CTCs in culture, cultures were harvested and characterized to identify blood cells that might persist in culture. Further on, the cultures were profiled by immunostaining, fluorescence *in situ* hybridization (DNA/RNA FISH), histopathological staining and other techniques to ascertain viability and to determine their characteristics (e.g. morphology, EMT phenotypes, invasiveness and copy number increase in cancer-associated genes). Peripheral blood of healthy volunteers was utilized as controls to evaluate the specificity of this method. Finally, the data obtained was also used to draw any possible correlations between culture occurrence with patient demographics or prognosis.

Chapter 2: Materials and Methods

2.1 Preparation of culture assay

Microwells were made on non-coated 60 mm polystyrene dishes (Becton Dickinson, Franklin Lakes, NJ) in an array pattern which maximized the coverage of microwells on the substrate (~ 48 microwells cm^{-2} , **Figure 2.1A**). The microwell array was drawn with the Auto Computer Aided Design software (Fortier et al.) (Autodesk, San Rafael, CA). Due to the flexibility of this method, microwells can be produced on other polystyrene substrates, including well plates (**Figure 2.1B**). An air-cooled $10.6 \mu\text{m}$ CO_2 laser engraving/cutting system (VLS-2.30, Universal Laser System Inc., Scottsdale, AZ) was used for the generation of microwells. Patterned dishes were sterilized with and kept in 70% ethanol until use.

2.2 Characterization of biochemical changes of patterned dishes

To estimate relative surface topography of the dish before and after laser ablation (i.e. to determine difference in surface roughness), atomic force microscopy (AFM) was used to trace the substrate surface at regions near or away from the microwells (laser-ablated regions). Scans were performed with the contact mode, in air, using a Bruker cantilever optic fiber probe of tip diameter of 20 nm (Msct tip, C triangle cantilever), as described in previous reports (Li et al. 2011). Imaging was done with the Nanowizard I AFM (JPK Instruments, Berlin), and analyzed with the JPK SPM software.

To determine changes in the surface energy after laser treatment, water contact measurements were obtained using a self-assembled goniometer consisting of a side-view microscope and camera (Prof Seeram Ramakrishna's lab, NUS) (Nikon, Japan). An automatic dispensing needle (VICI Precision Sampling, CA, USA) released a

single 1 μ l water droplet onto the substrate region tested, and images of the water droplet were immediately obtained. Water contact angles (WCAs) were estimated using the axisymmetric drop-shape analysis profile technique.

2.3 Blood collection

Informed consent from healthy volunteers and breast cancer patient individuals (see **Appendix Tables A1.1-1.4**) were obtained before blood extraction. Patients were participants of four clinical studies, including two neoadjuvant (doxorubicin /cyclophosphamide (AC) with or without Sunitinib and paclitaxel /carboplatin/ lapatinib), one for refractory patients under assorted treatments, and another which involved patients with early-stage breast cancer. All study protocols were approved by the institutional review board and local ethics committee (DSRB Reference 2012 / 00105, 2012 / 00979, 2010 / 00270, 2010 / 00691). Blood samples were collected from healthy volunteers for use in the study (DSRB-2013/00542) as controls for culture or validation of antibody specificity.

For both patients and healthy volunteers, 10 ml of blood was obtained after discarding the first 1 ml of blood collected to avoid contamination by skin fragments. Clinical blood samples were either sampled in a single draw or at different treatment time points. Collected blood was stored in ethylenediaminetetraacetic acid (EDTA) tubes (BD, Franklin Lakes, NJ, USA) at 4 °C prior to use. To retain viability of the cells and prevent coagulation of blood, blood samples were processed within 8 hrs from the time of sampling.

2.4 Maintenance of cancer cell lines

Human breast adenocarcinoma cell lines, MCF-7, SKBR3 and MDA-MB-231

(obtained from American Type Culture Collection (ATCC), were used for initial characterization of the culture assay or to validate antibody specificity. Cells were cultured in T-25 polylysine-coated tissue culture flasks (Falcon Plastics, Oxnard, Calif.) with either Dulbecco's Modified Eagle Medium (DMEM) (Sigma, St. Louis, MO, USA) for MCF-7 or Roswell Park Memorial Institute (RPMI) 1640 (Sigma, St. Louis, MO, USA) for SKBR3 and MDA-MB-231 respectively. Media was supplemented with 10% fetal bovine serum (FBS) and 1% penstrep (penicillin G and streptomycin) (all from Invitrogen, Carlsbad, CA). Fresh media was supplied to the cells every 2 days, and passaged upon close to 80% confluency.

Cancer cell line cultures were detached from the wells with the use of trypsin-EDTA (Gibco, Carlsbad, CA, USA) after being washed with 1× phosphate buffered saline (PBS), and incubated under 37 degrees C for 5 mins. Trypsinised cells were neutralized with the same volume of media (as trypsin) and transferred to a 15 ml falcon tube (Beckon Dickinson, San Jose, CA), which was then centrifuged at 1200 rpm for 3 minutes to concentrate the cells. Concentrated cells were split into 3 new flasks and incubated in the incubator at 37 °C, 5% CO₂ and high humidity.

2.5 Cancer cell line cultures for optimization of assay parameters

Breast cancer cell line SKBR3 was seeded at high concentrations ($>10^6$ cells) into a patterned 60 mm dish with or without surface treatment. Cell counts were carried out with a disposable hemocytometer (iN Cyto, Republic of Korea) and the cell stock was serially diluted till the required amount. Cultures were maintained under conditions suitable for cell lines (37°C, 5% CO₂, high humidity and normoxia).

2.6 Preparation of blood samples for culture

For certain optimization assays, Ficoll-Paque PLUS (GE Healthcare, cat. no. 17-1440-02), a reagent commonly used for separation of blood components, was used as recommended by supplier. For the rest, RBC lysis was done to obtain nucleated cells for culturing. 10 ml of each blood sample was mixed with RBC lysis buffer (1:3 ratio; Life Technologies, Carlsbad, CA) under gentle agitation for a maximum of 5 mins, and centrifuged at 1000 g for 5 mins to concentrate the intact nucleated cells (**Figure 2.2**). Supernatant containing lysed RBC debris and plasma were decanted, and the resultant cell pellet was immediately washed once with PBS. Cell suspension was again centrifuged and eventually resuspended with fresh supplemented DMEM media. In the optimized protocol, the final volume of nucleated cells was split into four portions and seeded into four individual 60 mm patterned dishes for culture.

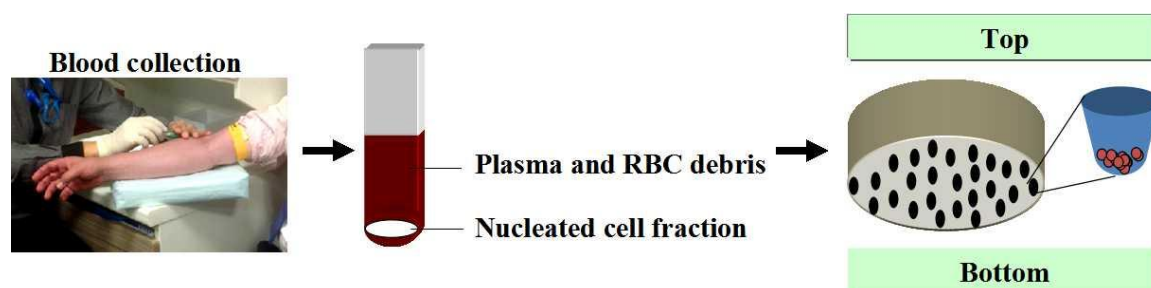


Figure 2.2 Preparatory procedures before culture. Whole blood was collected from healthy volunteers or patients via venipuncture. Collected blood was lysed with RBC lysis buffer to concentrate the nucleated cell fraction, which contained WBCs and CTCs. These cells were seeded onto patterned culture dishes with microwells for culture.

2.7 Primary human CTC culture

Seeded patterned dishes were kept in the humidified incubator maintained at 37 °C in 5% (v/v) CO₂ and 1 % O₂. Fresh media (supplemented DMEM) was introduced every 2 days, and media change was carried out gently at a consistent position of the dish to

reduce turbulence and disturbance to cell clusters. For proliferative cultures, media change intervals could be reduced to every 24hrs. Culture conditions might vary for certain experiments, due to the need for assay optimization (e.g. 21% O₂, normal dishes or RPMI instead of 1% O₂, microwells, or DMEM). During harvesting, clusters were lifted from the microwells with adequate washing (pipetting) with PBS, aided with dissociation using 0.01% trypsin and 5.3 mM EDTA (Lonza, Basel, Switzerland) solution in PBS, under 3 min incubation at 37 °C.

2.8 Cluster formation, imaging and diameter measurements

Viable cultures could be maintained within microwells up to 2 months or further passaged in suspension or gel assays (see **Section 4.2.4**) to form spheroids. Cultures were harvested or imaged with phase contrast microscopy (Nikon, Japan) at Days 8, 14 or 21. Average cluster diameter can be obtained using ImageJ (NIH, Bethesda, MD), by averaging the maximum and minimum length along a single Z plane for each cell aggregate (**Figure 2.3**).

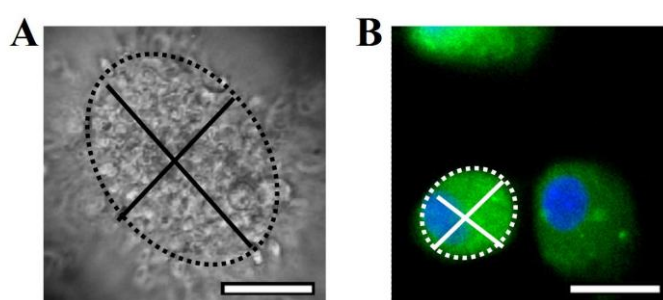


Figure 2.3 Measurement of average diameter for (A) clusters and (B) single cells. The maximum and minimum lengths along a single Z plane for each object were obtained and the average value calculated to get the average diameter values. Scale bar is 50 μm for (A) and 20 μm for (B).

2.9 Flow cytometry to determine proportion of viable cells

Proportion of viable cells was estimated by propidium iodide (PI) (Sigma-Aldrich) staining. Dead cells were stained by PI, leaving live cells unstained. Freshly harvested cells were incubated with PI on ice for 15 mins, washed thoroughly and processed with Accuri C6 (BD bioscience). Cells were gated based on PI expression and the resulted cell counts obtained with a data analysis program (BD CFlow Plus Software (Accuri)).

2.10 Histological staining of size-sorted cultured cells

Histopathological morphology of the cultured cells was observed via standard Papanicolaou (PAP) staining procedures at the Advanced Molecular Pathology Laboratory of Institute of Molecular and Cell Biology (IMCB; Singapore). PAP stain is a cytological technique adopted to distinguish phenotypes of cells via the differential staining of various cellular components.

Staining was done on frosted slides (Thermo Fisher Scientific) containing cytoplots. Cytoplots were concentrated cell spots prepared with 100 μ l of cell suspension (10^4 - 10^5 cells). The cell suspension was added into a Cytospin 4 cytocentrifuge (Thermo Fisher Scientific) and spun via centrifugation at 600 rpm for 5 min, to generate concentrated cell spots.

To better contrast the morphology between cultured cells of different sizes, harvested cultures were first size-sorted by a spiral inertial microfluidic biochip as previously described (Hou et al. 2013). The device allowed the pumping of cell suspension through this microfluidic biochip at $100 \mu\text{l min}^{-1}$ together with the sheath fluid (PBS) to allow separation of cells above $\sim 20 \mu\text{m}$ from the smaller cells. The size-sorting

principle was based on dominant inertial forces in a curvilinear channel, allowing the focusing of particles of varied sizes at different positions within the microchannel, followed by subsequent retrieval at separate outlets. The small and larger cells were cytopun separately onto the slides as described for PAP staining or Diff-QUIK Romanowsky staining (Pathology Department of the National University Hospital, Singapore). Diff-QUIK is another common histological staining method for distinguishing different cell populations, including blood smears.

2.11 Enumeration of putative CTCs

To estimate the amplification of CTCs in culture, cells were sampled at Day 0 before culture and at Days 8, 14 and 21 of culture. The current definition of CTCs (CK+/CD45-/Hoechst+) was used to provide an estimate of the number of CTCs present at each time point (see **Section 1.2**). It is important to note that these counts will be an underestimation of the actual CTC numbers, due to the heterogeneity of cancer cells.

Cytopun slides were prepared and fixed with 4% paraformaldehyde (PFA) (Sigma-Aldrich, St Louis, MO) and incubated at 10 min under room temperature. Fixed cells were permeabilised with 0.1% Triton X-100 (Thermo Fisher Scientific) for 1 min and stained with a cocktail of antibodies targeting cytokeratins 8, 18 and 19 (Pan-cytokeratin) and CD45 (all from Miltenyi Biotec, Auburn (MACS), CA) (diluted at 1:100 with 2% bovine serum albumin (BSA)) for 30 mins under dark conditions. The cell spot was washed extensively to remove unbound antibodies and reduce unspecific binding. Cell nuclei were labeled with Hoechst dye (Invitrogen, Carlsbad, CA). Cytopots were imaged with an upright epifluorescence microscope (Nikon, Japan) to quantify the CK+/CD45-/Hoechst+ cell counts ml^{-1} of blood.

2.12 Immunophenotyping of cell clusters

For direct staining of cell clusters, media was removed gently from the dish and clusters were fixed and permeabilized (as described in **Section 2.12**) directly within the microwells. Permeabilized cell clusters were then incubated with the respective antibody cocktail solution diluted in PBS/2% BSA for at least 2 hrs on ice. For respective dilution factors, refer to (**Tables 2.1 - 2.2**). For non-conjugated antibodies, primary antibodies were added accordingly (**Tables 2.1 - 2.2**) followed by the corresponding secondary Dylight 488 nm or 594 nm antibodies (Abcam, Cambridge, United Kingdom). Stained samples were washed with PBS and imaged under an inverted confocal microscope (Olympus Fluoview FV1000, USA).

Table 2.1 List of primary antibodies targeting MSC-derived cell types, WBCs and endothelial cells.

| Cell type | | Target | Company | Isotype | Specificity | Dilution |
|------------------|----------------|------------------|--------------------------|--------------------------|---------------------------|----------|
| MSC derivatives | Adipocyte | FABP4 | Abcam | IgG (Rabbit) | Mouse, Human | 1 to 250 |
| | Chondrocyte | Aggrecan | Abcam | IgG1 (Mouse) | Cow, Human | 1 to 250 |
| | Osteocyte | Osteocalcin | Abcam | IgG (Rabbit) | Human | 1 to 250 |
| | Cardiomyocytes | Troponin T | Abcam | IgG2b (Mouse) | Mouse, Rabbit, Human etc. | 1 to 250 |
| WBC | Leukocytes | CD45 | MACs | IgG2a (Mouse) | Human | 1:100 |
| | | CD18 | Abcam | IgG (Rabbit) | | 1 to 250 |
| | Macrophages | CD68 | Abcam | IgG ₁ (Mouse) | Mouse, Rat, Human | 1 to 250 |
| | | MIF | Abcam | IgG (Rabbit) | Mouse, Rat | 1 to 250 |
| | Monocytes | CD14 | Abcam | IgG (Goat) | Human | 1 to 250 |
| | | CD16 | Abcam | | | 1 to 250 |
| | Megakaryocytes | Thrombospondin-1 | Abcam | IgM (Mouse) | Cow, Human | 1 to 250 |
| | NK cells | CD56 | Abcam | IgG (Rabbit) | Human | 1 to 250 |
| Platelets | vWF | Abcam | IgG (Rabbit) | Rat, Cow, Human etc. | 1 to 250 | |
| Endothelial cell | CD31 | BD | IgG ₁ (Mouse) | Mouse | 1 to 250 | |

Table 2.2 List of primary antibodies targeting antigens expressed by a variety of stem cells or epithelial cells or mesenchymal cells, including an antibody to decorate actin microfilaments and another for cell proliferation status

| Cell type | | Target | Company | Isotype | Specificity | Dilution |
|------------------|-----------------|------------|--------------|---------------------------|------------------------|----------|
| Stem cells | ESC | Rex1 | Abcam | IgG (Rabbit) | Mouse | 1 to 250 |
| | | SOX2 | Abcam | | Mouse, Rat, Human etc. | 1 to 250 |
| | | OCT4 | Abcam | | Mouse, Rat, Human etc. | 1 to 250 |
| | | NANOG | Abcam | | Mouse, Human, Monkey | 1 to 250 |
| | CSC | CD44 | MACs | IgG1 (Rat) | Human, cow, horse etc. | 1 to 100 |
| | | CD24 | MACs | IgG1 (Rat) | Human, cow, horse etc. | 1 to 100 |
| | MSC | CD90 | Abcam | IgG (Rabbit) | Rat, Human | 1 to 250 |
| | HSC | CD34 | BD | IgG2a, κ (Rat) | Mouse | 1 to 250 |
| | Epithelial cell | E-cadherin | Abcam | IgG1 (Rat) | Mouse, Dog, Human | 1 to 250 |
| | | Pan-CK | MACs | IgG1 (Rat) | Human, cow, horse etc. | 1 to 100 |
| CK 5 | | Abcam | IgG (Rabbit) | Mouse, Human | 1 to 250 | |
| CK 7 | | Abcam | IgG1 (Mouse) | Human | 1 to 250 | |
| CK 8 | | Dako | | | 1 to 250 | |
| CK 18 | | Dako | | | 1 to 250 | |
| CK 19 | | Dako | | | 1 to 250 | |
| EpCAM | | MACs | | | 1 to 100 | |
| Mesenchymal cell | Vimentin | Sigma | IgG1 (Mouse) | Human, chicken, rat etc. | 1 to 250 | |
| Others | Ki67 | Abcam | IgG (Rabbit) | Mouse, Rabbit, Human etc. | 1 to 250 | |

2.13 Characterization of putative CTCs via immunophenotyping of cytopots

Cytopots of cultured cells were stained for 30 min at room temperature, using antibodies listed in **Tables 2.1 and 2.2**. Other cell types, including those of embryonic stem cells (ESCs), MSCs, blood cells (Day 0 nucleated cell portion after RBC lysis),

macrophages, endothelial cells and human breast cancer cell lines (MCF-7 and MDA-MB-231) were utilized accordingly as the relevant controls to determine antibody specificity or to act as a comparison for antigen expression with putative CTCs.

Senescence-associated beta-galactosidase (SA β -gal) activity was investigated in triplicates at pH 6 for the quantification of non-senescent cells. Cells were freshly lifted from the culture dishes, and fixed with 4% PFA for 10 min. Fixed cells were incubated overnight with SA β -gal staining solution adjusted to pH 6. Senescent cells appeared blue-green while non-senescent cells remained unstained.

For quantification of the proportions of residual blood cells, cytopots were prepared with Day 14 samples and stained with the respective antibodies targeting the blood cell antigen. Stained slides were imaged and enumerated to determine percentage of cells positive for the blood cell marker over total cell count (Hoechst positive cells).

2.14 RNA extraction, reverse transcription and Real-Time PCR quantification

Cells were lysed with RLT buffer included in the RNeasy MiniPrep kit (Invitrogen, Carlsbad, CA) according to the manufacturer's instructions. Cell lysates could be frozen at -80°C until further use. Lysates were processed to extract RNA according to the full protocol. RNA concentration was quantified with a NanoDrop Spectrophotometer (Thermo Fisher Scientific). Complementary deoxyribonucleic acid (cDNA) was synthesized from 300 ng of total RNA using the SuperScript™ III First-Strand Synthesis SuperMix for real-time quantitative reverse transcription polymerase chain reaction (qRT-PCR) kit (Invitrogen, Carlsbad, CA), according to recommended protocol and stored at -80°C until required.

Six genes (*ZEB1*, *CD44*, Vimentin (*VIM*), *CD24*, *EPCAM* and E-cadherin (*CDH1*))

were selected to distinguish between epithelial and mesenchymal phenotypes. Subsequently, genes for HIF1- α and SNAIL were used to evaluate mechanisms of CTC proliferation. Beta-actin was used as an endogenous control to normalize data. The primers used in this assay were from 1st Base (Singapore) and the base sequences are provided in **Table 2.3**. Two other genes (CD45 (*PTPRC*) and CD31 (*PECAM1*)) were selected to assess the relative proportion of WBCs and endothelial cells as compared with nucleated blood cells after RBC lysis. qRT-PCR was performed using a 7300 Sequence Detection System (Applied Biosystems, Foster City, CA) with SYBR Green (Invitrogen, Carlsbad, CA). PCR reactions were performed in a 96-well optical plate, with cycle conditions as follows: 95°C for 20 s, then 40 cycles of 95°C for 10 s and 60°C for 20 s. The threshold cycle (CT) was defined as the fractional cycle number at which the fluorescence passes the fixed threshold. CT values were obtained using default threshold settings.

Table 2.3 List of qRT-PCR probes

| Biomarker | Forward strand | Reverse strand |
|-------------------|--|--|
| CK 18 | 5'- GGCATCCAGAACGAGAAGGAG - 3' | 5'- ATTGTCCACAGTATTTGCGAAG A -3' |
| EPCAM | 5'- AATCGTCAATGCCAGTGTACTT- 3' | 5'- TTCATCGCAGTCAGGATCATA A-3' |
| <i>CD44</i> | 5'- CTGCCGCTTTGCAGGTGTA - 3' | 5'- CATTGTGGGCAAGGTGCTATT - 3' |
| <i>CD24</i> | 5'- CTCCTACCCACGCAGATTTATTC -3' | 5'- AGAGTGAGACCACGAAGAGAC - 3' |
| <i>CDH1</i> | 5'- CGAGAGCTACACGTTACGG- 3' | 5'- GGGTGTCGAGGGGAAAATAGG- 3'. |
| <i>ACTB</i> | 5'-GCGAGAAGATGACCCAGATC- 3' | 5'-CCAGTGGTACGGCCAGAGG-3' |
| <i>PECAM1</i> | 5'- AACAGTGTTGACATGAAGAGCC -3' | 5'- TGTA AACAGCACGTCATCCTT- 3' |
| <i>VIM</i> | 5'- GACGCCATCAACACCGAGTT -3' | 5'-CTTTGTCGTTGGTTAGCTGGT- 3' |
| SNAIL | 5'- TCGGAAGCCTAACTACAGCGA- 3' | 5'- AGATGAGCATTGGCAGCGAG - 3' |
| <i>HIF1-alpha</i> | 5'- GAACGTCGAAAAGAAAAGTCTC G -3' | 5'- CCTTATCAAGATGCGAACTCAC A -3' |
| Beta actin | 5'-GCGAGAAGATGACCCAGATC- 3' | 5'-CCAGTGGTACGGCCAGAGG-3' |

2.15 DNA FISH

Freshly prepared cytosspots were fixed with a 400 μ l mixture of acetic acid and methanol (1:3 ratio, Sigma-Aldrich) at room temperature. Fixed slides were dehydrated in a graded ethanol series (80%, 90%, and 100%) using a coplin jar (Wheaton Industries, USA), dried and incubated with 4 mg ml⁻¹ RNase (Sigma-Aldrich) in PBS within the humidified incubator at 37 °C for 45 min. Treated slides were washed thoroughly under shaking conditions with 1 \times PBS/0.2% Tween-20 thrice for 5 mins each, and denatured at 80°C for a maximum of 10 min in 70% formamide/2 \times saline sodium citrate (SSC) (Sigma-Aldrich) solution. Denatured slides were quickly chilled with a second round of graded ethanol series on ice, dried and then hybridized with either one or all of the pre-denatured probes (Spectrum Green or Spectrum Orange) (75°C for 5 min) (**Table 2.4**) overnight at 42 °C, as recommended by the supplier. These slides were sealed by applying rubber cement and kept under dark and humid conditions.

Hybridized slides were washed after 16 hours of incubation with 50% formamide/ 2 \times SSC pre-warmed solution (42 °C) thrice for 5 mins each under shaking conditions. This was then followed with further washing with pre-warmed 2 \times SSC solution (42 °C), and washed slides were counterstained with Hoechst (33342) dye for 1 min. Preservation of the fluorescence signals was done by applying Vectashield® mounting medium (Vector Laboratories, Burlingame, CA) before the glass coverslip was secured (Thermo Fisher Scientific) and sealed with transparent nail polish.

Hybridized slides were imaged with an upright epi-fluorescence microscope at 63X magnification (oil immersion) controlled by Metamorph software. Z-stacks were obtained and processed to get a compressed image (by maximum intensity) using

Image J. Single DNA spot signals were identified by subtraction of background. Proportions of cells displaying signals were compared to total cell count.

Table 2.4 List of DNA FISH probes

| Probes | CCND1 | HER2 | FGFR1 | MYC | TOP2A | ZNF217 | CEN17 |
|-------------|-----------------|----------|-----------------|-----------------|--------|--------|----------|
| Company | Empire Genomics | Kreatech | Empire Genomics | Empire Genomics | Abbott | Abbott | Kreatech |
| Chromophore | Red | Red | Red | Red | Red | Red | Green |

2.16 RNA FISH

The procedure for RNA FISH is similar with that described for DNA FISH. In this project, custom-made probes (**Table 2.5**) were obtained from Affymetrix (iDNA, Santa Clara, CA) and the full procedure was carried out with the Quantigene ViewRNA Cell Assay kit from Affymetrix as recommended. The target genes were selected based on the analysis of various breast cancer expression profiling databases (Akalay et al. 2013, Tan et al. 2014), in which the ones corresponding to either the highest or lowest EMT scores were selected to characterize the cells. Probes targeting epithelial cells were labeled green (488 nm excitation wavelength), while those selective for mesenchymal cells were labeled red (550 nm excitation wavelength). All labeled probes were incubated with a single sample to provide a striking contrast of the EMT phenotype in the sample tested (mostly red spot signals = mesenchymal-associated phenotypes; mostly green-associated phenotypes = epithelial). Washed hybridized slides were counterstained with Hoechst (33342) dye and sealed with transparent nail polish after application of mounting medium.

Hybridized slides were imaged as described in **Section 2.16**. In the case whereby single spots cannot be identified (due to saturation of probes), epithelial cells were

identified as those displaying green signals in the cytoplasm. Cells with intermediate EMT phenotypes will display green cytoplasmic signals with red dot signals.

Table 2.5 List of RNA FISH probes

| Specificity | Probes | Company | Chromophore |
|-------------------|------------|---------|-------------|
| Epithelial cells | E-cadherin | iDNA | Green |
| | TFF1 | iDNA | Green |
| | FOXA1 | iDNA | Green |
| | AGR2 | iDNA | Green |
| | GATA3 | iDNA | Green |
| | CK 7 | iDNA | Green |
| | CK 8 | iDNA | Green |
| | CK 18 | iDNA | Green |
| | CK 19 | iDNA | Green |
| Mesenchymal cells | Fascin | iDNA | Red |
| | Vimentin | iDNA | Red |
| | PTX3 | iDNA | Red |
| | SERPIN2 | iDNA | Red |

2.17 Validating presence of residual macrophages with a phagocytosis assay

Day 14 cultures were introduced evenly with high concentrations of fluorescein-labeled polystyrene microbeads (1 μ m; Roche Applied Science) and incubated overnight under optimal culture conditions. After incubation, excess microbeads were removed by gentle washing with PBS, followed by fixation and imaging as previously described with confocal microscopy (**Section 2.13**).

2.18 Establishment of spheroids from cultured CTCs

Day 14 cultures were passaged with trypsin-EDTA as described (**Section 2.4**), followed by seeding into 3D Geltrex® (Invitrogen, cat. no. 12760-013) within wells of 16-well glass chamber slides (Lab-Tek Products, Miles Laboratories, Naperville, IL) or 48-well plate chambers. Dissociated cells could also be cultured in 2D ultra-low adhesive dishes (Cat No; 3473 or 3473; Corning Inc., Corning, NY). Passaged samples were allowed to proliferate under optimal conditions for another week, fixed

then stained with either Tetramethylrhodamine (TRITC) -phalloidin (Dilution 1:1000, Sigma) or CK/CD45, coupled with Hoechst counterstaining. To trigger spheroid formation for established cultures, passaged cells were maintained with advanced DMEM/F12, reduced-serum medium (Ratio 1:1) (Gibco, Life Technologies, Carlsbad, CA) under normoxia, and could be passaged up to 5-6 times.

2.19 Invadopodia assay and phalloidin staining

Cultures were harvested and added (density of $\sim 10^4$ cells per well) to a thin layer of FITC-labeled gelatin in 8-well glass bottomed Lab-Tek (Nunc, Thermo Scientific) chamber slides. Cancer cell lines were handled separately in the same manner as a control. Gel matrix was obtained from the QCM Gelatin Invadopodia Assay Green (Millipore) kit. Seeded samples were incubated overnight and then fixed with 4% PFA, permeabilized and stained with phalloidin-rhodamine (Invitrogen) for 2 hrs. Stained samples were counterstained with Hoechst dye for 15 mins. Samples were imaged at 20X using an inverted confocal microscope (Olympus Fluoview FV1000, USA) and representative images were analyzed with ImageJ. Cell count and area of degraded matrix were obtained and contrasted for each sample.

2.20 Western blot

Samples were lysed within the dish with cold RIPA buffer from the NE-PER Nuclear and Cytoplasmic Protein Extraction Reagent kit (Pierce, Rockford, IL, USA). The protein concentration was compared to protein standards and estimated with components from the Bradford Protein Assay Kit (Bio-Rad). Purified protein was extracted and 20-50 μg of protein was processed with sodium dodecyl sulfate polyacrylamide gel electrophoresis (SDS-PAGE), transferred electrophoretically to

nitrocellulose membrane (Millipore Corp., MA, USA). Membranes were blocked with 5% milk for an hour then incubated with the respective antibodies overnight. This was followed by washing and further incubation for 1 hr at 25 °C with horseradish peroxidase (HRP) -tagged secondary antibody (GE Healthcare), before imaging (VersaDoc imaging system; Bio-Rad, Hercules, CA). Beta-actin protein level was similarly detected to confirm equal loading.

2.21 Cell cycle analysis

Harvested cells were fixed with cold 70% ethanol, treated with 10 µg ml⁻¹ RNase A (30 min at 37 °C) and incubated with PI for 30 min at room temperature. Stained cells were washed thoroughly and processed in a flow cytometer (LSRII; Becton Dickinson, Heidelberg, Germany). Analysis were done with a FL2-A (585/40) filter. To estimate the positions of G0/G1, S and G2 on the charts, a cancer cell line with known polyploidy (MDA-MB-231) was processed in a similar manner as a form of control. An event count of 10000 was used for all experiments.

2.22 Statistical analysis

The χ^2 (chi) test was used to access any associations between various variables (Table 5.1) with microwell cell cluster formation. For larger sample sets, verification was done with a two-way analysis of variance (ANOVA) for the two independent variables (culture positivity and patient survival status) (Finak et al.). 95% confidence intervals were determined. Adjusted multivariate analyses for continuous independent variables (to other variables) require larger sample sizes and were not utilized in this study. Further Cox regression (investigation of multiple variables) was also not carried out due to the small sample size. Based on previous studies, the minimum

number of cases required for a Cox regression analysis is 100 (Peduzzi et al. 1995).

Chapter 3: Microwell-based Culture and Expansion of Viable CTCs

3.1 Optimization of culture conditions

3.1.1 Microwell dimensions and surface treatment

Microwells were generated on uncoated dishes with a laser ablation technique, which provided the speed of fabrication (one 60 mm dish in ~20 mins) and the versatility of varying microwell dimensions for optimization. The microwell size could be varied with laser power, speed of ablation and focal plane (distance of laser from substrate) used during ablation (**Figure 3.1A**).

An invasive breast cancer cell line of enhanced spheroid-forming capability (SKBR3) was used for these optimization experiments. Small microwells of average 50 μm inner diameter were initially generated (using long focal length and low power), with negligible layer of recast (**Figure 3.1B (left; main and insert)**). However, these 50 μm wells were too small and shallow to capture and retain seeded cells after media changes (disturbance and removal during media change). This is similar for large and wide wells of average inner diameter 341.5 μm (**Figure 3.1B**) (using minimal focal length possible and high power). Hence, microwells of intermediate sizes are required. Since it is difficult to fine-tune the focal plane quantitatively (to obtain microwells of intermediate sizes), the focal distance was fixed at the minimal distance possible for the laser to be positioned away from the substrate.

Microwells of intermediate sizes were then fabricated by variation of laser power and ablation speed (**Figure 3.1C**). Higher power percentage and lower speed percentage values for the laser were desired to obtain deeper microwells, as the percentage of laser power correlates positively with depth, and the percentage of speed correlates negatively with depth. Deeper wells serve to reduce the disturbance of non-adherent

cultures in microwells during handling.

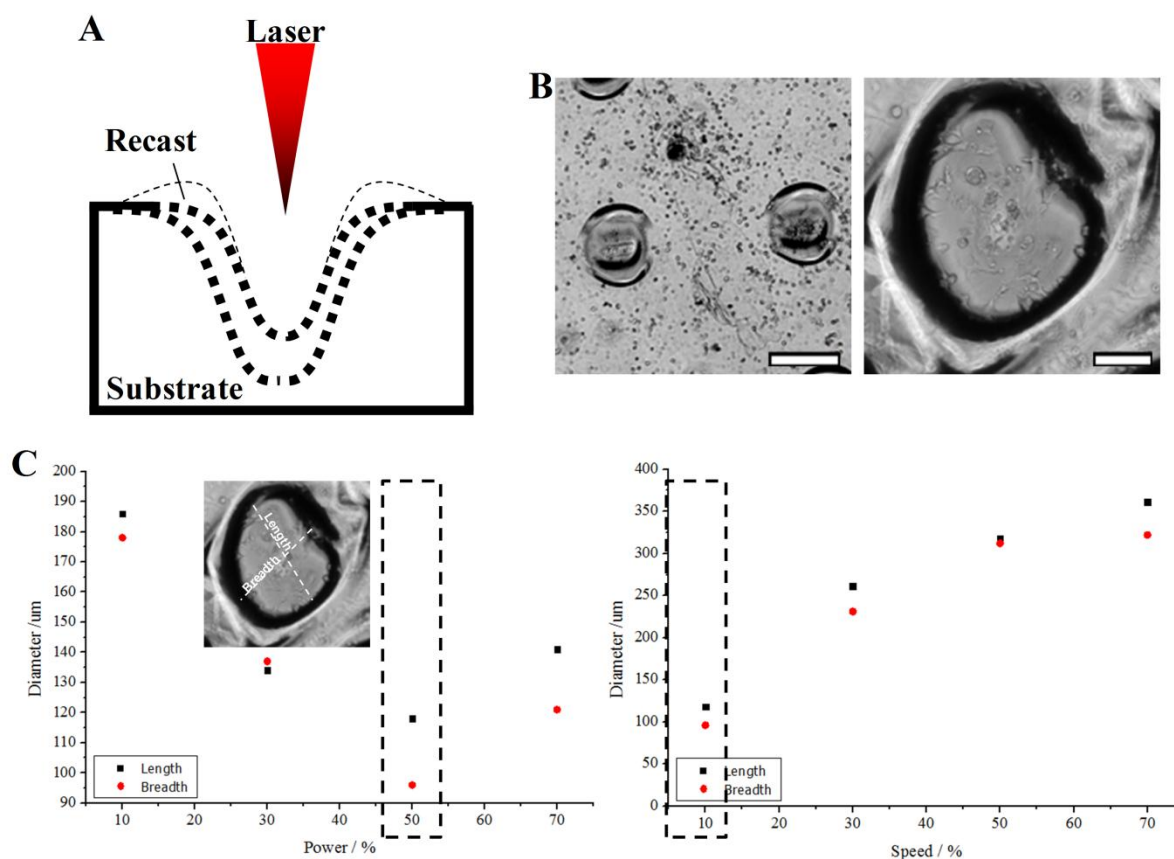


Figure 3.1 Optimization of microwell fabrication. (A) Schematics illustrating the formation of a microwell. The distance of the laser from the substrate, speed of laser ablation as well as laser power affects the depth and width of microwell formed. The higher the laser power, the deeper and wider the resultant microwell becomes. The layer of recast is an artifact generated by the laser process, which becomes prominent with stronger laser power. (B) Phase contrast images of the smallest (left; average inner diameter 50 μm; Scale bar is 50 μm) and largest possible microwell that can be fabricated (right; average inner diameter 341.5 μm; Scale bar is 100 μm.) (C) (Left) Microwells of different dimensions can be created by varying laser power and ablation speed. Average inner diameter of the microwells was obtained by averaging the length and breadth dimensions as shown in insert of left image. 50% power (when speed is standardized at 10%) yields the smallest microwells. (Right) 10% speed (when power is standardized at 50%) yields the smallest microwells. Focal plane is fixed to the minimal possible distance of the laser away from substrate.

With an uncoated substrate, most SKBR3 cells were washed away from the larger microwells (~341.5 μm), while a majority of cells were retained in the smaller microwells (~107 μm and 187.5 μm) (**Figure 3.2A**). Coating of surfactants (e.g. 5%

BSA or pluronic acid) reduced cell-substrate interaction, thus preventing any degree of adhesion of cell lines and indirectly promoting formation of cell aggregates or spheroids in smaller microwells (~107 μm and 187.5 μm). Spheroid formation was more apparent in microwells of average inner diameter ~187.5 μm , possibly due to the higher amount of cells captured in wells. For larger microwell dimensions (~341.5 μm), only a high seeding cell density ($>50 \times 10^6$ cells), used in addition to surfactant treatment, would result in cluster formation. However, the surfactant coating effect was temporary, and spheroids obtained from cell line cultures would start to disperse after three days in culture (**Figure 3.2B**).

Using microwells of ~187.5 μm in inner diameter, clinical samples containing putative CTCs were processed and seeded for culture under conditions recommended for the proliferation of CSCs (1% hypoxia) (Heddleston et al. 2009, Soeda et al. 2009). It was observed that the resultant clusters from clinical samples did not behave like spheroids generated from robust cell lines. Clusters obtained from blood samples were loose clusters, unlike tightly packed aggregates or spheroids (**Figure 3.2C**). Surfactant treatment was also not required for cluster formation from clinical samples, due to the lower adhesive capability of cells from the clinical samples. Since blood samples were likely to require longer culture periods to obtain clusters, surfactants cannot be opted for use in the protocol. This section determined that non-coated microwells of ~187.5 μm in inner diameter, fabricated at 10% speed and 50% laser power, should be utilized for subsequent experiments.

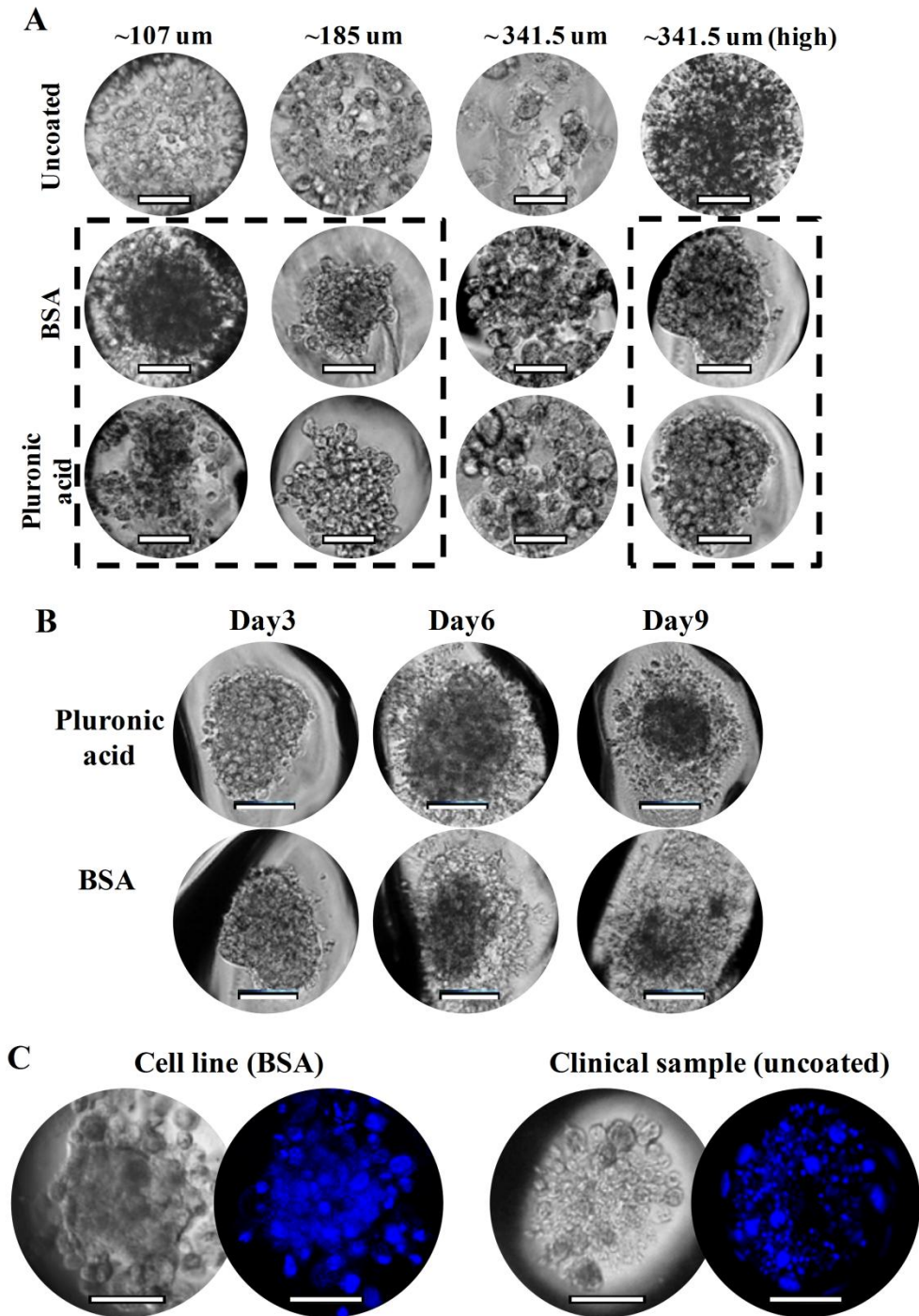


Figure 3.2 Optimization of assay parameters with SKBR3 breast cancer cell line. Images were obtained with a 20X objective lens. (A) Phase contrast images of SKBR3 cells seeded into wells of different average diameters ($\sim 107 \mu\text{m}$ and $187.5 \mu\text{m}$ and $341.5 \mu\text{m}$). Surfactants (5% BSA and pluronic acid) were used to treat patterned substrates respectively. Scale bar is $50 \mu\text{m}$. (B) Surfactant treatments of substrates is temporary, and spheroids of cell lines cultured in microwells dispersed after three days in culture. Scale bar is $50 \mu\text{m}$. (C) Clinical samples can form loose clusters with microwells of $187.5 \mu\text{m}$ diameter in the absence of surfactant treatment. Scale bar is $50 \mu\text{m}$.

3.1.2 Characterization of microwell surface chemistry

The patterned dish was characterized to determine changes in the substrate biochemistry induced by laser ablation. The effects of substrate roughness (induced by even nano-topographies) on cell proliferation and migration have been disputed (Biggs et al. 2010, Nikkhah et al. 2012), but some studies report weakened cell-substrate adhesion and heightened proliferation of cells on substrates exposed to laser (Hao et al. 2005).

AFM was first utilized to trace the roughness of the substrate surface near and away from the laser-ablated regions, and graphical representations of the substrate surface were constructed accordingly (**Figure 3.3A**). The regions nearer to the microwells were found to be significantly rougher than those further from the laser-ablated regions (**Figure 3.3B**, $p < 0.05$). Using WCA estimates, it was found that the regions nearer to the microwell had increased contact angles, demonstrating higher hydrophobicity (**Figure 3.3C**). The combination of high hydrophobicity and roughness may promote protein adsorption and increased cell-substrate interactions (Lampin et al. 1997, Mager et al. 2011), possibly aiding the initial clustering of cells within the microwell regions and reducing loss of target cells to the non-microwell regions (**Figure 3.3D**).

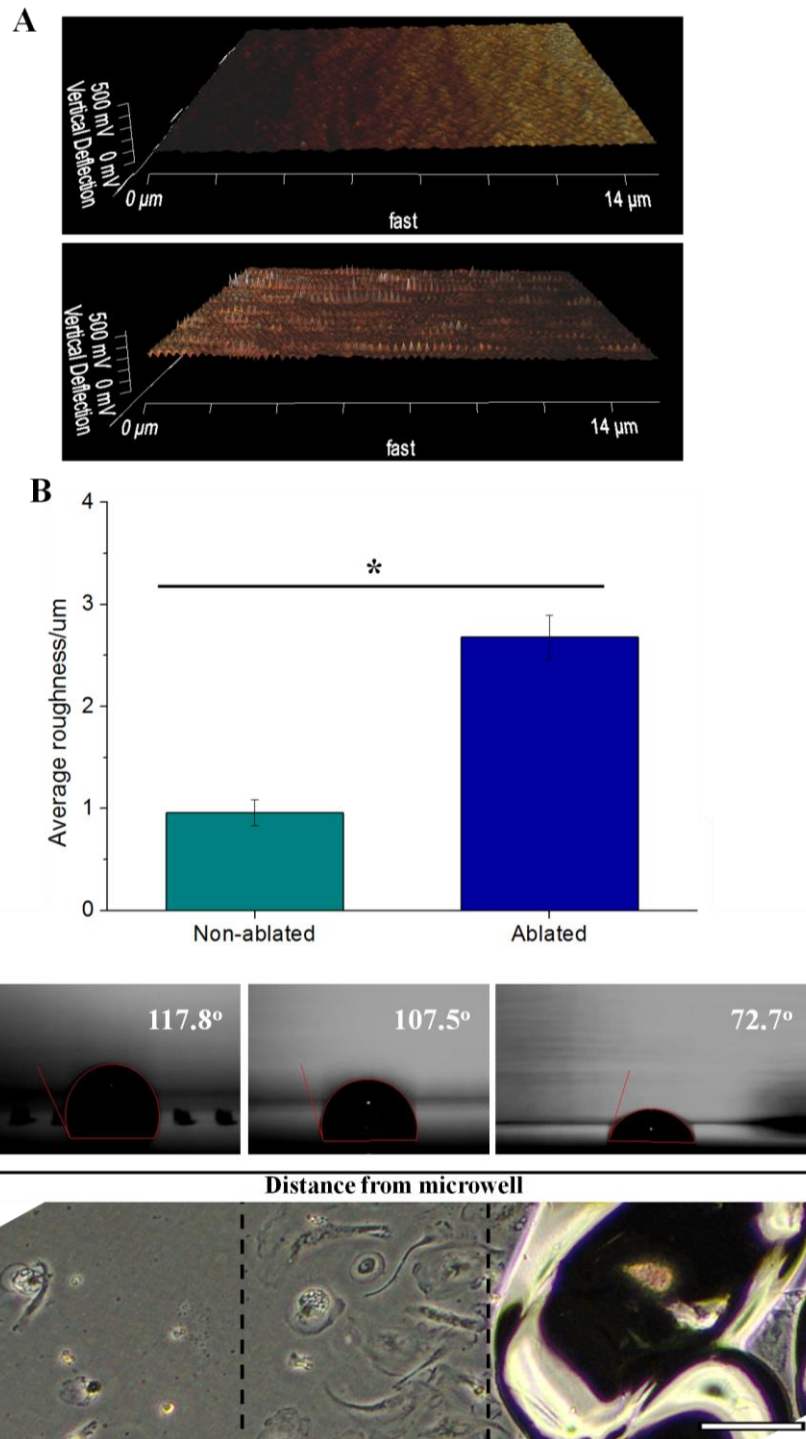


Figure 3.3 Characterization of laser-ablated surfaces to determine changes in surface chemistry. (A) Image reconstruction of the substrate surface after scanning with AFM on contact mode in air. (B) Graphical representation demonstrating the significant increase of average roughness for laser-ablated regions as compared to non-ablated regions. Single asterisk indicates $P < 0.05$ as compared to average roughness of non-ablated regions. All error bars represent standard deviation (SD) of triplicates. (C) WCA estimates for regions adjacent to or away from microwell regions (above). Cells seeded in a patterned dish tend to collect in regions within and surrounding the microwells, as compared to regions further away from the microwell (below) Scale bar is 100 μm .

3.1.3 Culture preparation and maintenance

3.1.3.1 Length of culture period

To establish the optimal length of culture period, clinical samples (10 ml separated equally into four 60 mm patterned dishes) were harvested at Day 0, 8, 14 and 21 to determine the proportion of proliferative putative CTCs using proliferation marker Ki-67 (**Figure 3.4A**). Proportion of Ki67+/CD45- cells increased with culture, being highest at Day 14 (27.7%), which is at a proportion comparable to that of most cell lines and breast tumors (~20%) (Zabaglo et al. 2003, Rhodes et al. 2010, Machowska et al. 2014).

To determine if this time point corresponded to the highest proportion of putative CTCs, immunostaining of CK+/CD45- cells were carried out with cytopots prepared from either Day 0 (RBC-lysed nucleated cells) or Day 8, 14 and 21 cultured cells. Small CK+/CD45- cell counts with respect to total cell counts increased in culture over time (**Figure 3.4B**), especially from Day 0 to Day 8 and Day 14 in culture.

The proportion of Small CK+/CD45- cells beyond Day 14 was observed for most samples (70%, n=10) (**Figure 3.4C**). This could be due to decreased CK expression after EMT, and the proportion of EMT phenotypes may vary with cancer type (see **Section 4.2**). Since the time-point with highest CK+/CD45- proportion for most samples correlated with the highest number of Ki67+ cells, thus subsequent cultures were harvested at Day 14 for characterization.

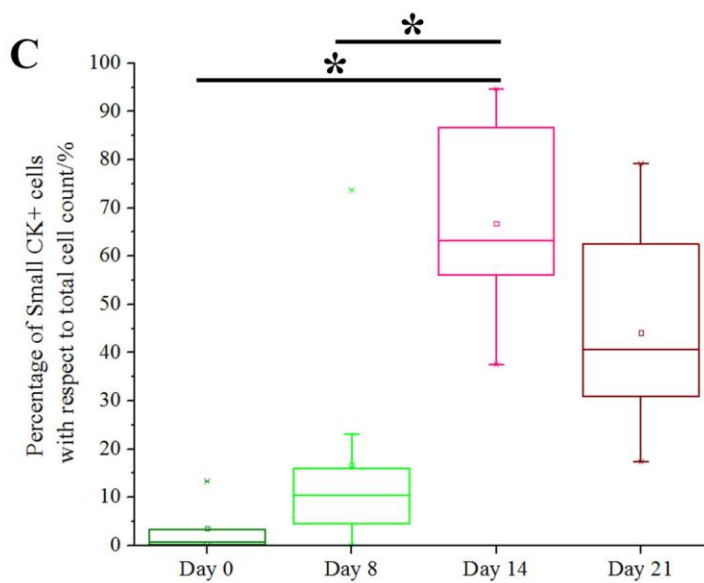
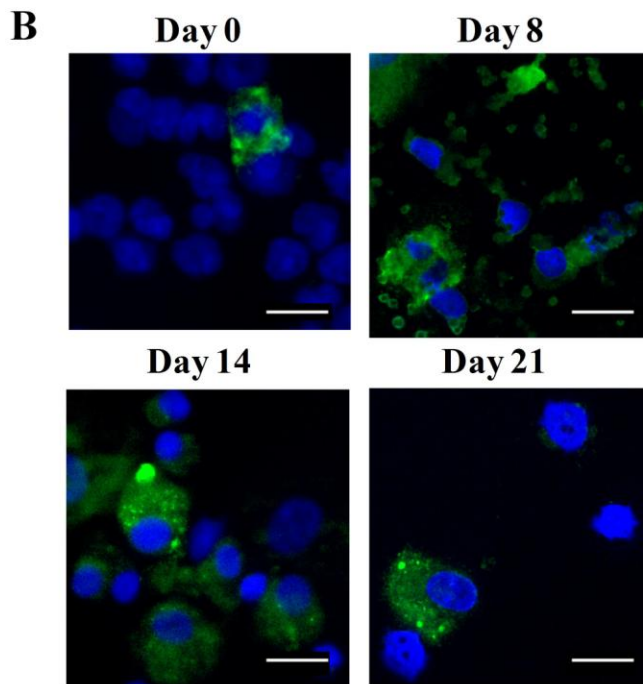
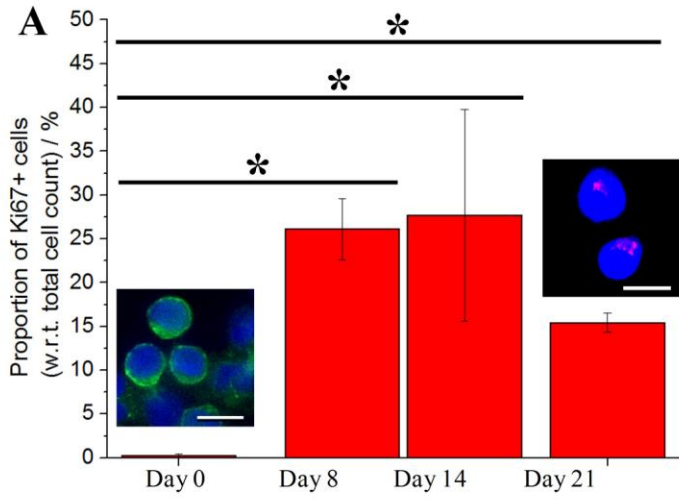


Figure 3.4 Determining time point for culture characterization. (A) Staining of proliferation-associated marker, Ki67 at pH 6, for cultures of clinical samples. Proportion of Ki67+/CD45- cells for cultures at different time points (Day 0, 8, 14 and 21) were shown. Representative images of cells stained with CD45- Fluorescein isothiocyanate (FITC), Ki67-Alexa Fluor 628 and Hoechst are embedded in top left and right boxes respectively. Scale bar is 20 μm . All error bars represent standard deviation (SD) of triplicates. Single asterisk indicates $P < 0.01$. (B) Representative images of cells harvested at different culture time points (Day 0, 8, 14 and 21) and stained with pan-cytokeratin antibodies targeting CK8, 18 and 19. Scale bar, 20 μm . (C) Percentage of Small CK+ cells (15–25 μm) with respect to total cell count (Hoechst+) at various time points (Days 0, 8, 14 and 21). Significant expansion of CK+ cells can be observed by Day 14. Single asterisk indicates $P < 0.01$.

3.1.3.2 Preparation of nucleated cell fraction

Nucleated cells can be obtained from blood samples either after Ficoll gradient centrifugation (Martin-Ramirez et al. 2012) or RBC lysis (Khoo et al. 2014). To determine which procedure is more suitable for the cultures of clinical samples, samples were split into two equal portions and cultured after Ficoll Paque reagent treatment or RBC lysis buffer processing. Samples processed with RBC lysis yielded larger clusters than Ficoll-Paque processed samples (possibly due to lower cell loss) (Average cluster diameter of samples after Ficoll-Paque processing = $52.1 \pm 7.5 \mu\text{m}$; Average cluster diameter of samples after RBC lysis processing = $85.4 \pm 17.5 \mu\text{m}$; $n = 3$ each) (**Figure 3.5A**), and the resultant cell counts were also lower in cultures obtained after Ficoll-Paque processing (Ficoll-processed to lysis-processed: 0.7:1; **Figure 3.5B**). There was also no significant difference in the proportion of residual white blood cell portion (CK-/CD45+) cells observed (**Figure 3.5C-D**).

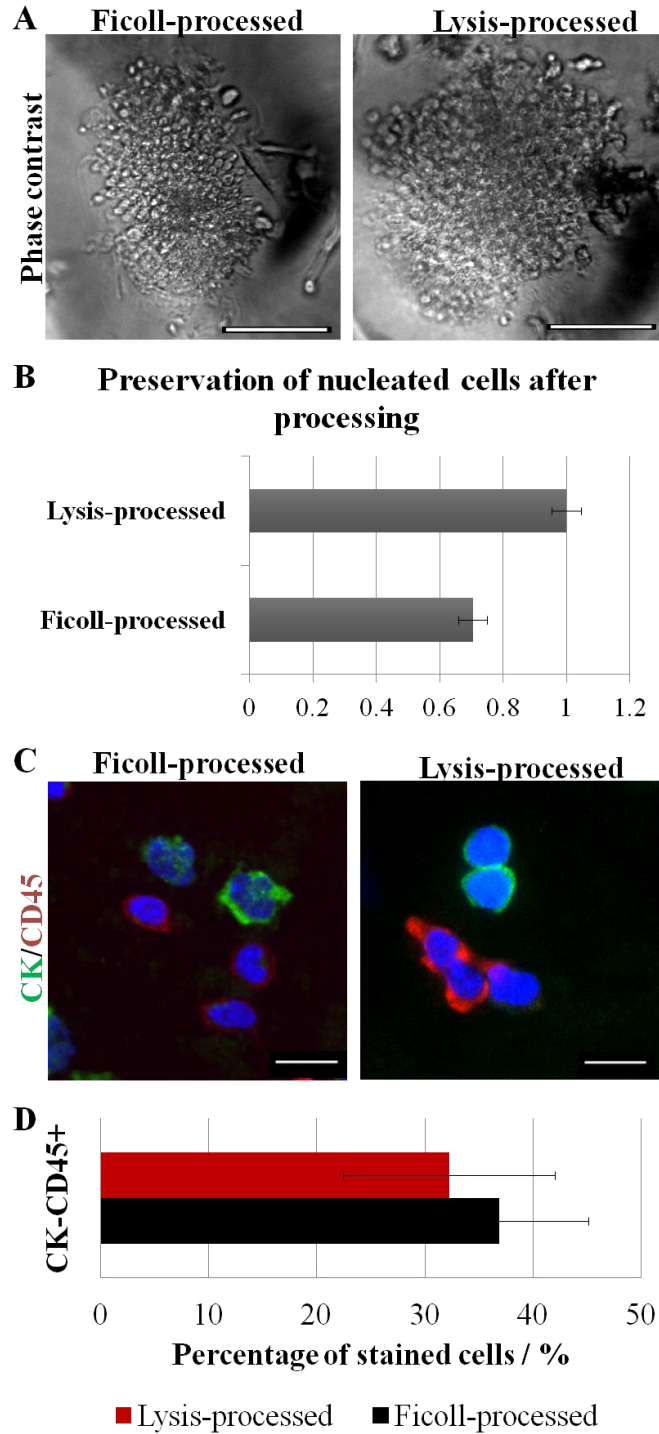


Figure 3.5 Optimization of pre-processing procedure to obtain nucleated cells for culture. (A) Blood samples were processed with either Ficoll-Paque reagent or RBC lysis buffer, and then cultured for two weeks. Heightened cell loss was observed with the Ficoll Paque technique, leading to smaller clusters. Scale bar is 50 μ m. (B) Graphic representation of the cell count after culture, normalized to the cell count of cultures obtained with lysis buffer. All error bars represent standard deviation (SD) of triplicates. (C) No significant difference in the presence and proportion of residual CK-CD45⁺ (white blood cell) cells was observed. Scale bar is 20 μ m. (D) Graphical representation of proportion of residual CK-CD45⁺ portion. All error bars represent standard deviation (SD) of triplicate cultures from the same sample.

3.1.3.3 Culture media and incubator conditions

Cultures of clinical samples were maintained with a range of different media to determine the influence of different components on CK⁺ and CD45⁺ proportions. A series of samples were split and separately cultured with growth factor Il6 (at 10ng/ml or 20mg/ml), conditioned media (from endothelial cell, MSC or WBC) or RPMI medium. Resultant cell cultures at Day 14 were stained for various markers associated with epithelial cancer types (CK) or leukocytes (CD45) and their proportions were normalized with those obtained from cultures maintained with DMEM media (**Figure 3.6A**). Overall, there was some reduction in the CD45⁺ cell counts in cultures maintained with conditioned media or Il6-supplemented media, as compared to those in DMEM. However, these differences were not significant (P value = 0.104578, 0.9-1.2 fold change). Hence, DMEM media was continued for use in subsequent cultures.

To determine the importance of microwells (W) and hypoxia (H) for promoting putative CTC expansion from clinical samples, blood samples were split into different dishes and maintained under varying conditions. Day 14 cultures were harvested and stained with pan-CK, CD45 and Hoechst. Blood cells (CK⁻/CD45⁺) were present in all four conditions, but the H+W⁺ condition yielded the highest proportion of putative CTCs (CK⁺/CD45⁻ cells) (**Figure 3.6B-C**). CK⁺/CD45⁺ cells were also found in all conditions, and were later found to comprise mainly of reactive leukocytes or macrophages (see **Figure 3.12**). Multilayered clusters were only formed under the H+W⁺ condition. Few cells were retained in cultures maintained with H⁻/W⁻, and only a monolayer of CK⁺CD45⁺ or CK⁻CD45⁺ cells were found in the microwells under normoxia (residual blood cells) (**Figure 3.6D**). These demonstrated that both hypoxia and microwells were required for establishing multilayered clusters comprising of CK⁺/CD45⁻ putative CTCs.

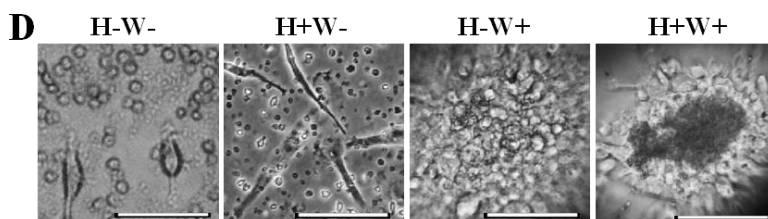
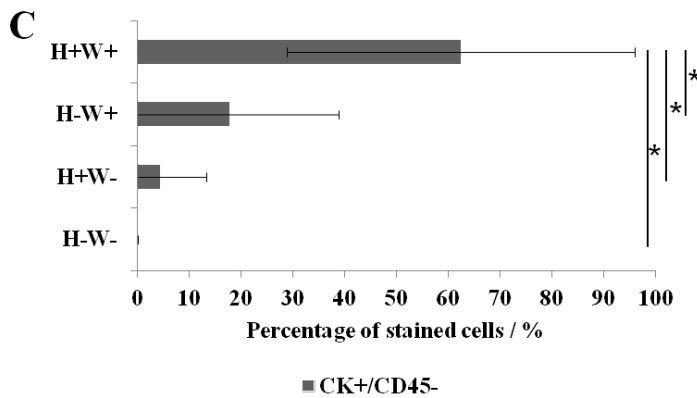
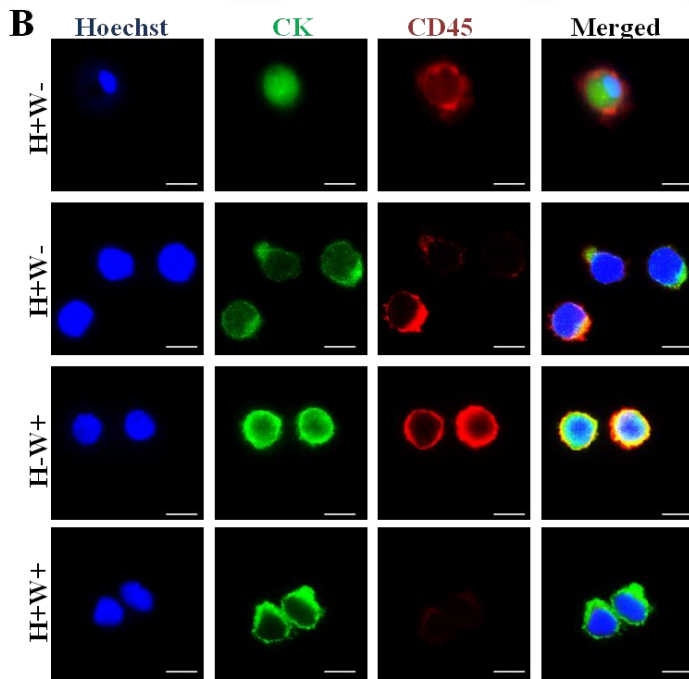
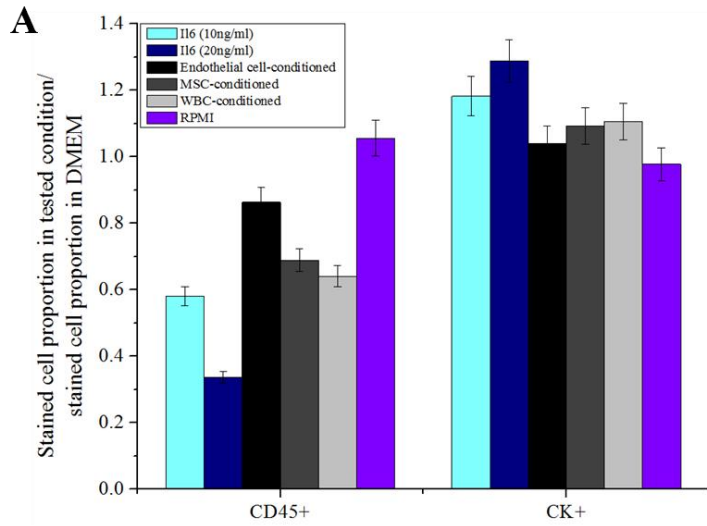


Figure 3.6 Determination of media and incubator conditions for putative CTC culture. H: Hypoxia (1% O₂) and W: Microwells. (A) Representative graph demonstrating the proportions of putative CTCs (CK+/CD45- cells) and leukocytes (CD45+ cells). CD45+ cell counts were reduced in conditioned media as well as Il6-supplemented media. However, the differences were not significant. All error bars represent standard deviation (SD) of triplicates. (B) Representative images of pan-CK-FITC/CD45-APC stained cells from cultures maintained under different conditions. Cells from cultures maintained under H-W-, H-W+ or H+W- conditions had CK+/CD45+ cells, but there were likely to be blood cells such as reactive leukocytes or macrophages. These cells formed only a minority proportion in H+W+ cultures (not shown). Scale bar is 20 μm. (C) Representative bar chart demonstrating the proportion of putative CTCs (CK+/CD45-) after culture under different conditions. All error bars represent standard deviation (SD) of culture triplicates obtained from different samples. Asterisks indicate p < 0.05. (D) Phase contrast images of Day 14 cultures under different culture conditions. Multilayered clusters were only formed in the presence of microwells under hypoxia. In microwells under normoxia, only a loose monolayer of cells (possibly blood cells) was found. No clusters were obtained under H-/W- condition. Scale bar is 50 μm.

To determine the volume of blood that should be cultured in each 60 mm patterned dish, six samples obtained from advanced metastatic breast cancer patients before treatment were cultured in patterned dishes to determine the volume threshold required for the detection of a positive sample. Smaller dishes (35 mm) were utilized for these experiments to enable the same sample to be used while comparing different parameters.

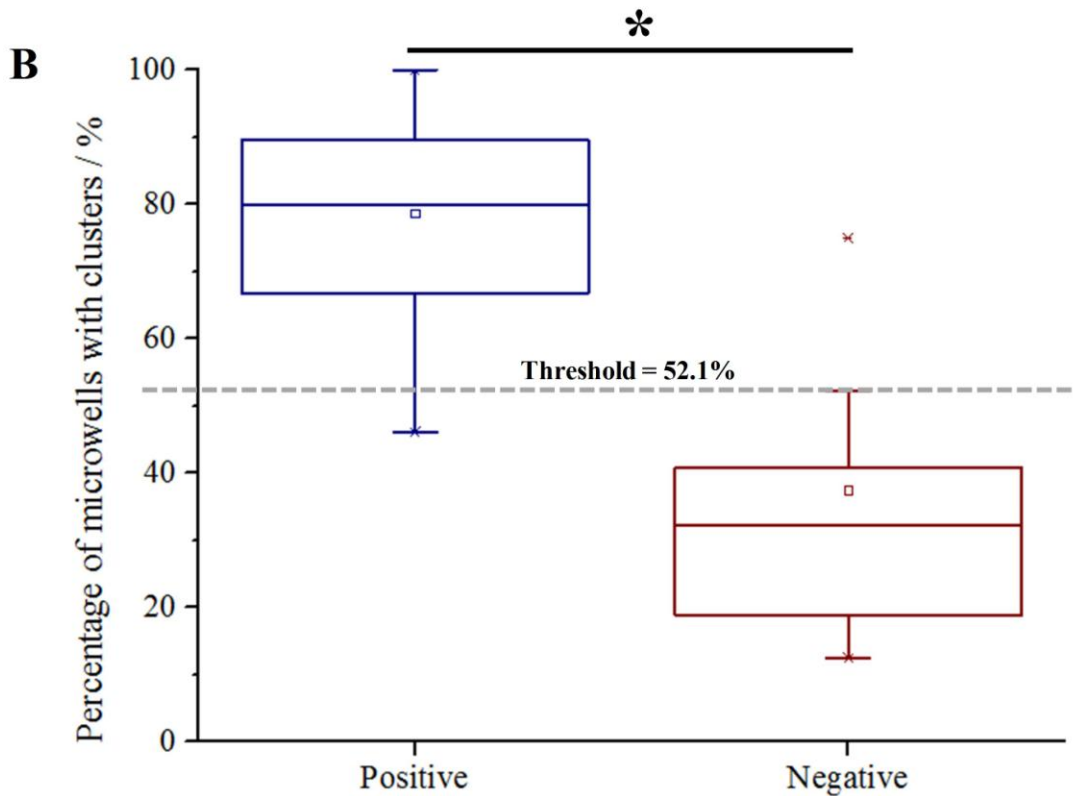
Different volumes of each sample (0.6-1.5 ml) were added to the dishes with ~ 9 cm² surface area. Proportion of microwells with clusters obtained from each sample were tabulated (**Figure 3.7A**). As a preliminary screening, samples with cluster formation in ≥50% of ten microwells for 3 out of 4 of sample volume used were regarded as positive. The proportion of clusters present in positive (≥50%) and negative (<50%) samples was then compared with more elaborate quantification (n=120). Analysis of the median values of overall cluster formation proportion in positive and negative samples provided confirmation that a threshold of ≥50% (Median of positive samples = 72.0%; Median of negative samples = 23.1%; Average of median values from

positive and negative samples = 52.1%) could be used to quantitatively distinguish between positive and negative samples (**Figure 3.7B**).

To evaluate the volume of blood required per cm^2 of culture substrate, the rate of false positives from negative samples and false negatives from positive samples (using the threshold of $\geq 50\%$) obtained from cultures established with different blood volumes were tabulated. Samples obtained from 1 ml sample correspond to the minimal number of false positives and false negatives. Hence, it was established that the minimum volume of patient blood required to correctly evaluate a sample was 1 ml per 9 cm^2 , which corresponds to ~ 2.3 ml of blood for a patterned 60 mm dish (**Figure 3.7C**). For all subsequent experiments, 10 ml of clinical blood sample were separated and cultured in four 60 mm patterned dishes (2.5 ml each).

A

| | Cultured sample 1/% | Cultured sample 2/% | Cultured sample 3/% | Cultured sample 4/% | Cultured sample 5/% | Cultured sample 6/% |
|-------|---------------------|---------------------|---------------------|---------------------|---------------------|---------------------|
| 1.5ml | 100 | 52.3 | 80 | 94.7 | 75 | 89.6 |
| 1ml | 100 | 40.8 | 73.9 | 88.6 | 36.5 | 70.1 |
| 0.8ml | 100 | 32.2 | 69.6 | 84.2 | 32 | 65.8 |
| 0.6ml | 66.7 | 18.9 | 50.1 | 80.6 | 12.5 | 46.1 |



C

| Proportion of microwells with clusters/% | 1.5ml | | 1ml | | 0.8ml | | 0.6ml | |
|--|-----------------|----------------|-----------------|----------------|-----------------|----------------|-----------------|----------------|
| | False positives | False negative | False positives | False negative | False positives | False negative | False positives | False negative |
| 72.0 | 0.5 | 0 | 0 | -0.25 | 0 | -0.5 | 0 | -0.75 |
| 52.1 | 1 | 0 | 0 | 0 | 0 | 0 | 0 | -0.5 |
| 32.1 | 1 | 0 | 1 | 0 | 0.5 | 0 | 0 | 0 |

Figure 3.7 Estimation of the minimal sample volume required for clinical sample culture. (A) Proportion of microwells with clusters. Samples with cluster formation in less than 50% of microwells using most volume amounts (3 out of 4) were considered negative. (B) Confirmation of threshold (Average of median values from positive and negative samples = 52.1%) using a box plot. Median of positive samples = 72.0%. Median of negative samples = 32.1%. Single asterisk indicates $P < 0.01$. (C) Table listing false positives from negative samples and false negatives from positive samples. Samples obtained from 1 ml sample correspond to the minimal number of false positives and false negatives. Single asterisk indicates $P < 0.01$.

Section 3.1.4 Section Summary and Discussion

Section 3.1 described the optimization of culture conditions using either breast cancer cell lines and clinical samples (**Figure 3.8**). Various microwell dimensions and substrate surface treatments were explored, and preliminary characterization of the microwell surface chemistry was carried out. Culture preparation procedures, mainly the length of culture, pre-preparation steps and incubation conditions were optimized directly with clinical samples.

One of the critical issues of cultures involving clusters or aggregates is the possibility of cell necrosis due to the inability of oxygen penetration into the depth of the aggregate (Hirschhaeuser et al. 2010). In this project, a reduction of the proportion of Small CK+/CD45- cells beyond Day 14 was observed for most samples (70%, n=10) (**Figure 3.4C**). According to prior reports on hepatocyte spheroid cultures, the maximum threshold of spheroid diameter to maintain viability is ~100–150 μm (Curcio et al. 2007). The clusters obtained with the microwell assay described in this project mostly ranged within 30-100 μm (see **Figure 3.13**), hence cell necrosis due to lack of oxygen penetration might not be a dominant factor. However, it is possible that this phenomenon will be observable in more proliferative cultures generating larger or tighter clusters.

On the other hand, induction of EMT by hypoxia via Notch signaling has been suggested by various findings (Sahlgren et al. 2008, Chen et al. 2010). qRT-PCR analysis of the microwell-based cultures similarly revealed significant gene expression increase of hypoxia-inducible factor 1 (HIF-1 α) and SNAIL-1, both of which are downstream components of the Notch pathway (see **Figure 4.10A**). Hence

reduction of CK⁺/CD45⁻ cell portion could be due to induction of EMT.

Ki-67 is a marker that closely correlates with proliferation (Urruticoechea et al. 2005). In this study, proportion of Ki67⁺/CD45⁻ cells increased with culture, being highest at Day 14 (27.7%). As the cultures were subsequently harvested for other downstream analysis (including further proliferation as spheroids), it is desirable to select a time point where the cultures were most proliferative.

The time-point with the highest Ki-67⁺ cell portion coincides with the time point with highest CK⁺/CD45⁻ proportion. Since the current consensus defines CTCs as nucleated cells that express epithelial markers (e.g. Cytokeratin (CK)), maximum CK⁺ cell portion was used as a gauge to determine the time point with the highest amount of putative CTCs in culture. It is noteworthy to mention that this definition is now known to be inadequate for cancer cell identification, and hence might not reflect the time point with the highest amount of total CTCs (epithelial or mesenchymal).

After optimization, 10 ml of clinical blood sample were cultured in four 60 mm non-coated patterned dishes comprising of ~187.5 μm microwells in inner diameter to culture for all subsequent samples. Cultures were maintained under hypoxia to establish multilayered clusters comprising of CK⁺/CD45⁻ putative CTCs, and evaluated at Day 14 of culture.

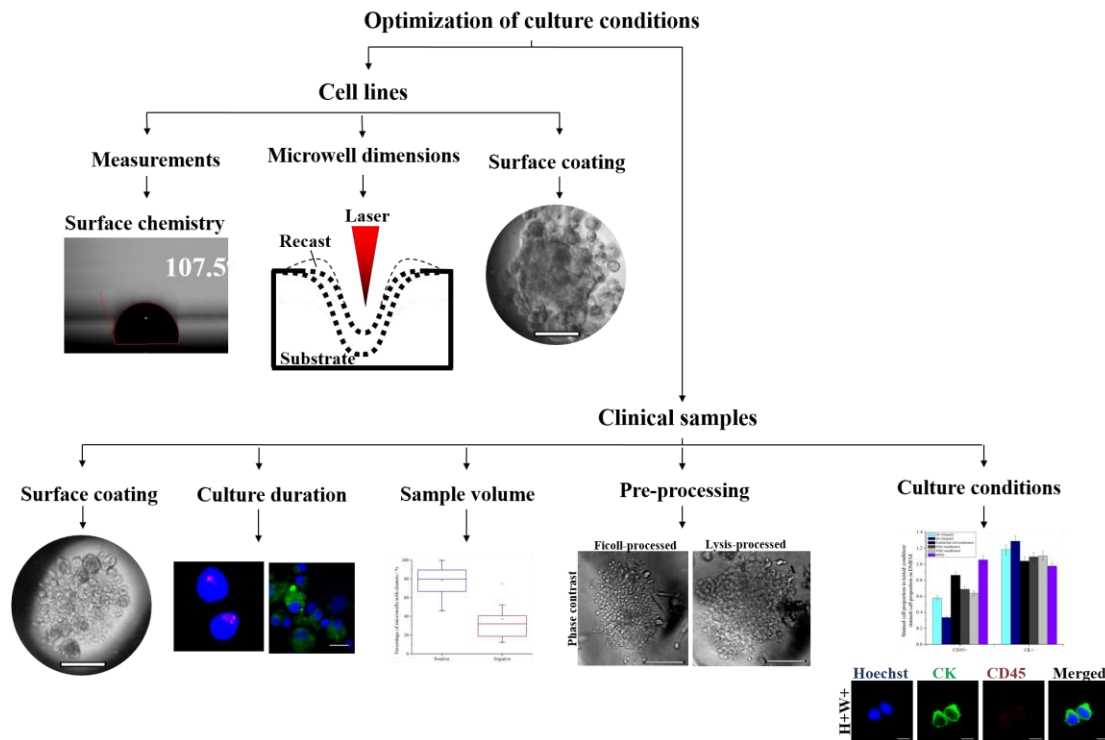


Figure 3.8 Schematics of the optimization procedures. Either breast cancer cell lines or clinical samples were utilized when applicable.

3.2 Overview of resultant cultures of clinical samples

To visualize the cross section of microwells, PDMS replicas were produced. PDMS was coated and lifted off from the patterned dish (**Figure 3.9**), sliced and sectioned vertically (y-direction). PDMS is first mixed thoroughly with solvent at a 10:1 ratio (Sylgard 184, Dow Corning, USA), degassed in a mini-vacuum desiccator (Scienceware, Pequannock, NJ) for an hour, poured onto a patterned dish and cured at 80 degrees Celsius (°C) for another hour. The cured PDMS was then demolded from the patterned dish gently, sectioned and imaged accordingly under phase contrast microscopy.

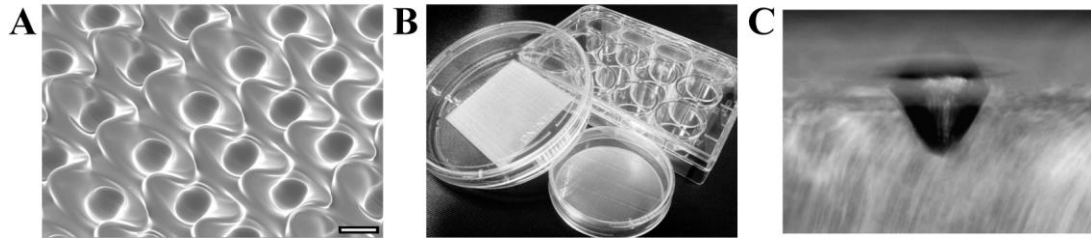


Figure 3.9 Fabrication of microwell assay via laser ablation. (A) Scanning electron microscope image illustrating the packed array of microwells for maximizing space. Scale bar is 100 μm . (B) Types of polystyrene substrates which can be patterned with microwells using the laser ablation technique. (C) Cross section of a PDMS replica demolded from a patterned dish.

60 mm dishes with ellipsoidal microwells of $\sim 225 \mu\text{m} \times 145 \mu\text{m} \times 150 \mu\text{m}$ dimensions (length x breadth x depth) were used for all subsequent cultures of clinical samples (**Figure 3.10A-D**).

Using the optimized conditions as previously discussed, cultures comprising of putative CTCs were obtained from clinical samples from various breast cancer cohorts, and compared against samples from healthy volunteers. Observation of the cultures at Day 8 shows either the formation of single cell monolayers or only cell debris. Cultures might be expanded to form either multilayered clusters (for positive samples; 100s of cells per cluster) or be reduced to cellular debris (for negative patient or healthy volunteer blood samples) (**Figure 3.10E**) after two weeks.

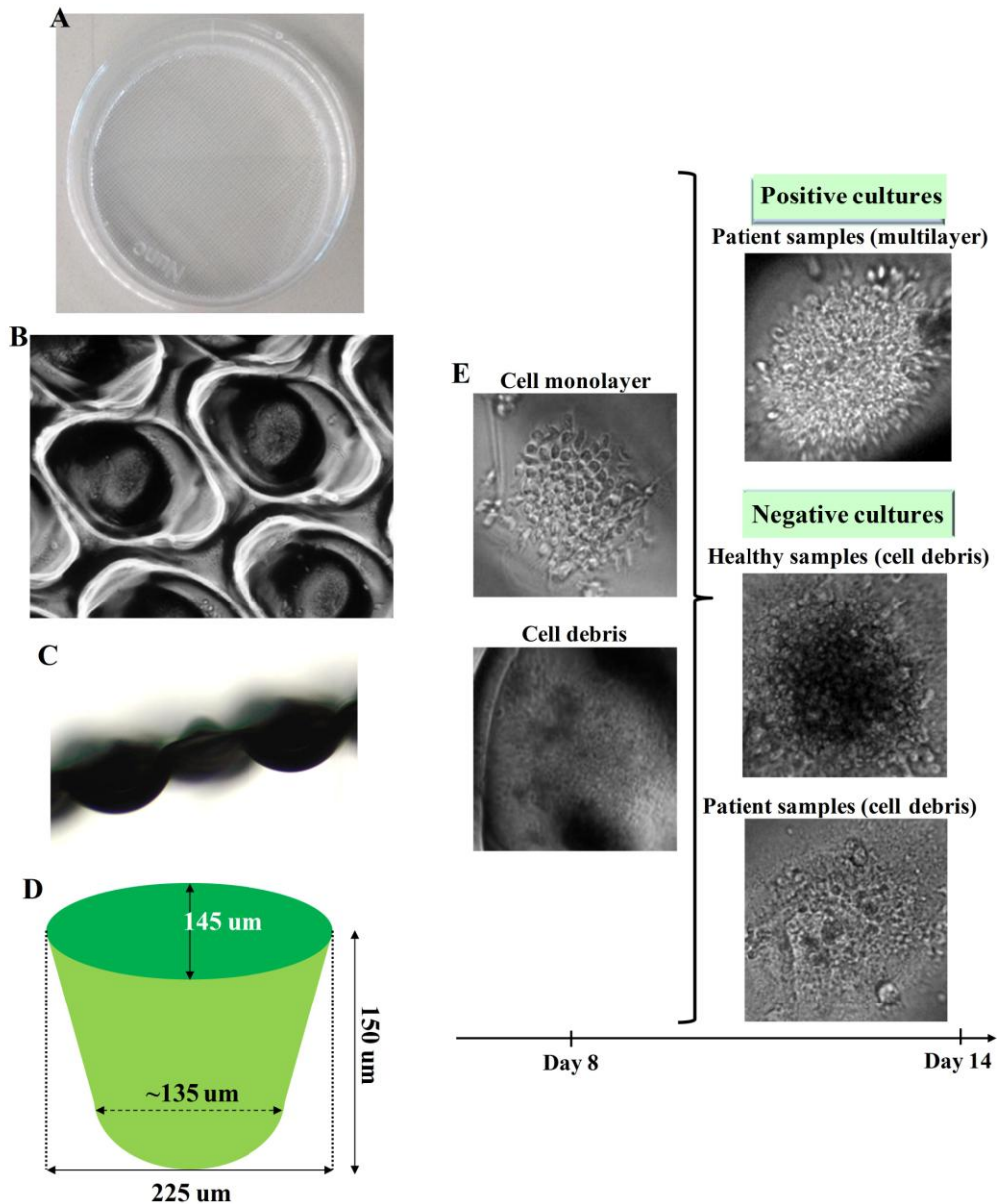


Figure 3.10 Workflow for culture of clinical samples. (A-D) 60mm non coated dishes were patterned with an array of closely arranged microwells with estimated dimensions $225\ \mu\text{m} \times 145\ \mu\text{m} \times 150\ \mu\text{m}$. (E) Nucleated cells were seeded at Day 0 and cultured. Either cell monolayers or debris could be observed by Day 8 of culture. Positive samples proliferated to form multilayered clusters, while negative samples were reduced to cell debris or retained only a monolayer of residual blood cells.

To characterize the resultant cultures, Day 14 samples were harvested and subjected to a series of downstream analysis, as summarized in **Figure 3.11**.

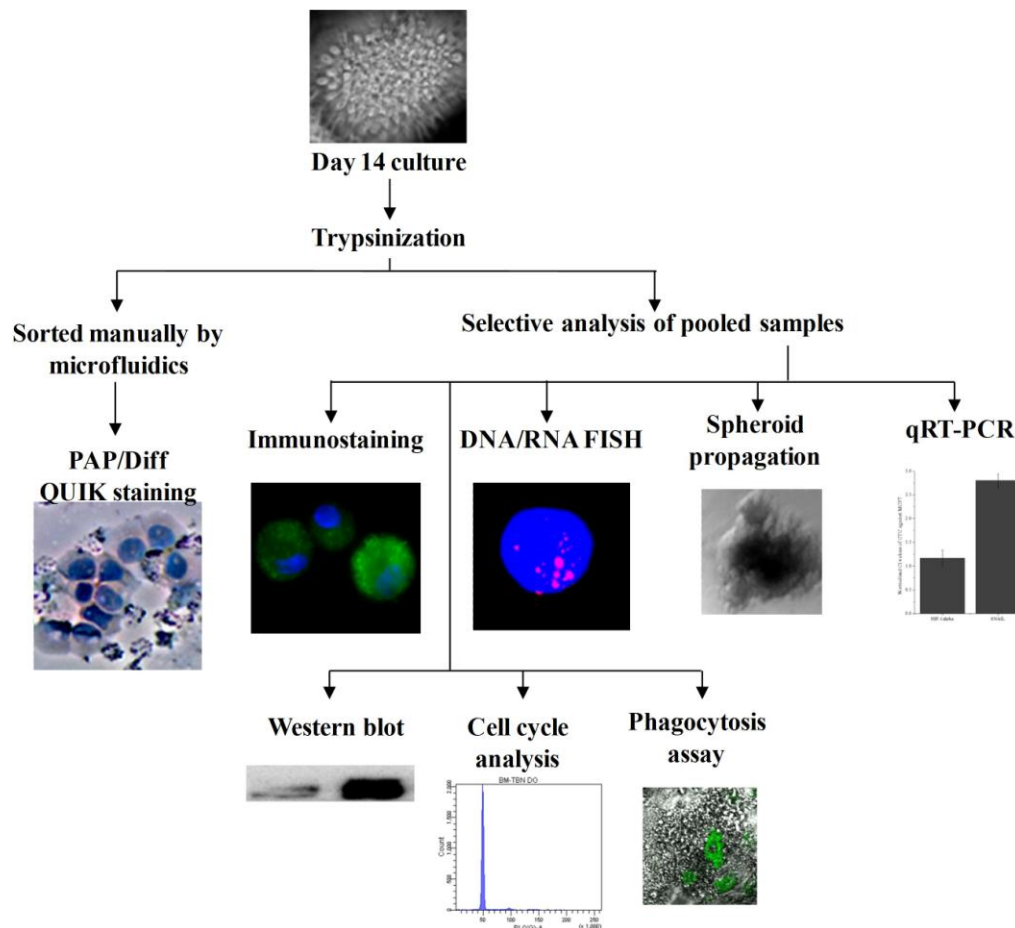


Figure 3.11 Schematic illustrating the series of downstream experiments done on cells obtained from established putative CTC cultures. Cells were sorted manually for PAP stain with microfluidics to provide a better contrast of Large and Small cells in culture, while the rest were processed without pre-sorting and selectively analyzed. For samples which were not sorted, only Small ($\leq 25 \mu\text{m}$) cells with a single round nucleus displaying high N/C ratio were considered for analysis.

3.2.1 Cell viability

Day 14 positive cultures were harvested and stained with propidium iodide (PI) to determine the proportion of cells that were viable. Most cells ($87.5 \pm 8.9\%$, **Figure 3.12A**) were PI⁻, suggesting that they were not apoptotic. On the other hand, viability was markedly decreased in negative cultures ($56.6 \pm 6.2\%$). To further verify the proportion of cells that might be viable but undergoing senescence, cultures were stained for SA β -gal at pH 6 to screen for the proportion of senescent cells. It is determined that the majority of the culture was not senescent (90.1% were negative

for SA β -gal, **Figure 3.12B**).

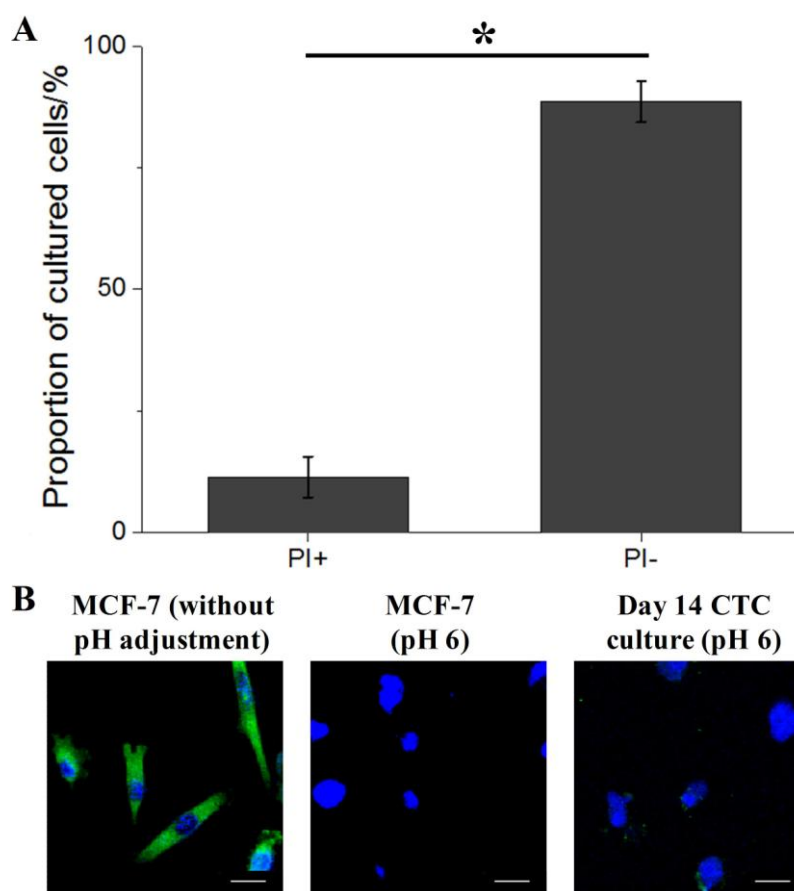


Figure 3.12 Determination of the proportion of apoptotic or senescent cells in established putative CTC cultures. (A) Graphical representation of the proportion of cultured cells stained with PI dye to determine viability. Most cells were not apoptotic (87.5%). All error bars represent standard deviation (SD) of triplicates. Single asterisk indicates $P < 0.01$. (B) Representative images of cells stained with SA β -gal. MCF-7 cells stained without pH adjustment served as a positive control for the antibody, while those stained at pH6 served as a negative control. Day 14 cultured cells stained at pH 6 demonstrate low percentage of β -gal positive cells (9.9%). Scale bar, 20 μ m.

3.2.2 Size heterogeneity of clusters and individual cells

The size of clusters obtained from a single sample varies, typically ranging from 30-100 μ m (**Figure 3.13A**). However, the range of heterogeneity for cultures across different dishes for the same sample should be the same, assuming the sample is resuspended homogeneously and seeded evenly across the dish.

Cultured cells could be harvested and separated into two distinct populations of different cell sizes, via size-based sorting with a microfluidic device (Khoo et al. 2014). Measurements of the average cell diameter revealed a Small cell population of $\leq 25 \mu\text{m}$, while the larger cells were $>25 \mu\text{m}$ (**Figure 3.13B**). The size range of the cultured Small cells were smaller (Median: $13.2 \pm 1.2 \mu\text{m}$) than the CK+/CD45- cells detected on Day 0 nucleated cell spots of corresponding samples (Median: $16.3 \pm 3.9 \mu\text{m}$). Sorted cultured cells processed with Papanicolaou (PAP) stain revealed different morphology between the two sub-populations by size. Small cells exhibited strongly stained nuclei and high nuclear/cytoplasmic (N/C) ratio, which resembled malignant-like features. Larger cells had relatively lightly stained nuclei with low N/C ratio (**Figure 3.13C**). These Large cells were also detected in a majority of cultures from healthy samples (76.5%, n=17) (**Table 3.1**) with no multilayered cluster formation (**Figure 3.13D**). As observed from their morphology, these Large cells were probably non-malignant cell types. Since the significance for the presence of Large cells is currently unclear, further evaluation (quantification of Large cell counts per sample), as well as correlation of the presence of Large cells with various factors (e.g. demographics or patient survival statistics) were not pursued.

Table 3.1 Demographics for healthy volunteers (n=17). C = Chinese; M = Malay; I = Indian; O = Others; Y: Positive. N: Negative.

| No | Race | Age | Multilayered cluster | With Large cells |
|----|------|-----|----------------------|------------------|
| 1 | I | 26 | N | Y |
| 2 | C | 31 | N | Y |
| 3 | C | 28 | N | Y |
| 4 | C | 24 | N | N |
| 5 | C | 25 | N | Y |
| 6 | C | 25 | N | Y |
| 7 | C | 40 | N | Y |
| 8 | M | 25 | N | Y |
| 9 | C | 36 | N | Y |
| 10 | I | 36 | N | Y |
| 11 | C | 30 | N | N |
| 12 | O | 67 | N | Y |
| 13 | C | 26 | N | Y |
| 14 | C | 27 | N | Y |
| 15 | C | 28 | N | N |
| 16 | I | 27 | N | Y |
| 17 | C | 29 | N | N |

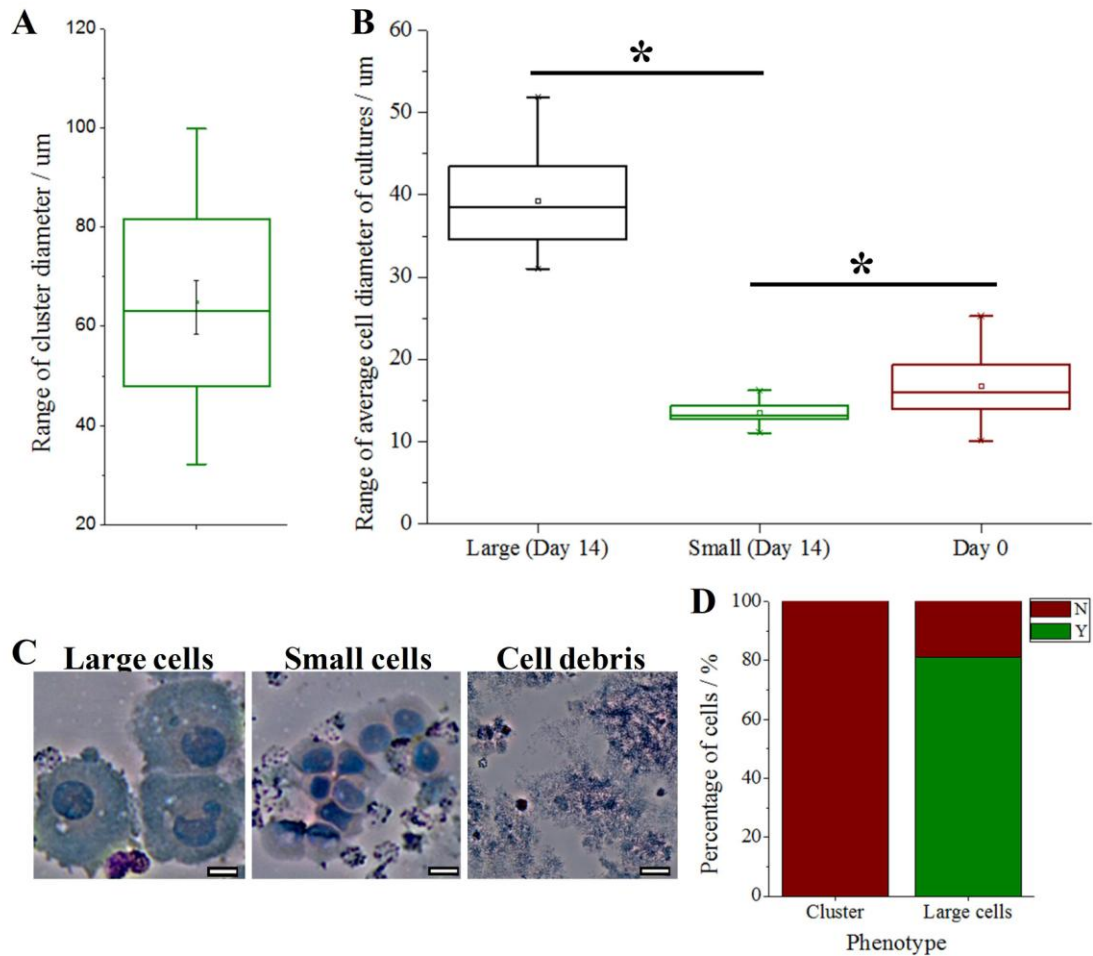


Figure 3.13 Cultures obtained from clinical samples vary from those generated with healthy blood. (A) Box plot demonstrating range of average diameter for resultant clusters within microwells. (B) Day 14 cultures consist of two distinct cell populations by size (Small cells: $\leq 25 \mu\text{m}$, Large cells: $>25 \mu\text{m}$). Single asterisk indicates $P < 0.01$. (C) Representative images of sorted cultures stained with Papanicolaou (PAP) dyes, highlighting their differences in morphology. Cultures from positive samples (patient) generated two distinct populations by size (Large and Small cells), while those from negative samples (healthy) led to cell debris or monolayer of residual blood cells. Scale bar is $10 \mu\text{m}$. (D) 17 samples were obtained from healthy volunteers. Bar charts depicted the proportion of healthy samples displaying clusters, and if Large cells ($>25 \mu\text{m}$, possibly residual blood cells) were present. Cultures of healthy samples did not generate clusters (N), but Large cells were observed in some of these cultures (Y).

To determine the identity of the Large cells, antibodies for several leukocyte and CTC associated markers were selected (**Tables 2.1-2.2**) to screen the cultures. Staining of the clusters *in situ* revealed that the larger cells were CD18⁺/CD68⁺ (leukocyte and macrophage markers respectively) (**Figure 3.14A**). Larger cells outside the

microwells were also CD18⁺/CD68⁺. Incubation with immunoglobulin G (IgG)-coated 1 μ m fluorescein-labeled polystyrene microbeads overnight showed that the Large cells had the phagocytic capability to ingest microbeads (**Figure 3.14B**), confirming that these Large cells were likely to be macrophages.

Macrophages had been previously detected from blood via microfiltration, and were believed to potentially promote CTC dissemination and subsequent metastasis (Adams et al. 2014). Immunostaining of cells revealed that the CD68⁺ cells were also often positive for CK (**Figure 3.14C**), likely due to the expression of Fc receptors. Expression of epithelial markers is also common on activated leukocytes (Jung et al. 1998, Kowalewska et al. 2006) (see **Section 1.4**). Time-lapse imaging of cultures showed that the Large macrophage-like cells appeared after 10 days in culture (**Figure 3.14D**).

The proportion of CD18⁻/CD68⁻ cells under different culture conditions (H+W⁻, H-W⁺ and H+W⁺) (**Figure 3.14E-F**) were investigated. It was observed that the cells derived from cultures maintained under H+W⁻, H-W⁺ were mostly CD18⁺/CD68⁺, while the majority of cells maintained under H+W⁺ conditions are CD18⁻/CD68⁻ ($\sim 67 \pm 26\%$).

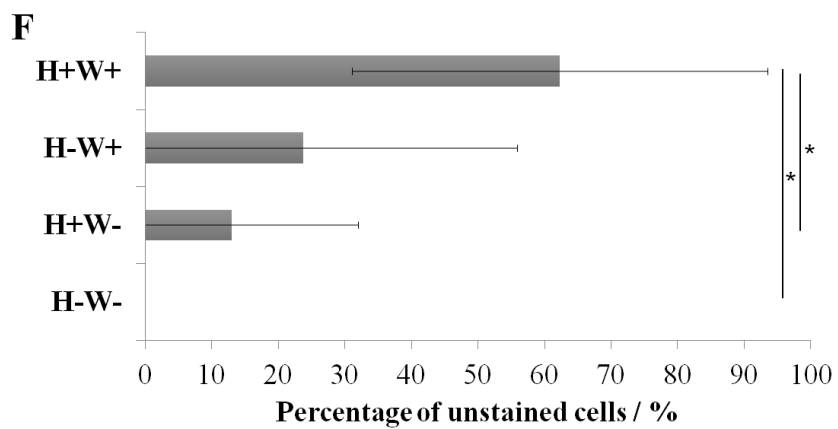
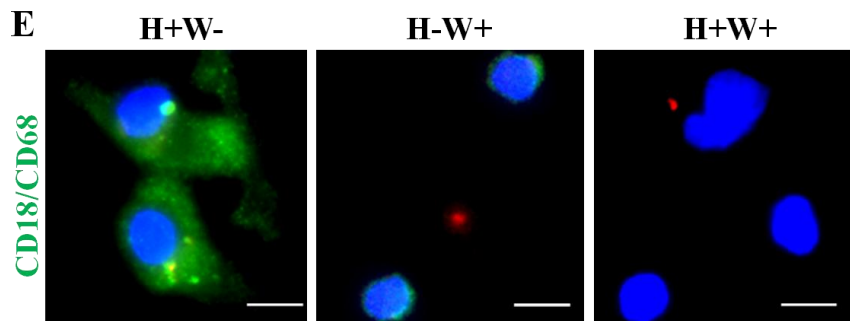
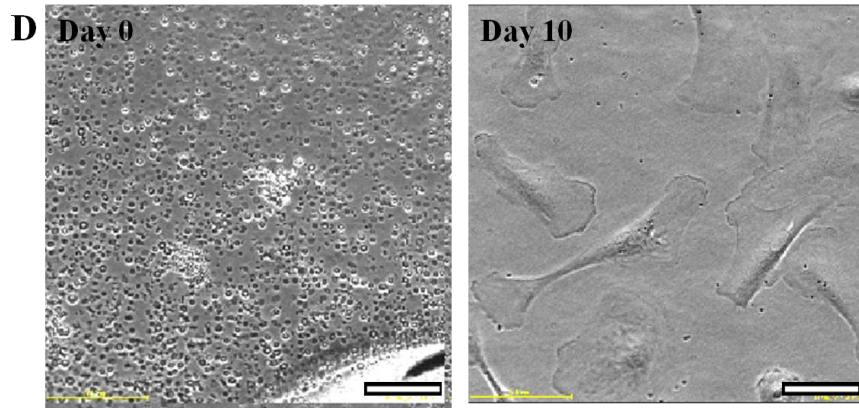
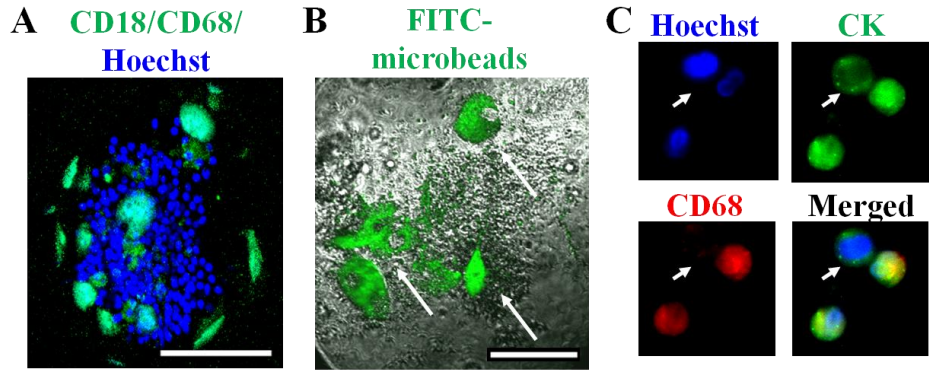


Figure 3.14 Phenotyping Large cells of cultures from clinical samples. (A) Immunostaining of cultures *in situ* for leukocyte (CD18) and macrophage (CD68) markers. Primary antibodies were counterstained with Alexa Fluor 488 secondary antibodies. Scale bar is 100 μm . (B) Bright-field image demonstrating result of a phagocytic assay using 1 μm polystyrene microbeads. Cells which took up the fluorescein-labeled microbeads displayed green fluorescence in the cytoplasmic regions (marked by white arrows), suggesting that they were macrophages. Scale bar is 50 μm . (C) Immunostaining of cells with pan-CK-FITC, CD68-Alexa Fluor 546 antibodies. CK⁺/CD68⁺ cells were detected in culture. Scale bar is 20 μm . (D) Time-lapse imaging of cultures demonstrated the appearance of large macrophage-like cells after Day 10 of culture. (E) Representative bar chart demonstrating proportion of unstained (CD68-CD18-) cells. All error bars represent standard deviation (SD) of triplicate cultures from different samples. (F) Characterization for the proportion of CD18⁺/CD68⁺ cells in cultures maintained under different culture conditions (H+W-, H-W+ and H+W+). Macrophage-like cells were detected in cultures maintained under H+W-, H-W+, while the majority of cells detected from cultures maintained under H+W+ were CD18-/CD68-. Scale bar is 20 μm .

3.2.2 Detection of residual blood cells

To analyze the presence of other blood cells, cells were harvested at different time points in culture (Day 0, 8 and 14) and split into portions for screening with a vast panel of antibodies (**Tables 2.1 and 2.2**) corresponding to haematopoietic precursors, endothelial markers, leukocyte markers, MSC, MSC-derived cell types and various other blood cell types. Screening with CD34 (haematopoietic precursor), CD45 and CD18 (leukocyte markers) demonstrated the progressive removal of blood cells over time (**Figure 3.15A-B**). CD34⁺ cells were completely absent after 14 days in culture, while a minority of CD45⁺ and CD18⁺ cells were detected.

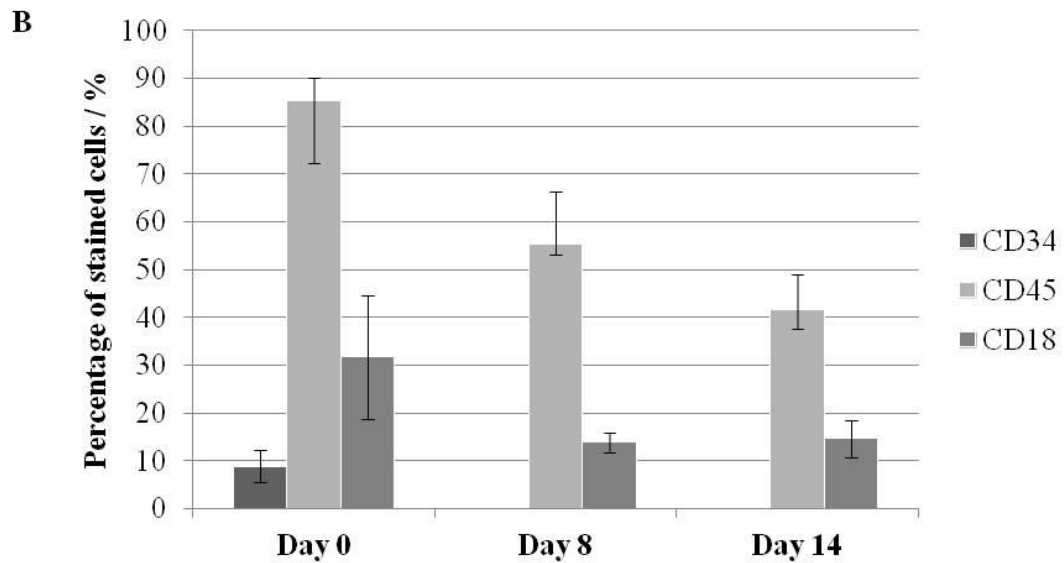
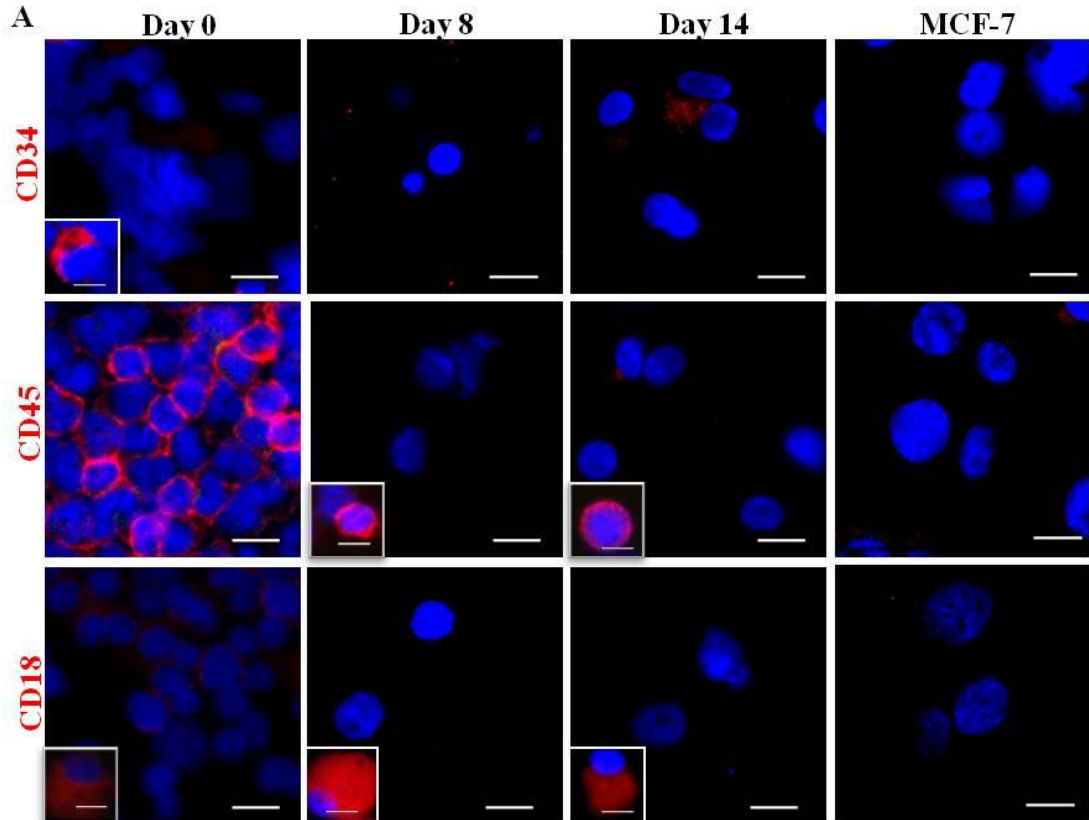


Figure 3.15 Immunostaining of cultures at different time points with antibodies targeting haematopoietic precursors and leukocytes. (A) Antibodies target haematopoietic precursors (CD34) and leukocytes (CD45 and CD18). Cultures from different time points (Day 0, 8, 14) were processed, and MCF-7 cells were used as a negative control to validate antibody specificity. Day 0 samples provided cells for a positive control. Representative images of the minority population (< ~50%) were provided in the box at the bottom left corner of the main image. Scale bar is 20 μ m. (B) Bar charts demonstrating the percentage of CD34, CD45 or CD18 stained cells obtained from samples at different time points. All error bars represent standard deviation (SD) of triplicate cultures from different samples.

Further screening was done with antibodies targeting monocytes, macrophages and other blood components such as platelets, natural killer (NK) cells and endothelial cells (**Figure 3.16-3.17**). Monocytes (CD14+ and CD16+ cells) were absent from cultures at Day 8 and 14. Macrophages (Macrophage inhibiting factor (MIF+ and CD68+) were detected as a minority population (<50%) in Day 8 and 14 samples. Platelets (Thrombospondin-1+ and Von Willebrand factor (vWF)+) and endothelial cells (CD31+) were also undetected in most cells for all time points, with the exception of NK cells (CD56+) (~33±26%). Proportion of macrophages and NK cells vary across patient samples, and may likely reflect worsened disease prognosis (Adams et al. 2014).

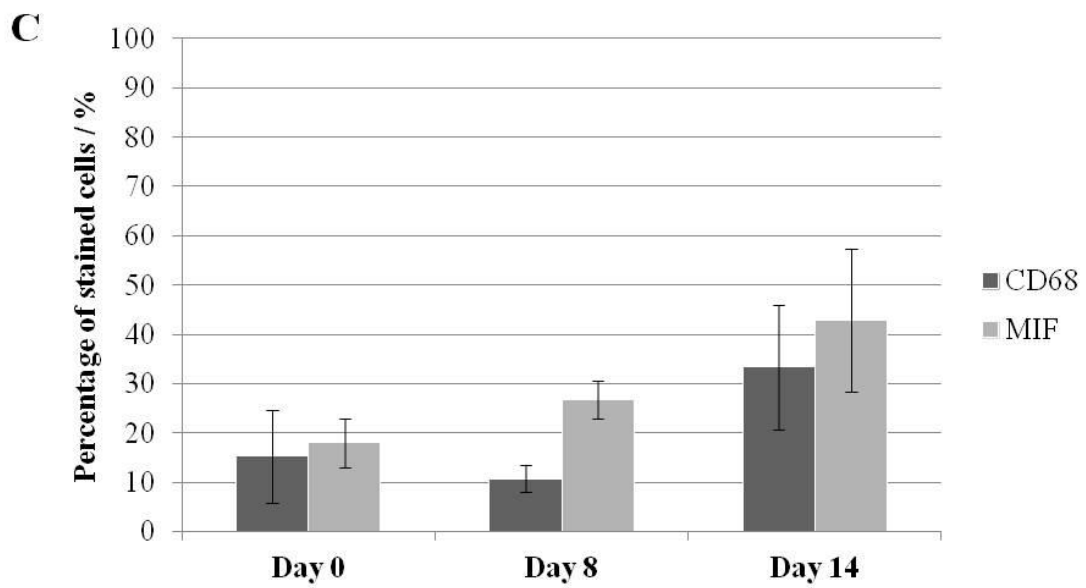
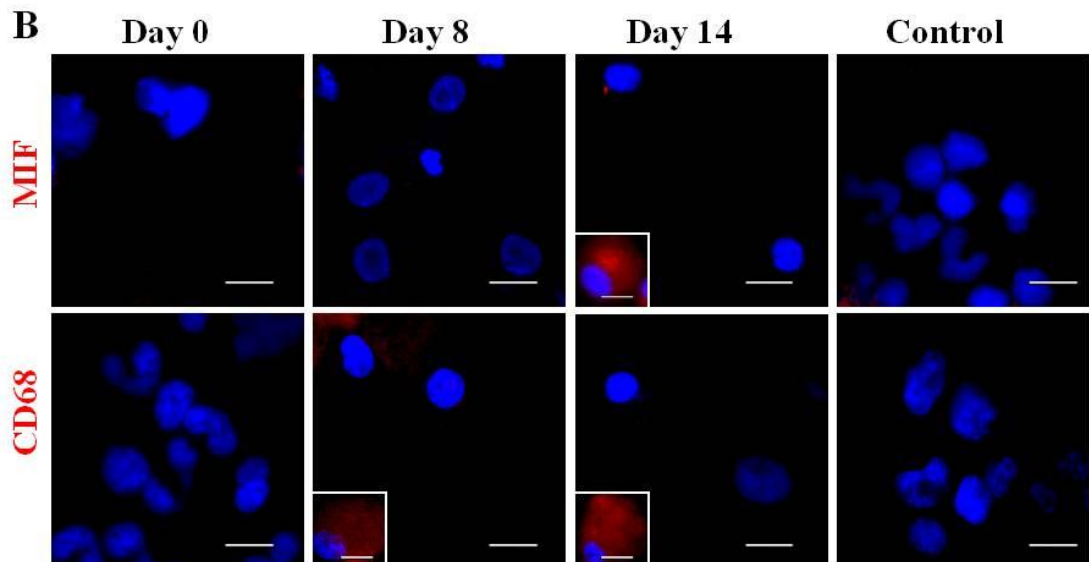
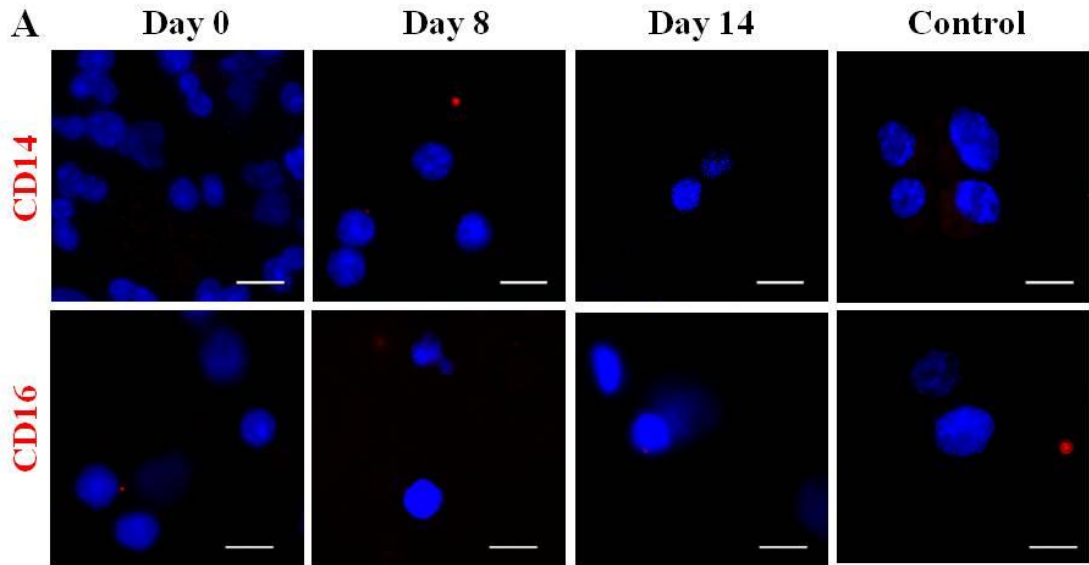


Figure 3.16 Immunostaining of cultures at different time points with antibodies targeting (A) monocytes, (B) macrophages. Antibodies targeting monocytes (CD14 and CD16) and macrophages (MIF) were utilized. Samples from different time points (Day 0, 8, 14) were processed, and MCF-7 cells were used as a negative control to validate antibody specificity. Day 0 samples provided cells for a positive control. Representative images of the minority population (<50%) were provided in the box at the bottom left corner of the main image. Scale bar is 20 μm . (B) Bar charts demonstrating the percentage of CD68 or MIF stained cells obtained from samples at different time points. All error bars represent standard deviation (SD) of triplicate cultures from different samples.

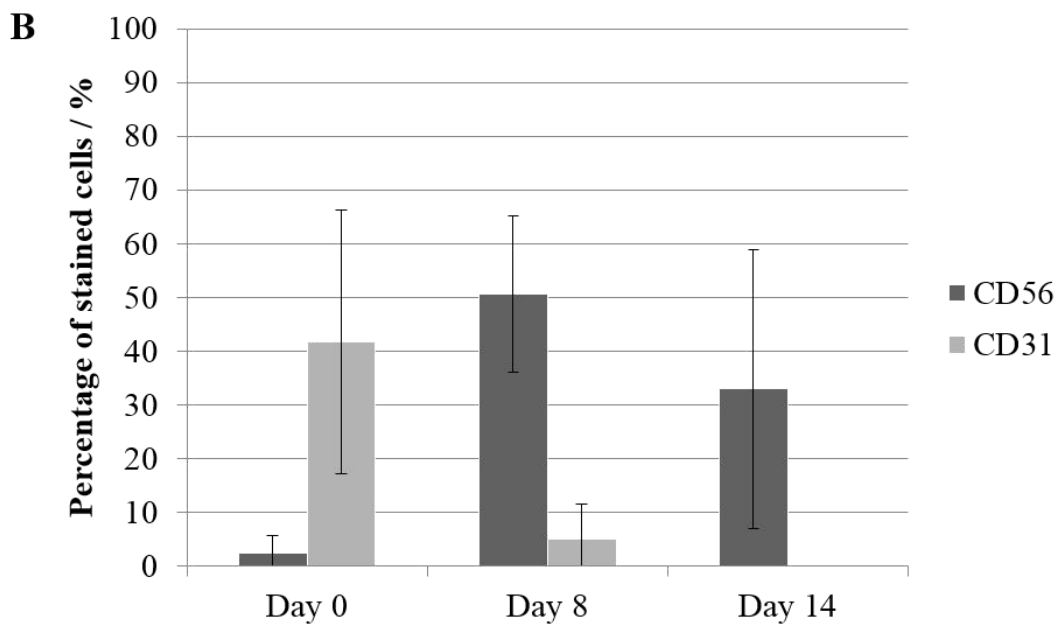
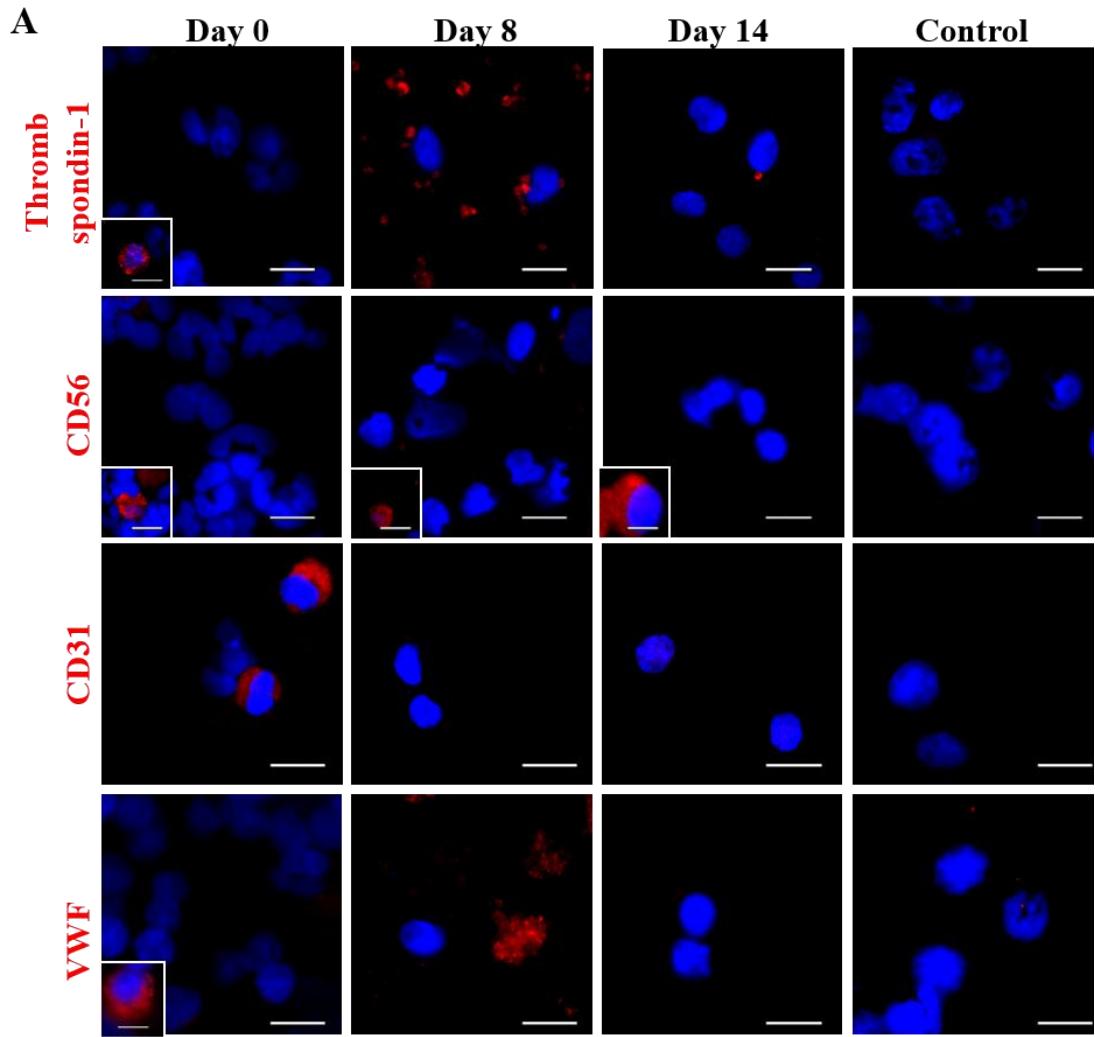


Figure 3.17 Immunostaining of cultures at different time points with antibodies targeting other blood components. Antibodies targeting other blood components including megakaryocytes or platelets (Thrombospondin-1 and vWF), NK cells (CD56) and endothelial cells (CD31) were utilized. Samples from different time points (Day 0, 8, 14) were processed, and MCF-7 cells were used as a negative control to validate antibody specificity. Day 0 samples provided cells for a positive control (C). Representative images of the minority population (<50%) were provided in the box at the bottom left corner of the main image. Scale bar is 20 μ m. (B) Bar charts demonstrating the percentage of CD56 or CD31 stained cells obtained from samples at different time points. All error bars represent standard deviation (SD) of triplicate cultures from different samples.

3.2.3 Amplification of CK+ cells in culture

After validating the progressive removal of blood cells from culture (with the exception of NK cells and macrophages), the proportion of putative CTCs before and after culture were estimated by detection of pan-CK+/CD45-/Hoechst+ cells at different culture time points. Direct staining of clusters within microwells revealed a random distribution of large macrophage-like CK+ cells. Small CK+ cells (either brightly or faintly stained due to heterogeneous expression level of CK) were present adjacent to the periphery of CD45+ cells, while those in the core were typically CK-/CD45- (**Figure 3.18A inset**). These double negative cells are likely to be putative CTCs with more mesenchymal-like expression.

Cells were also harvested on Day 0, 8, 14 and 21 and concentrated into cell spots for CK+ putative CTC enumeration. It is worthy to note that the determination of putative CTCs via CK staining only provides an underestimation of CTC counts, since CTCs may not express CK to an observable extent (Schilling et al. 2012).

Cytospots were stained with antibodies targeting CK8, 18 and 19 (pan-CK) and CD45 while counterstained with Hoechst dye. Enumeration of the CK+/CD45-/Hoechst Small cell count revealed a gradual increase of the percentage of putative CK+ CTCs

over time, usually peaking at Day 14 of culture (**Figure 3.18A**) (Median of CK+ cells corresponding to per ml of blood: Day 0 is 1; Day 8 is 12; Day 14 is 64; Day 21 is 42). The peak appearance of CK+ putative CTCs in Day 14 samples (37.5% to 94.6%) support the decision to characterize cultures after two weeks in culture. Thus, subsequent downstream analyses were carried out with cultures up to 2 weeks culture.

On the other hand, the proportion of putative CTCs after culture was found to correlate with the initial CTC counts at Day 0. Samples with >100 CK+ CTCs at Day 0 generally lead to cultures with a higher CK+ CTC count at Day 14 of culture (5/6, 83.3%) (**Table 5.3**). Interestingly, some of the samples with no detectable CTC fraction at Day 0 were later detected with CK+ putative CTCs after culture. Decrease in CK+ putative CTCs after Day 14 could be either due to cell death or an initiation of EMT, which reduces epithelial marker (e.g. cytokeratin) expression.

The gene expression of CK18 in cultures were specifically determined by qRT-PCR, and compared to that of epithelial (MCF-7) and mesenchymal (MDA-MB-231) breast cancer cell lines (**Figure 3.18B**). Loss of CK18 has been reported to correlate with the onset of EMT, which promotes tumor progression via cell migration (Fortier et al. 2013). It was apparent that the cultures had intermediate expression of CK18 after a week in culture, which was then also reduced at Day 14. This supports the finding that some putative CTCs in culture convert to a more mesenchymal phenotype.

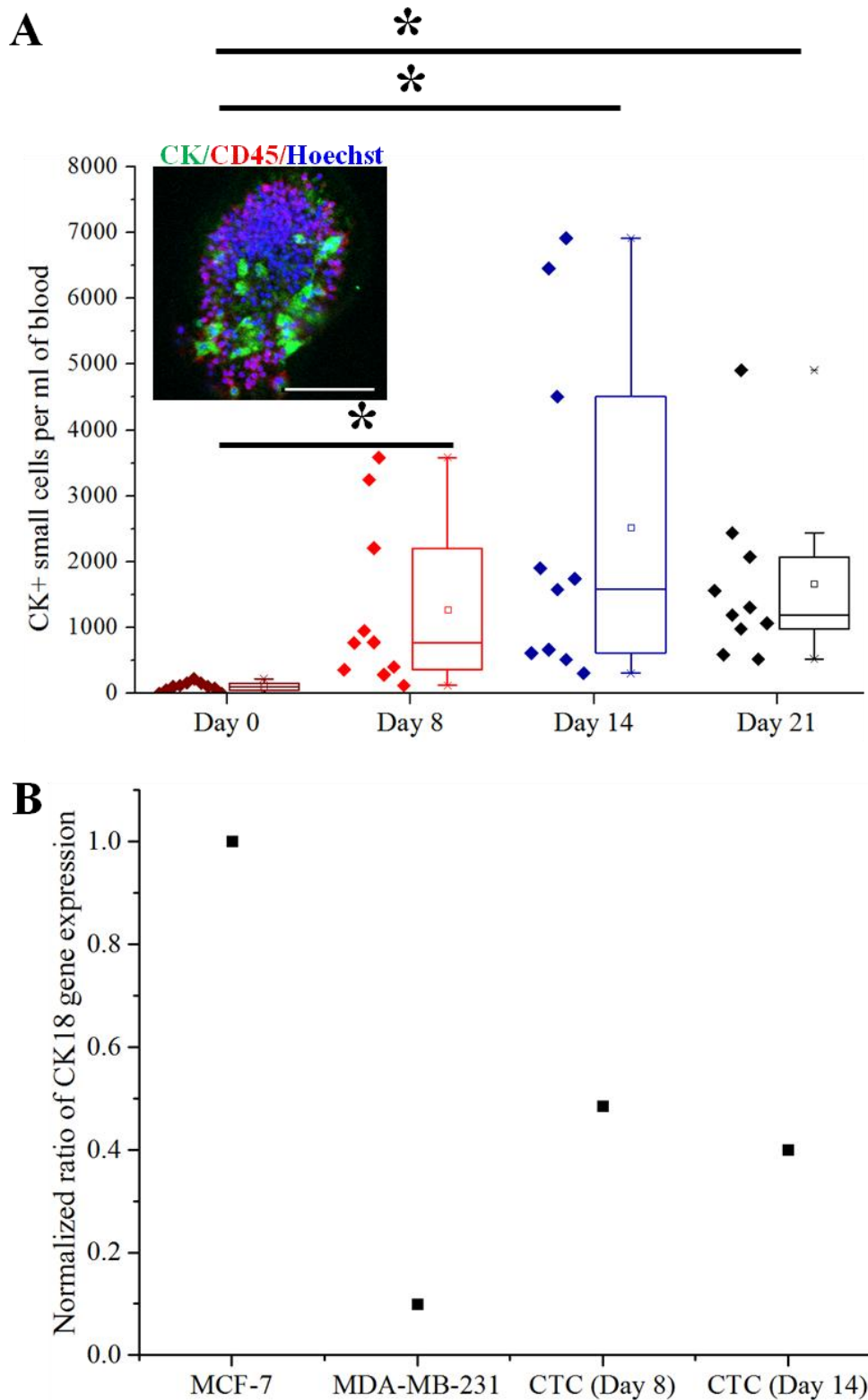


Figure 3.18 Characterizing putative CTCs (Small CK+ cells) in culture. (A) Box plot illustrating range of putative CTCs (CK+/CD45-/Hoechst+) corresponding to per ml of blood, for cultures harvested at various time points. Image of cluster stained with pan-CK-FITC, CD45-APC and Hoechst is provided (inset; Scale bar is 50 μ m). Single asterisk indicates $P < 0.01$. (B) Ratio of CK18 gene expression of Day 8 and 14 cultures, as well as MDA-MB-231 cell line, in contrast (normalized) to that of MCF-7 cell line. Day 0 samples were not analyzed due to insufficient CTC counts.

To eradicate the possibility that CK+/CD45-/Hoechst+ cells could be MSC or MSC-associated derivatives (since they also express epithelial cell markers), Day 14 cultures were harvested and stained for a range of MSC (CD90) and MSC-associated (Aggrecan, FABP4, osteocalcin and Troponin T) specific markers (**Table 2.1, Figure 3.19**). The MSC and MSC-associated cells were generally absent from the cultures. However, a portion of cells were positive for CD90, which is a marker for mesenchymal stem cells, but have also been recently reported to be expressed in breast cancer stem cells (Lu et al. 2014).

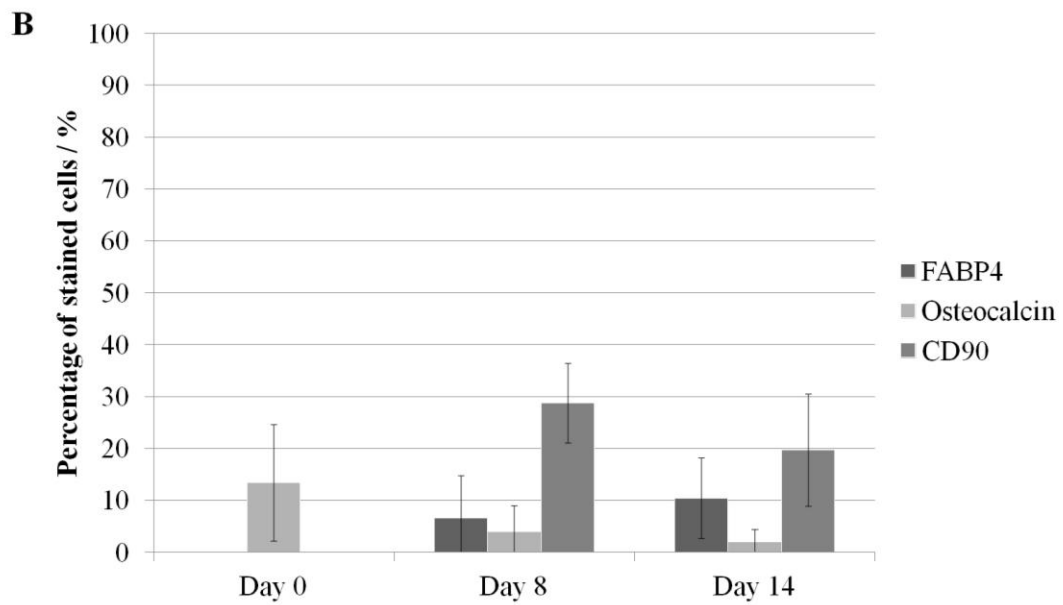
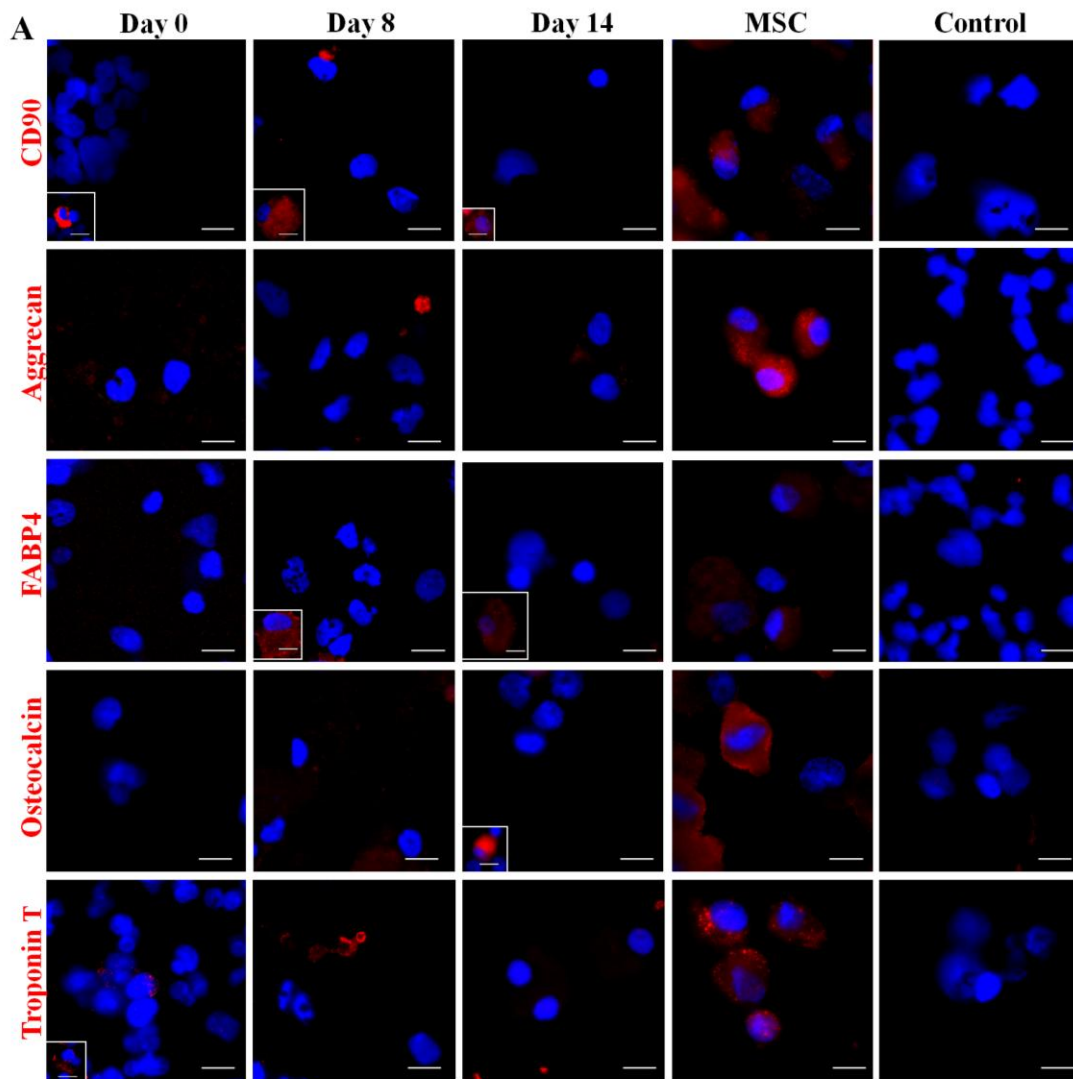


Figure 3.19 Immunostaining of cultures at different time points with antibodies targeting MSCs or MSC derivatives. Samples from different time points (Day 0, 8, 14) were processed, and MSCs and MCF-7 cells were used as positive and negative controls respectively to validate antibody specificity. Representative images of the minority population (<50%) were provided in the box at the bottom left corner of the main image. Scale bar is 20 μm . (B) Bar charts demonstrating the percentage of FABP4, osteocalcin or CD90 stained cells obtained from samples at different time points. All error bars represent standard deviation (SD) of triplicate cultures from different samples.

3.3 Chapter summary

A culture protocol for primary cancer cells using microwells was designed and optimized. Microwells of $\sim 187.5 \mu\text{m}$ in inner diameter were generated on uncoated dishes with a laser ablation technique at 10% speed and 50% laser power. Length of culture was established to be Day 14, when most samples were found to have the highest CK+/CD45- and Ki67+ cell proportions. Nucleated cells were obtained with RBC lysis buffer processing, and supplemented DMEM is used for all cultures for consistency. A combination of hypoxia and the presence of microwells were required for the establishment of multilayered clusters. The minimum volume of patient blood required to correctly evaluate a sample was found to be $\sim 2.3 \text{ ml}$ of blood per patterned 60 mm dish.

Actual clinical samples were used to validate the protocol. It was found that cultures might be expanded to form either multilayered clusters (positive) or be reduced to cellular debris (negative) after two weeks. Majority of the cultured cells were not senescent. Cultures consist of a heterogeneous range of cells, including double negative cells which are likely to be putative CTCs with more mesenchymal-like expression.

Sorted cultured cells revealed small cells which exhibited malignant-like features with strongly stained nuclei and high nuclear/cytoplasmic (N/C) ratio, as well as larger

cells with relatively lightly stained nuclei with low N/C ratio. Phagocytosis assay and immunolabeling confirmed that these large cells were macrophages. Apart from macrophages, NK cells were also presented in the residual leukocyte portion. Proportion of macrophages and NK cells vary across patient samples, and may likely reflect worsened disease prognosis (Adams et al. 2014). Haematopoietic precursors, endothelial cells, MSC, MSC-derived cell types and various other blood cell types were not detected.

Proportion of putative CTCs after culture was found to correlate with the initial CTC counts at Day 0. However, some of the samples with no detectable CTC fraction at Day 0 were also later detected with CK+ putative CTCs after culture.

Chapter 4: Characterization of Cultured CTCs

4.1 Detection of cultured CTCs with genetic alterations

4.1.1 DNA FISH

Enumeration of putative CTCs in culture via detection of EpCAM⁺ or CK⁺ cells could only provide an underestimate of CTC counts. The epithelial markers used for identifying CTCs were also not specific to carcinoma cells. Hence, detection of cells overexpressing cancer-specific genes might provide a more relevant estimate of the actual CTC counts.

Cancer cells are commonly accumulated with various genetic alterations, possibly due to their genetic instability which generates a vast heterogeneity within the tumor. CTCs are believed to be conferred with a similar degree of genetic variation, as they are shed directly from either primary and/or secondary tumors.

To validate this, Day 14 cultures were harvested and concentrated as cell spots for DNA FISH as described in **Materials and Methods**. The six genes selected for screening (FGFR1, MYC, CCND1, HER2, TOP2A and ZNF217; **Table 2.4**) are commonly altered in breast cancer. They constitute about 44% of driver mutations in combination (Davies et al. 2002, Magbanua et al. 2012), which may be detected as a copy number increase or presence of amplicons.

Probes corresponding to these six genes were first hybridized to cell spots individually (**Figure 4.1A**). 10 samples at Day 14 of culture were harvested and sorted into portions for hybridization to each Spectrum Orange-labeled probe. Putative cancer cells with copy number increase in cancer genes were defined as those expressing ≥ 3 red signals. Amplification of the breast cancer associated genes was not observed in WBCs (1 or 2 red signals for haploid and diploid cells respectively)

(Figure 4.1B). The gene expression amongst cultured cells were heterogeneous and 4/10 samples had copy number increase in 1 or more genes for at least 40% (~90th percentile) of the culture (**Figure 4.2**).

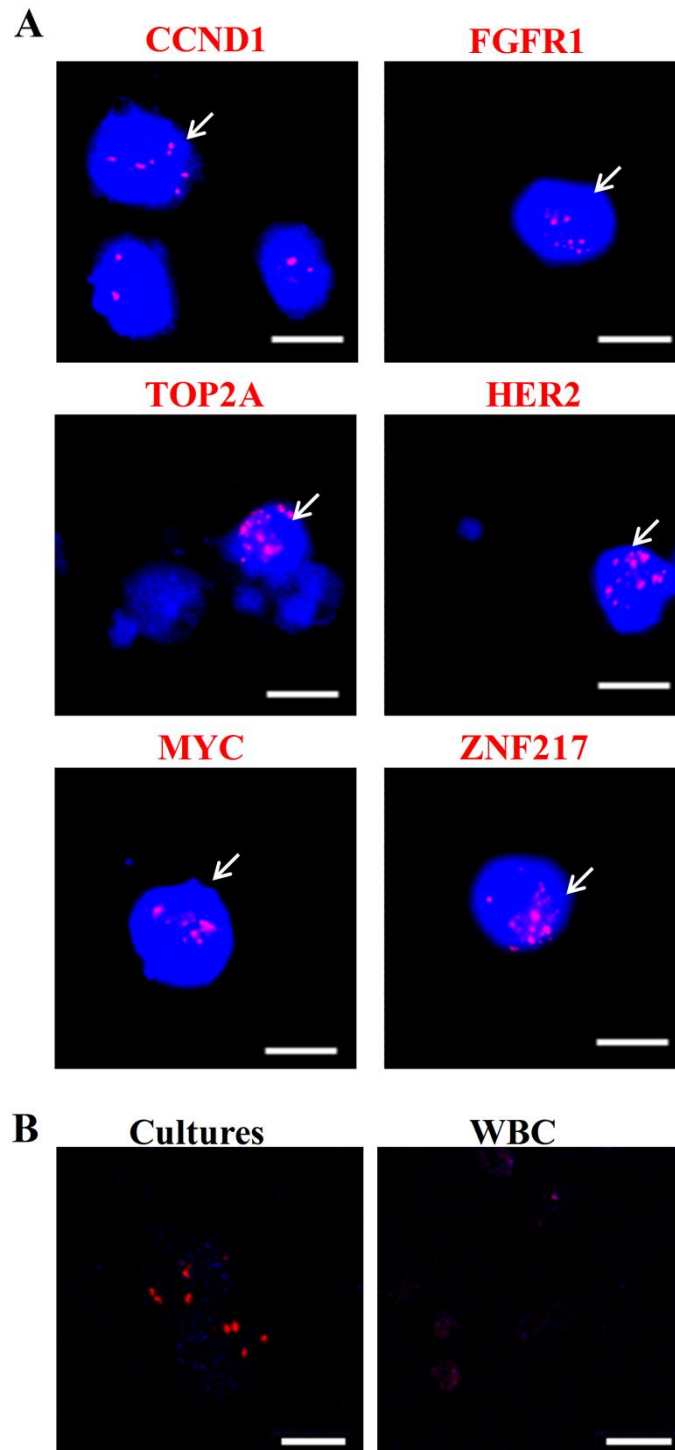


Figure 4.1 DNA FISH of cultured cells and controls (1 probe to 1 sample). (A) Representative images of cultured putative CTCs hybridized with single DNA probes corresponding to genes commonly altered in breast cancer (FGFR1, MYC, CCND1, HER2, TOP2A and ZNF217). Scale bar is 20 μ m. (B) Freshly lysed blood sample, consisting mostly of WBCs, was used as a negative control (right) to validate the specificity of probes. WBCs do not demonstrate copy number increase for the probes targeting breast cancer associated genes (mostly with one or a pair of faint red signals), unlike cultures (left). Scale bar is 20 μ m.

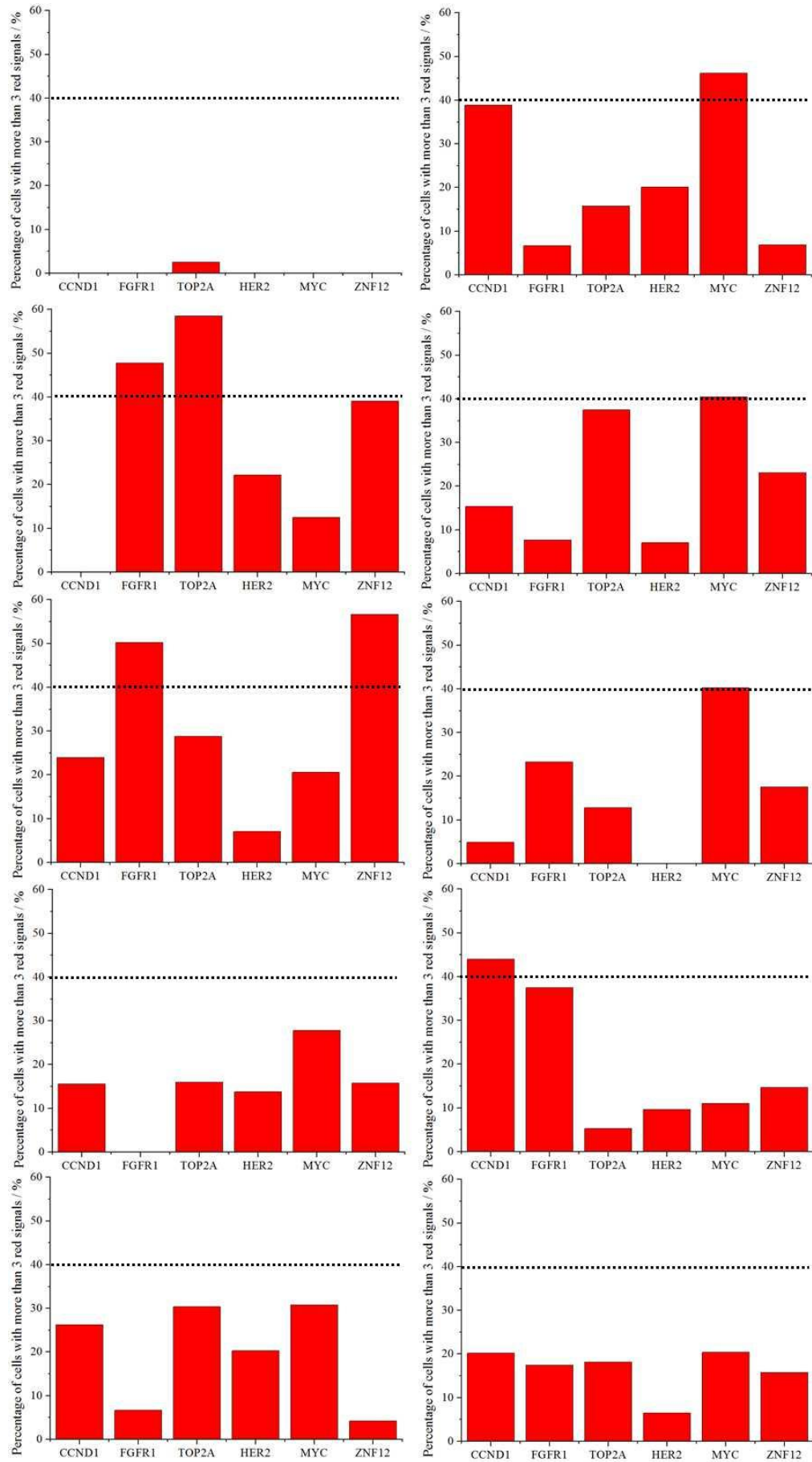


Figure 4.2 Quantification of the percentage of cells with ≥ 3 red signals after DNA FISH (1 probe to 1 sample). Each chart corresponds to analysis from a single sample. Proportion of cultured cells with increase in copy number of cancer genes vary, with some samples having more than 40% (90th percentile) with ≥ 3 red signals for single or multiple probes.

To determine the total percentage of cells with copy number increase in cancer genes, another 27 samples were harvested and hybridized individually to all six probes, on top of a CEN17 probe (**Figure 4.3A**). Increase in copy number of CEN17 indicates cell polyploidy, which is associated with cancer progression. Due to the combination of the six spectrum-orange labeled probes, cells with copy number increase in target genes were defined as cells expressing ≥ 13 red signals. Cells with copy number increase in CEN17 were defined as those with ≥ 3 green signals.

Not all samples were found to have copy number increase in CEN17 (92.6%, n=27; Range: 10.3-85.7%, Mean: 46.2%), an observation which could be attributed to the heterogeneity of the samples (**Figure 4.3B**). Two samples did not express copy number increase in both CEN17 and target genes. This was expected, since the target genes only constitute about 44% of driver mutations in combination (Davies et al. 2002, Magbanua et al. 2012). It was observed that some samples expressing copy number increase in CEN17 might also not be detected with copy number increase in target genes (85.2%, n=27; Range: 7.1-80%, Mean: 35.9%). There appeared to be a lack of association between copy number increase of CEN17 and cancer-associated genes, which was similar to that reported in other studies (Lehmann-Che et al. 2011). Detection of copy number increase in the target genes (constituting ~ 44% of driver mutations in combination) represented the likely presence of a cancer cell, thus these results provided another underestimate of the total proportion of cancer cells in culture.

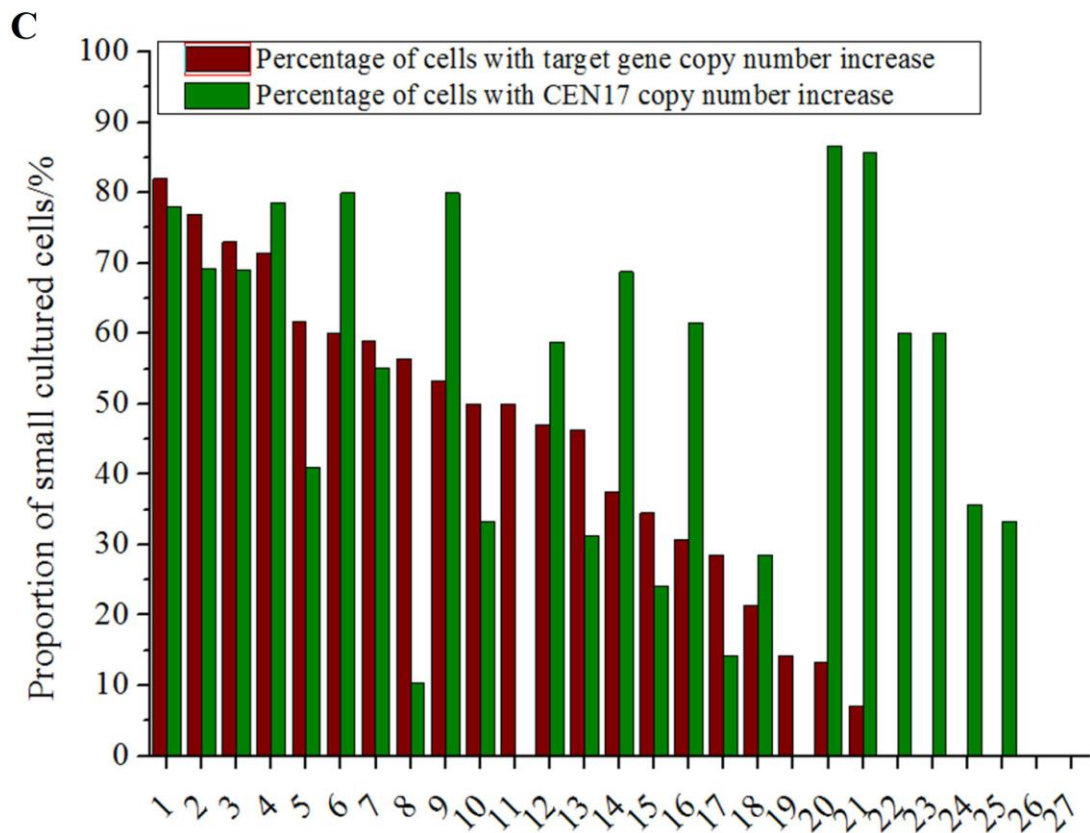
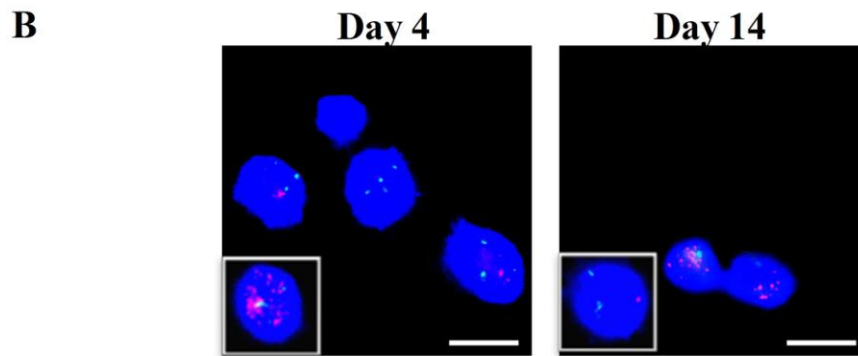
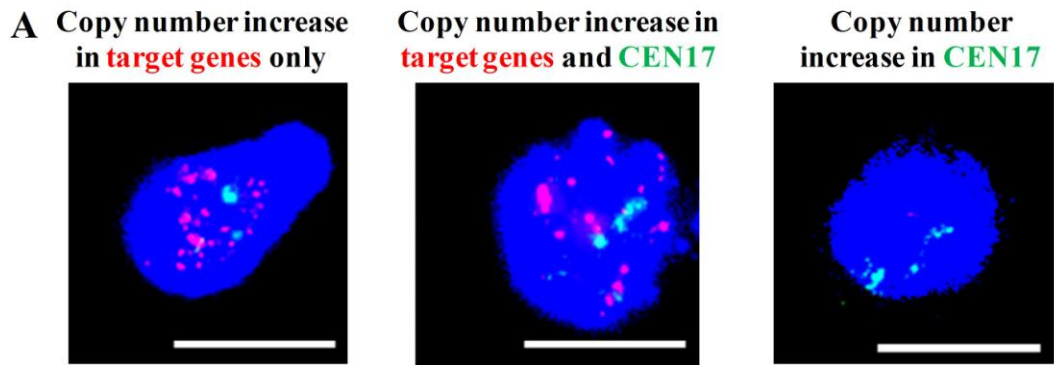


Figure 4.3 Combined DNA FISH (6 probes to 1 sample) for cultured cells. (A) Representative merged images (DAPI, spectrum green, spectrum orange) of cells hybridized with all six target probes (FGFR1, MYC, CCND1, HER2, TOP2A and ZNF217, all red) per sample. Cells with copy number increase in target genes were defined as cells expressing ≥ 13 red signals. Cells with copy number increase in CEN17 were defined as those with ≥ 3 green signals. Scale bar, 20 μm . (B) DNA FISH for Day 4 culture (which consisted mainly of blood cells) and Day 14 culture. Boxed images (marked in white) provided examples of a distinct minority phenotype ($< 50\%$) from the majority of cells. Scale bar, 20 μm . (C) Bar charts demonstrating the percentage of cells of Small cells with target gene or CEN17 copy number increase in 27 cultured samples. Each chart corresponds to analysis from a single sample. The combined prevalence of copy number increase in the six target genes correspond to $\sim 44\%$ of all breast cancers. Each bar refers to a respective sample as numbered (x-axis).

4.2 EMT phenotypes

EpCAM⁺ cancer cells are not associated at all with 30% of tumor subtypes (Went et al. 2004), while CK⁺ cancer cells may not be observed in certain CTC populations (Fehm et al. 2002). Similar phenotypic changes in cell lines obtained from disseminated carcinoma cells (DTCs) from the bone marrow were also often observed (Willipinski-Stapelfeldt et al. 2005), supporting that EpCAM⁻ and CK⁻ phenotypes could also be detected with cultured CTCs.

It is believed that CTCs were as heterogeneous as the tumor *in vivo*, as reported by others for breast (Kallergi et al. 2011), prostate (Armstrong et al. 2011, Chen et al. 2013) and head and neck cancer (Balasubramanian et al. 2012). CTC heterogeneity could be attributed to a partial or complete reversible process of EMT (Thiery and Lim 2013), and might even exhibit one or more phenotypes in their entire transit time within the peripheral circulation (Labelle et al. 2011). EMT phenotypes are of great interest as the EMT process has been closely linked to stem cell-like properties (Wicha 2014) and invasive potential of cells (Tam and Weinberg 2013).

4.2.1 Pooled sample analysis with qRT-PCR

In this project, EMT phenotypes were first investigated via qRT-PCR of pooled samples harvested at different culture time points (Day 8 and 14). Several epithelial (EPCAM and CDH1) and mesenchymal (Vimentin) associated genes, along with two breast cancer markers associated with stemness properties (CD44 and CD24) were investigated. The expression profiles of cultured samples were normalized to that of MCF-7 cells (**Figure 4.4**). There was a general decrease in the expression of epithelial markers and an overall increase of mesenchymal genes in cultured samples. The changes in phenotypic expression appeared to stabilize over time as the culture develops. However, these data were inconclusive due to the presence of blood cells in the pooled samples.

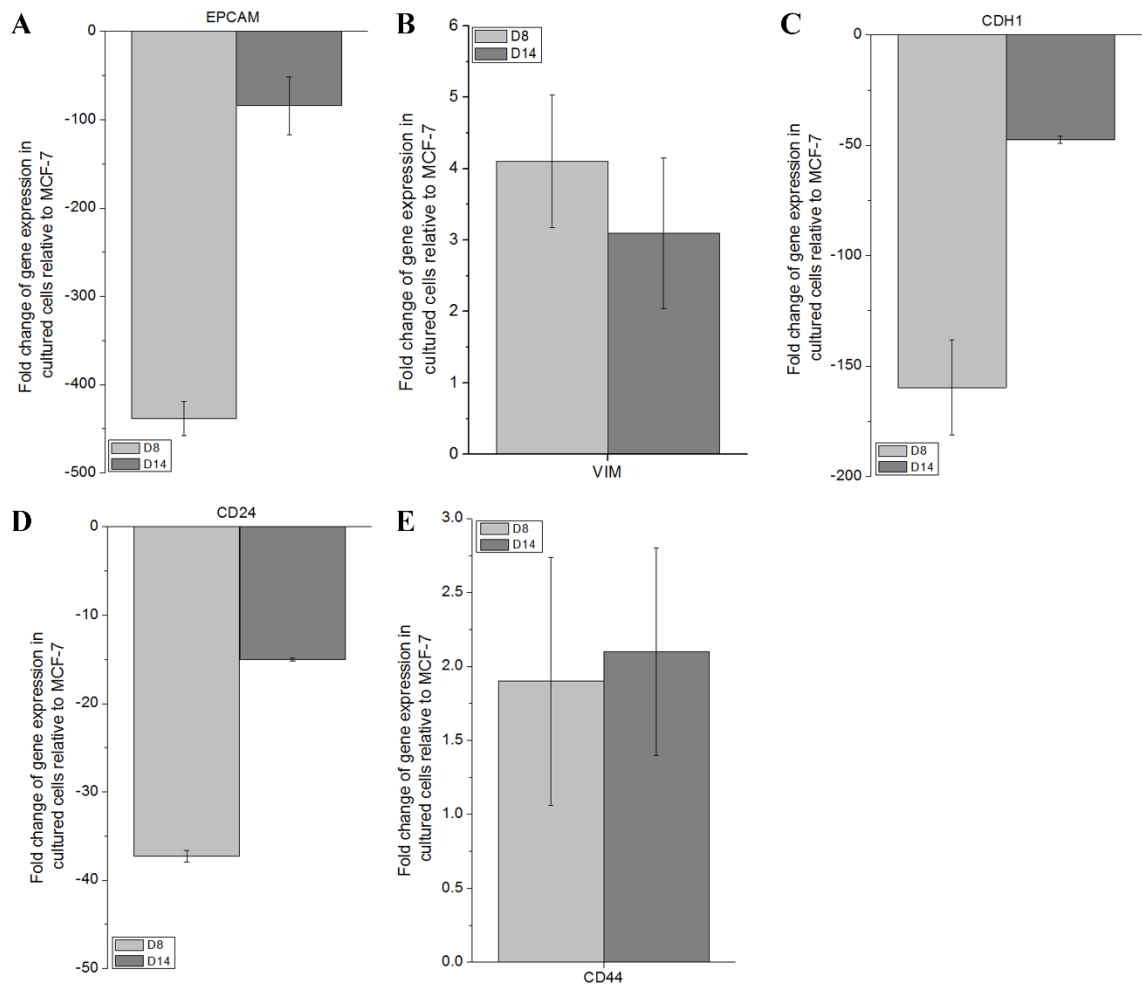


Figure 4.4 Gene expression profiles of EMT associated genes via qRT-PCR. (A) EPCAM, (B) Vimentin and (C) CDH1, as well as stemness associated genes (D) CD24 and (E) CD44 were obtained and normalized to that of MCF-7 cells. All error bars represent standard deviation (SD) of triplicates.

4.2.2 Single cell characterization with immunostaining

To validate this trend more specifically, single cell characterization were carried out on the Small cell portion of samples before and after culture, using antibodies or probes targeting known EMT markers. A list of markers associated with epithelial (E) and mesenchymal (M) expression (Epithelial: E-cadherin, CK5, CK7, CK18, CK19 and EpCAM; Mesenchymal: Vimentin and Fascin) (Akalay et al. 2013) were selected for immunochemical screening of the Small cell cohort (**Table 2.2, Figure 4.5**). MCF-7 and MDA-MB-231 cell lines were used as positive controls, representing epithelial

and mesenchymal carcinomas respectively. Day 0 cultures (freshly RBC lysed blood sample) act as a negative control for most markers (except vimentin staining, where MCF-7 acts as the negative control) as they consist mostly of leukocytes. EMT status of putative CTCs at Day 14 was heterogeneous, with a majority of cells positive for Vimentin, while negative for E-cadherin and EpCAM. Loss of E-cadherin was important as this had been often associated with gain of metastatic traits (Onder et al. 2008). Staining of cultures from Day 8 and 14 time points suggested that the cultured cells became increasingly more mesenchymal-like. Individual CK immunolabelling demonstrated that cultured cells had a higher expression of CK5 (associated with mesenchymal phenotypes) as compared with CK7, CK18 and CK19 (associated with epithelial phenotypes). The expressions of these cytokeratins in cultured cells appeared to be at intermediate levels in contrast to that in full blown epithelial (MCF-7) and mesenchymal (MDA-MB-231) cell types.

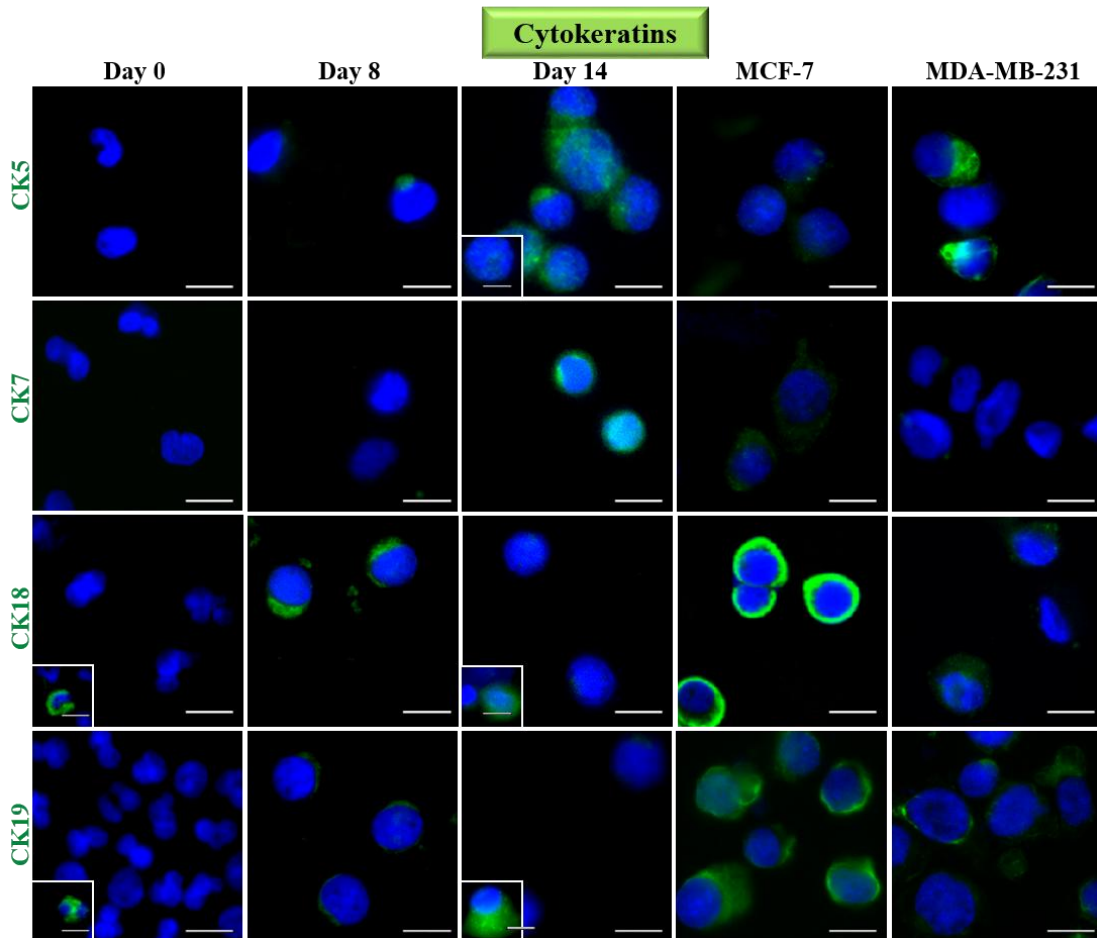
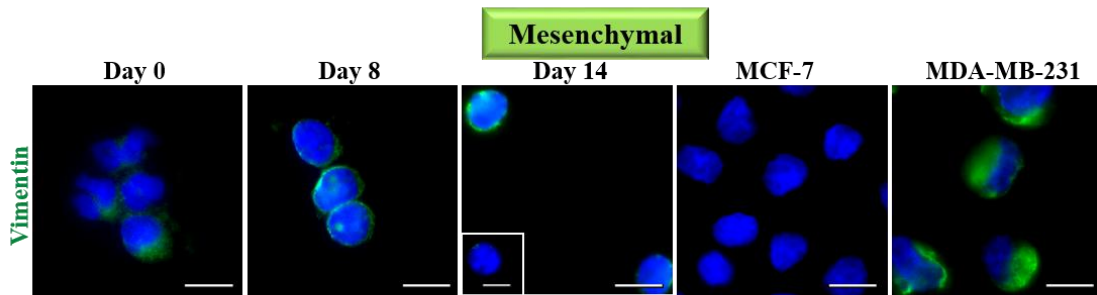
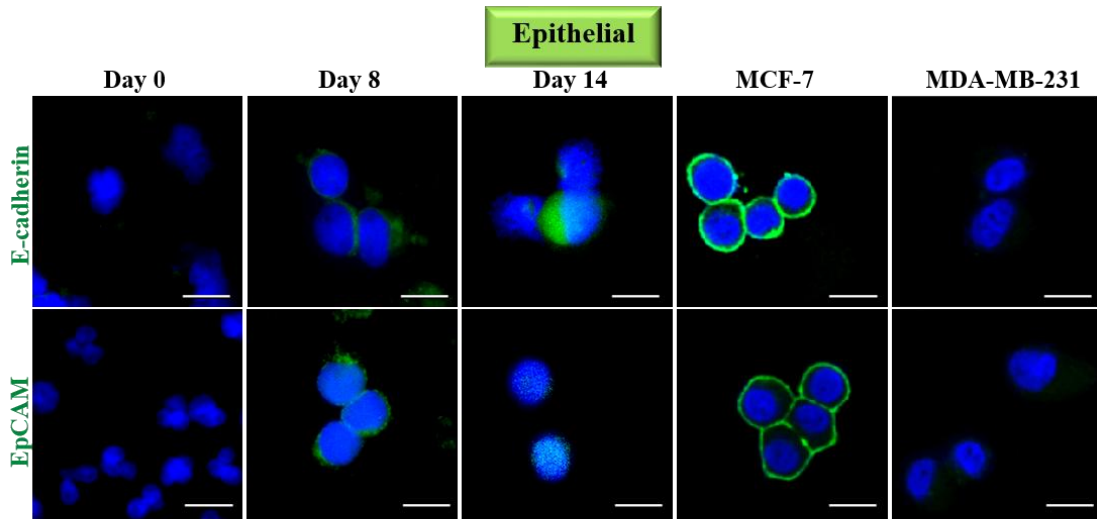


Figure 4.5 Immunostaining of epithelial and mesenchymal markers for Day 14 cultures. Boxed images (marked in white) provided examples of a distinct minority phenotype from the majority of cells (<50%). Cells generally demonstrated increased expression of mesenchymal markers (Vimentin and Fascin), and decreased expression of epithelial markers (EpCAM and E-cadherin). Individual cytokeratin staining (CK 5, 7, 18 and 19) demonstrated that the cultured cells were more positive for CK5 and 7 as compared to CK18 and 19. MCF-7 and MDA-MB-231 breast cancer cell lines were used as references for epithelial and mesenchymal carcinoma cell lines, respectively. Scale bar, 20 μ m.

4.2.3 RNA FISH

To consider the proportion of cells transcribing EMT-associated genes but not translating them into proteins, RNA FISH was carried out to better determine the amount of epithelial-like (E) and mesenchymal-like (M) cells. Thirteen genes, including nine epithelial (E: CK7, 8, 18, 19, CDH1, TFF1, FOXA1, AGR2 and GATA3) and 4 mesenchymal (M: PTX3, SERPINE2, VIM, FASCIN) (**Table 2.5**) genes were targeted with probes from Affymetrix. E probes were labeled green (emission: 488 nm) and M probes were labeled red (emission: 550 nm). Due to the density of E probes (9 probes per sample), cells expressing a high amount of epithelial associated genes would appear green, instead of having distinct green signals (Yu et al. 2012). M cells displayed distinct red signals (**Figure 4.6A**). Cell lines (MCF-7 and MDA-MB-231) were utilized as epithelial and mesenchymal cell line references respectively (**Figure 4.6B**).

RNA FISH processing of 10 samples from individual patients revealed variation of EMT phenotypes across cultures. The 10 patients were previously determined by the clinician for their oestrogen receptor (ER), progesterone receptor (PR) and HER2 status. In a further attempt to evaluate any correlations between the EMT statuses of samples with patient's ER/PR/HER2 status, EMT status data were classified according to patients of respective ER/PR/HER2 status combination. Cluster

formation appeared to demonstrate no correlation to ER, PR or HER2 status (**Figure 4.6C**). However, ER positive/PR positive/HER2 negative samples (PPN) (n=8) did contain a higher proportion of E and EM (intermediate) cell types, even though one sample appeared to be fully M. Overall, the genomic and proteomic expression of EMT markers were heterogeneous, which was consistent with other reports on CTCs of other cancer types (Armstrong et al. 2011, Kallergi et al. 2011, Balasubramanian et al. 2012).

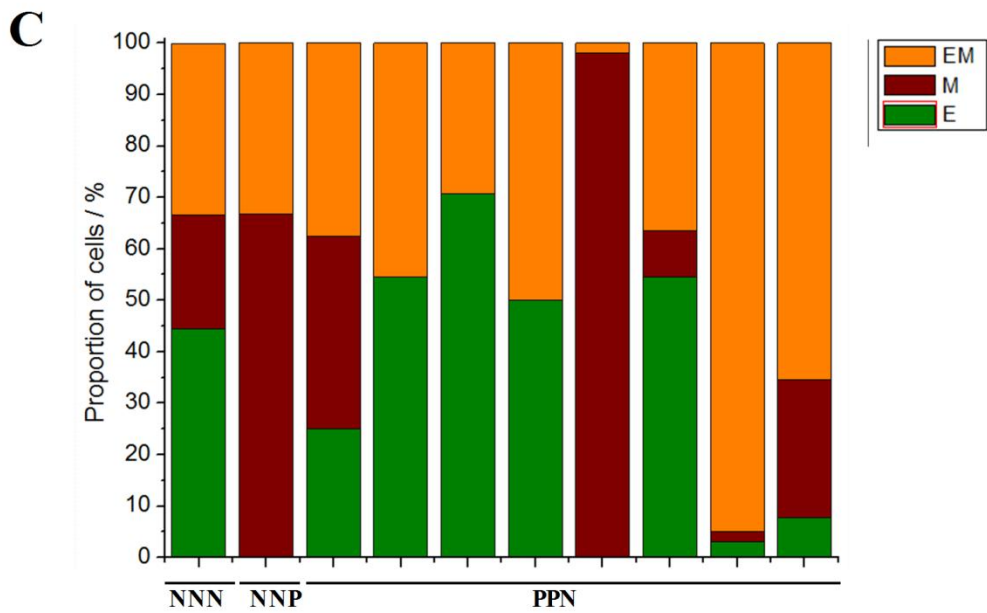
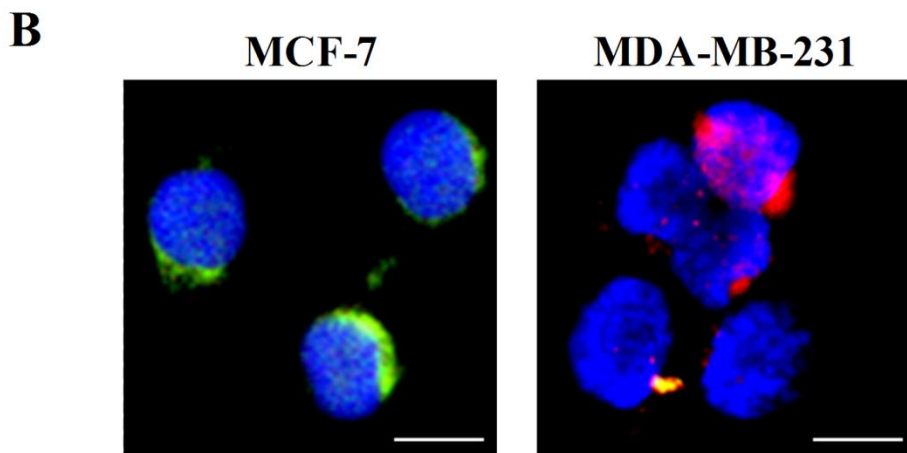
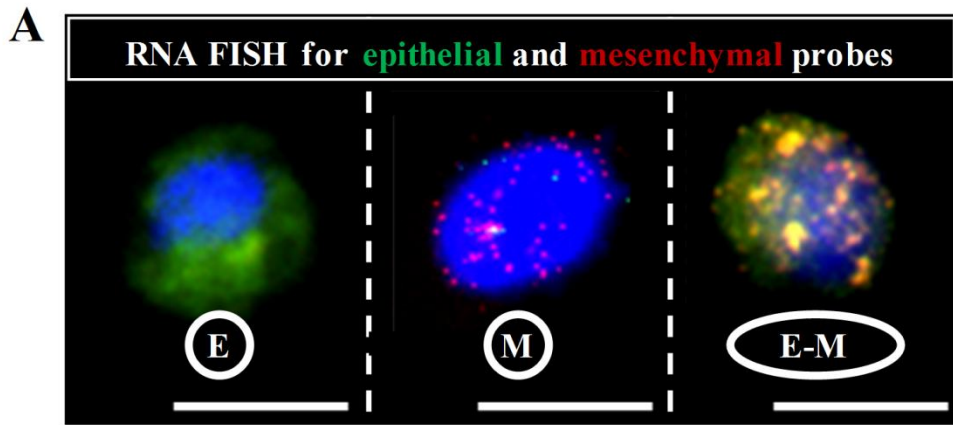


Figure 4.6 RNA FISH with probes targeting EMT markers. (A) Epithelial genes were hybridized to green (488)-labeled probes targeting CK7, 8, 18, 19, CDH1, TFF1, FOXA1, AGR2 and GATA, while mesenchymal genes were hybridized to red (550)-labeled probes targeting PTX3, SERPINE2, Vimentin and Fascin. E: Epithelial-like, M: Mesenchymal-like, EM: Epithelial-Mesenchymal-like. Scale bar, 20 μm . (B) RNA FISH of the same probe combination with control cell lines MCF-7 (epithelial) and MDA-MB-231 (mesenchymal). MCF-7 cells were labeled green and MDA-MB-231 cells demonstrated red signals respectively. Scale bar, 20 μm . (C) Proportion of cells in 10 samples with E, M or EM status. Cells were considered as E if the cytoplasm display green signal with few red signals or if the green: red signal ratio is >2 . Cells were classified as M if green: red signal ratio is <2 . The rest were classified under EM. EMT phenotypes were heterogeneous across samples with different ER, PR and HER2 status. PPN: ER positive/PR positive/HER2 negative samples, NNN: ER negative/PR negative/HER2 negative, NNP: ER negative/PR negative/HER2 positive status. Each bar corresponds to a respective sample as numbered. X axis indicates the ER, PR and HER2 status of the patient.

4.2.4 Cancer stem cells (CSCs)

CSCs belong to a rare subpopulation of stem-like carcinoma cells (Al-Hajj et al. 2003, Ho et al. 2007), usually isolated from tumors via affinity binding techniques (Eramo et al. 2008, Li et al. 2009). They were first observed in the 1960s, from the generation of teratomas from primordial germ cells (Stevens 1964). They have now been detected in various cancer types (including blood cancers) (Lapidot et al. 1994, Bui and Reiter 1998, Singh et al. 2003), and were known to express intermediate EMT phenotypes (Mani et al. 2008, Thiery and Lim 2013, Wicha 2014).

EMT is a process that generates a spectrum of cell phenotypes, and is hypothesized to contribute to the generation of CSC sub-population (Brabletz 2012). *In vitro* CSC cultures obtained from tumors were established typically with non-adhesive substrates (Al-Hajj et al. 2003, Tosoni et al. 2012) and hypoxia (Soeda et al. 2009, Lu et al. 2010), which are conditions similar to that used in the CTC method described in this project. In addition, CSC-like cells were also reported to be present amongst the enriched CTC populations (Kasimir-Bauer et al. 2012, Hou et al. 2013). Hence it is assumed that CSCs might be amplified in the CTC culture.

To demonstrate this, markers used to identify breast CSCs (CD44+/CD24-) (Al-Hajj et al. 2003) were utilized to investigate their expression in cultured cells. Under the absence of either microwells (W) or hypoxia (H), relative proportion of CD44+/CD24- (phenotype of CSCs) was reduced as compared to cells cultured under H+W+ (Figure 4.7; W-H+ to W+H- to W+H+ is 0.62 to 0.42 to 1). No CD44+/CD24- cells were found under samples maintained under H-W- conditions.

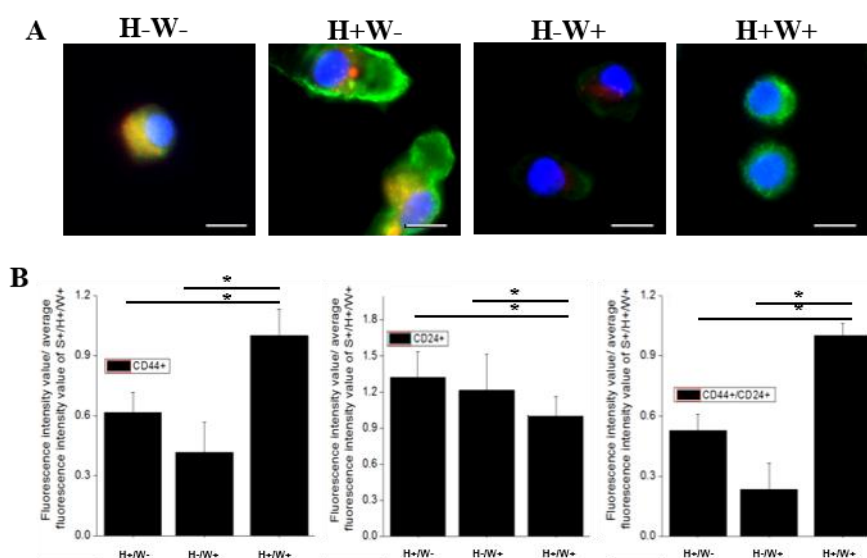


Figure 4.7 Proportion of putative breast CSCs (CD44+/CD24-) in cultures. (A) Representative images of immunostained cells derived from cultures maintained under different conditions. Scale bar, 20 μ m. (B) Bar graphs illustrating the quantitative proportions of CD44+/CD24-, CD44-/CD24+ or CD44+/CD24+. CD44+/CD24+ cells are those at intermediate EMT stages. All error bars represent standard deviation (SD) of triplicates. Asterisks indicate significance of $P \leq 0.05$.

On the other hand, several markers of embryonic stem cells (SOX2, Rex1, Nanog and Oct4) (Kim et al. 2008) were screened to determine presence of cells expressing markers corresponding to embryonic stem cells (ESCs). Intriguingly, only Rex1 was detected in both Day 8 and Day 14 samples (Day 14: $78.5 \pm 17\%$ of positive cells; Figure 4.8). Rex1 has been reported to be expressed in murine teracarcinoma stem

cells (Hosler et al. 1993), and could also suggest the presence of CSCs in these cultures. SOX2 was detected in Day 8 cultures, but not in Day 14. This downregulation of SOX2 could have contributed to the cell growth inhibition observed at later culture time points (see **Section 4.3**) (Herrerros-Villanueva, 2013 #271).

In vitro cultures of spheroids are often used to select and grow tumorigenic cancer cells (Liu et al. 2012). It was found that the cultured samples could also be passaged at Day 14 and transferred into 3D Geltrex® or ultra-low adhesive dishes to form spheroids (**Figure 4.9**), supporting that tumorigenic cells were present in the cultures of clinical samples.

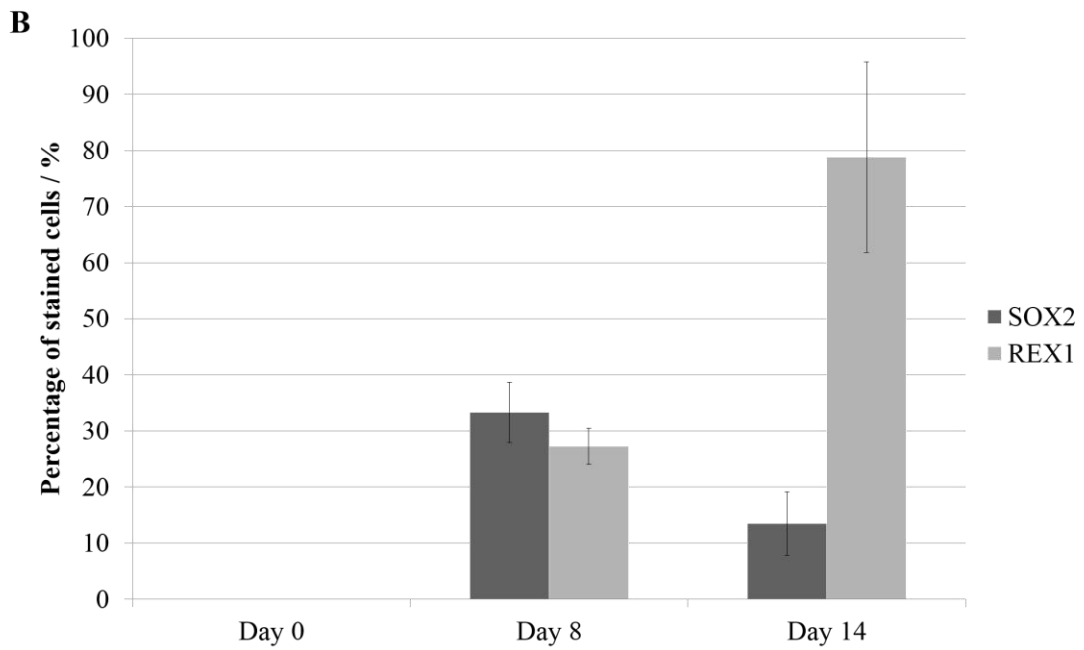
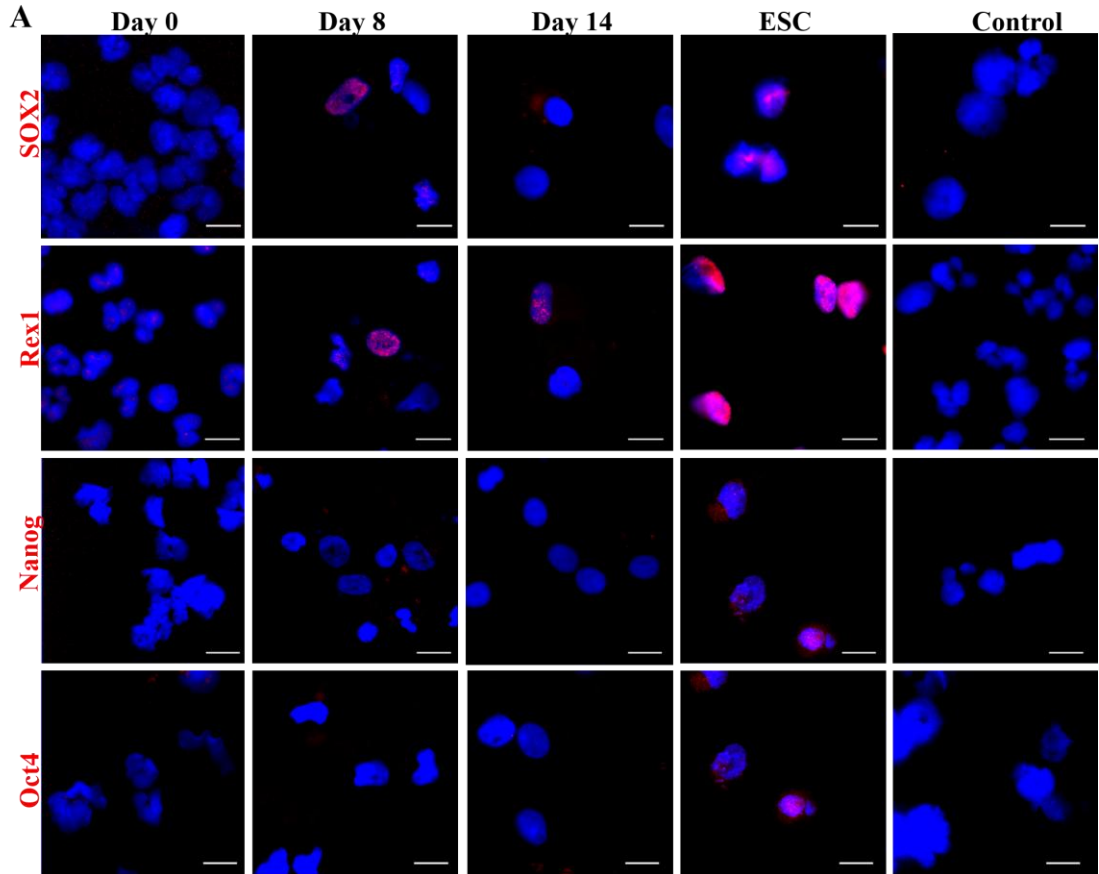


Figure 4.8 Immunostaining of cultured cells from different sample time points with antibodies targeting ESC-associated markers. (A) Cells were positive for an ESC marker (Rex1) at Day 14 but not for the others (SOX2, Nanog and Oct4). Boxed images (marked in white) provide examples of a distinct minority phenotype from the majority of cells (<50%). Representative images of the positive and negative controls for the antibodies are provided in the 2nd last and last columns using ESC and blood cells from Day 0 lysed blood respectively. Scale bar, 20 μ m. (B) Bar charts demonstrating the percentage of SOX2 or REX1 stained cells obtained from samples at different time points. All error bars represent standard deviation (SD) of triplicate cultures from different samples.

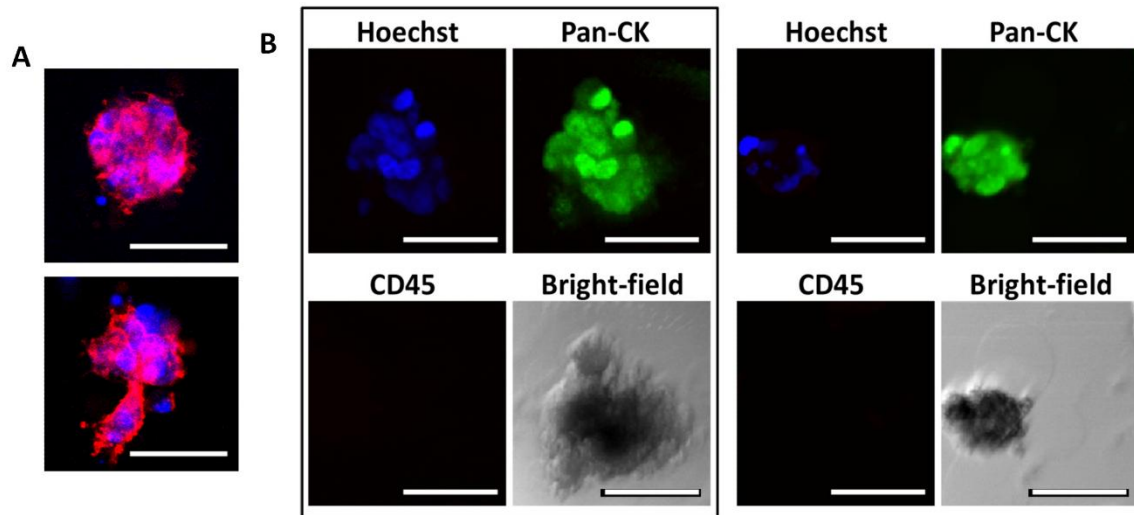


Figure 4.9 Formation of spheroids in 3D Geltrex or low adhesive substrates. (A) Day 14 cultures can be transferred into 3D Geltrex® for further expansion into spheroids. (Top) Spheroids stained for F-actin and Hoechst. (Bottom) Some cells were observed to be migrating out of the spheroids into the surrounding matrix. Scale bar is 100 μm . (B) Cultures could also be transferred into ultra-low adhesive dishes for propagation as spheroids over 10 days, and can withstand passages for at least 4 to 6 times. Resultant spheroids were stained for Hoechst, pan-CK and CD45 antibodies. Cells were mostly Hoechst+/pan-CK+/CD45-. 2 panels (left, right) displaying representative spheroids were shown here. Scale bar is 100 μm .

4.3 Functional characteristics and mechanisms of cultured CTCs

The functional characteristics of CTCs are still an uncharted territory. A key question facing CTC culture protocols would be regarding the mechanisms of proliferation. A hypothesis could be that the induction of EMT triggers the formation of CSC (sub-population of CTCs) (Brabletz 2012), which then proliferate to form clusters.

However, the exact signals of EMT are often unclear. One possibility is the induction of EMT by hypoxia via Notch signaling, as suggested by previous findings (Sahlgren et al. 2008). qRT-PCR analysis of cultures revealed significant gene expression increase of hypoxia-inducible factor 1 (HIF-1 α) and SNAIL-1, both of which are downstream components of the Notch pathway (**Figure 4.10A**). SNAIL-1 is also

termed as the ‘survival factor’ that leads to protective traits and induce partial G1/S cell-cycle arrest (Barrallo-Gimeno and Nieto 2005). A similar observation has been detected in the CSC subpopulations (Ho et al. 2007), with the majority of cells being reported in the G₀ quiescent state. Interestingly, cell cycle analysis with PI staining seemed to suggest the presence of a similar cell cycle arrest (enhanced S phase) in flow cytometry analysis of Day 14 cultured samples (**Figure 4.10B**).

Other regulatory systems such as the claudin or Wnt pathways (Visvader 2011) might also be working in parallel to generate the unique heterogeneity of CTCs. Western blot analysis supports previous findings (that most cultured cells approach a more mesenchymal-like phenotype)(**Figure 4.5, Figure 4.7**), as suggested by the downregulation (EpCAM, E-cadherin and CD24) as well as up-regulation (ZEB-1, c-kit, vimentin, CD44 and SNAIL-1) of epithelial and mesenchymal associated proteins respectively (**Figure 4.10C**). However, western blot analysis is not a favored mode of characterization for CTC samples, as it usually requires large amounts of sample input and does not provide quantitative analysis.

There are few indicators to evaluate cancer cells for their metastatic potential, and most are of low efficiency. Xenografts are the most direct way to confirm tumorigenic properties, but the method is costly and success rate is often low (Baccelli et al. 2013). CTC xenograft experiments were not attempted at this point of time, because the cultures appeared to contain cells which mostly become arrested in the intermediate S phase, and might not be able to divide further (**Figure 4.10B**). Similar reduction of proliferative capability in the progeny as compared to the progenitors has been often reported in stem cells(Tosoni et al. 2012). Intriguingly for some samples, passage of 2 weeks culture into fresh Geltrex® or non-adherent dishes appeared to trigger

proliferation again, forming spheroids (~50% of cultures tested, n=6) (**Figure 4.9**).

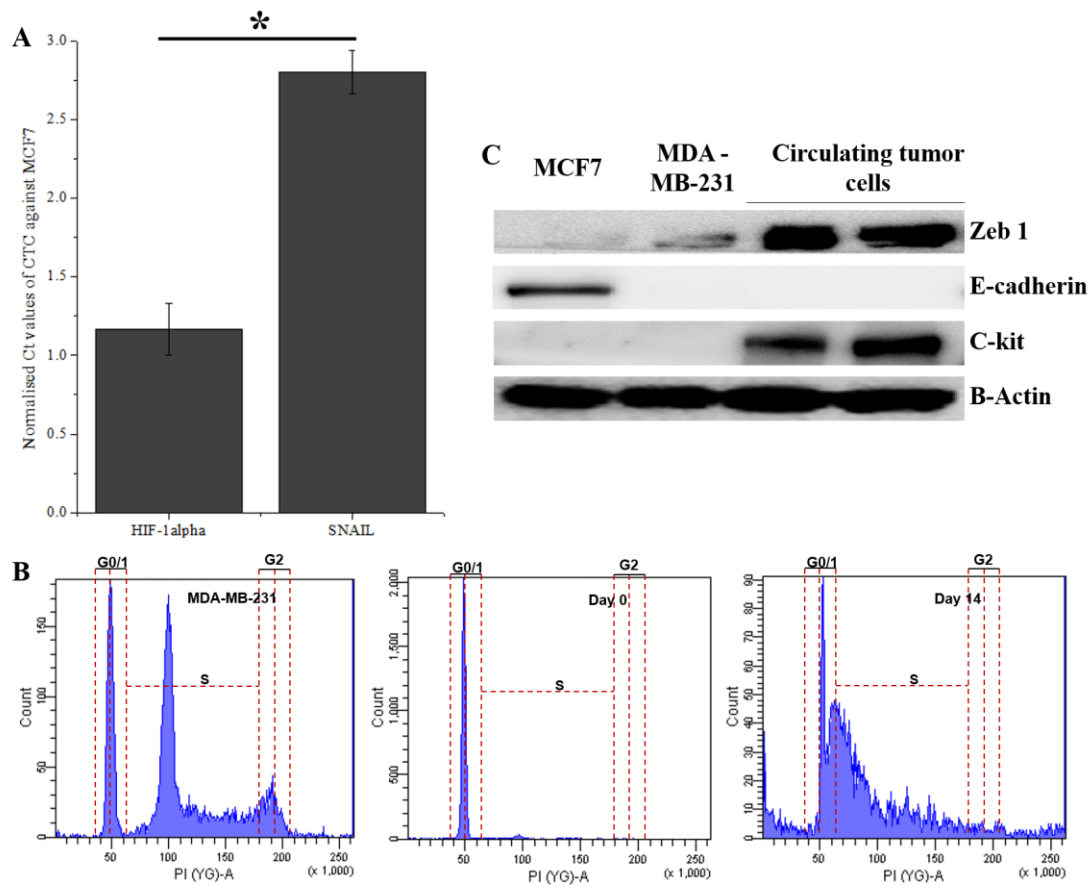


Figure 4.10 Gene or protein expression analyses to suggest mechanisms for CTC proliferation. (A) Normalized Ct value correlating to gene expression of Small cell CTC culture cohort as compared to that of MCF-7 cell line. All error bars represent standard deviation (SD) of triplicates. Asterisks indicate a significance of $p < 0.05$. (B) Flow cytometry analysis of PI-stained Small cell culture cohort (Day 14), blood cells (Day 0 lysed sample) or polyploidy cancer cell line (MDA-MB-231). CTC cultures exhibited a distinct enlarged S-phase in contrast to freshly lysed blood samples at Day 0. (C) Western blot analysis indicating up- or down- regulation of EMT associated proteins in contrast to expression of beta-actin.

Potential invasiveness of cultures was explored with invadopodia assays. Results suggested that a proportion of cultured cells could lead to the degradation of matrix (**Figure 4.11A**), and the proportion of invasive cells vary across samples. Most degraded areas due to invadopodia or podosome formation were 'blotchy', while some gave rise to 'punctate' patterns. Some cultures contained cells which were more

migratory or were able to degrade the extracellular matrix more efficiently than others (**Figure 4.11B-C**). Cells which were more migratory generated a larger degraded matrix to cell area ratio.

Invasiveness is often associated with higher migratory speeds (Christofori 2006). Filamentous (F)-actin polarization is crucial for physically inducing a cell's migration (van Oudenaarden and Theriot 1999, Snapper et al. 2001). To determine the pattern of F-actin expression in CTCs, four cultures were stained with phalloidin, and the resultant images were contrasted with those obtained with stained cancer cell lines (MCF-7 and MDA-MB-231) (**Figure 4.11D**). MDA-MB-231 formed distinct F-actin stress fibers, while MCF-7 cells displayed F-actin fibers of higher bundle density. Cultured CTCs appeared to demonstrate high expression of condensed F-actin within the perinuclear zone, which is an observation usually associated with exposure to certain anticancer drugs (Rosenblum and Shivers 2000).

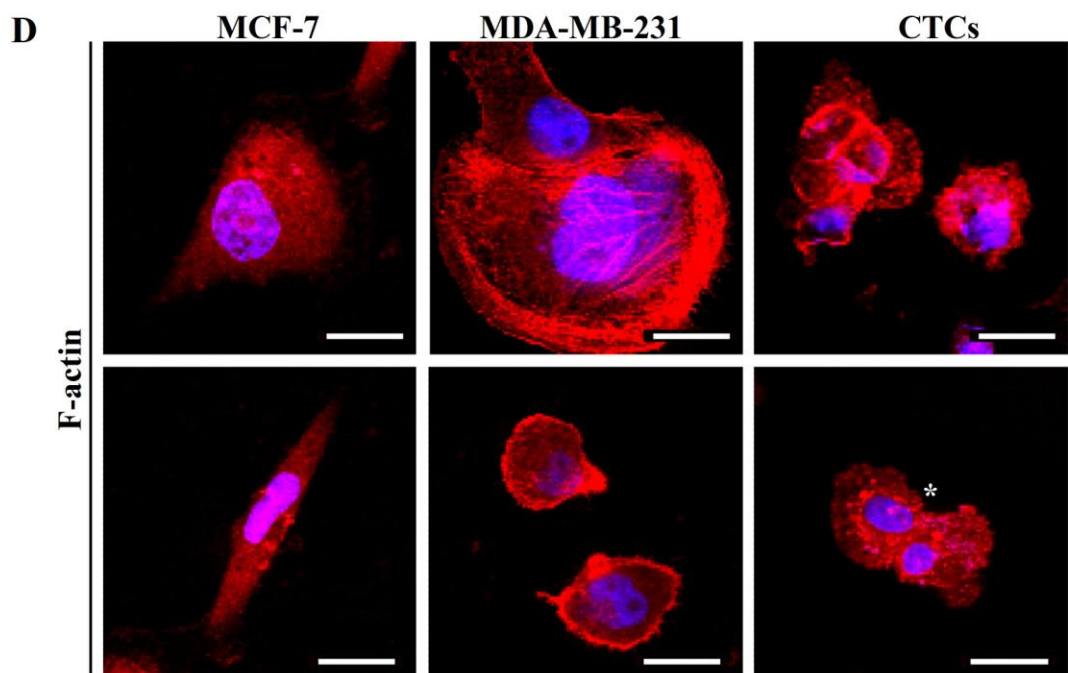
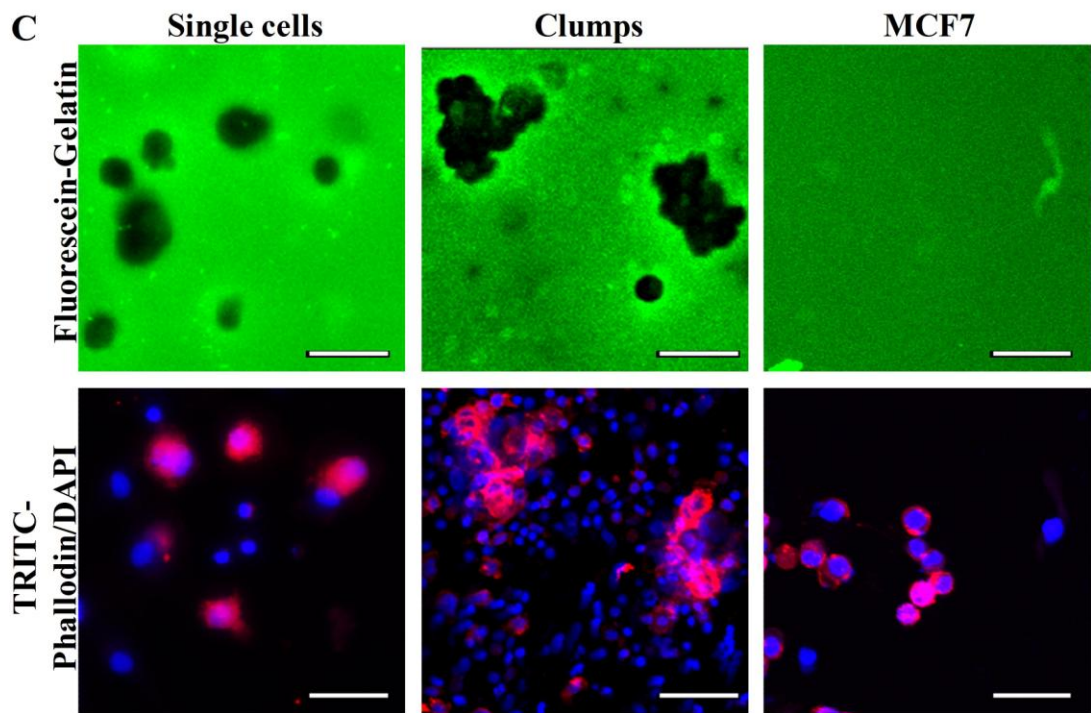
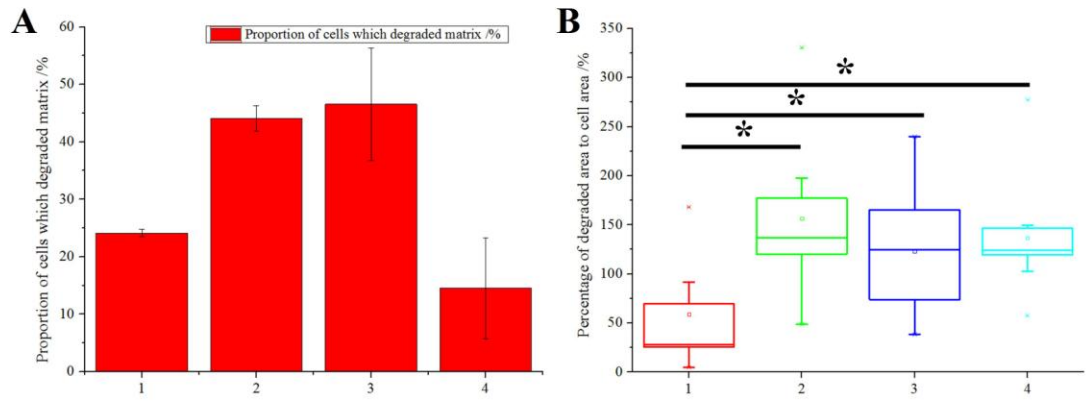


Figure 4.11 Invasiveness and migratory aspects of cultured CTCs. (A) Proportion of cultured cells which led to matrix degradation. Each bar graph (numbered 1-4) represents an individual sample. All error bars represent standard deviation (SD) of data from cells in each individual sample. (B) Percentage of degraded matrix area to cell area. Each box chart (numbered 1-4) represents an individual sample. Some percentages were higher than 100% due to migration of cells which generated a wider degradation area with respect to cell size. Single asterisk indicates $P < 0.01$. (C) Imaging of gelatin substrate (green)/TRITC-phalloidin/DAPI stained cells. Scale bar is 100 μm . (D) Phalloidin staining to reveal F-actin expression of cell lines (MCF-7 and MDA-MB-231) and cultured CTCs respectively. Two representative images of each cell type were provided (top and bottom panels). White asterisk indicates cell displaying high expression of condensed F-actin within the perinuclear zone. Scale bar is 20 μm .

4.4 Chapter summary

Extensive screening of samples with a range of DNA FISH probes corresponding to ~44% of driver mutations in combination confirmed the presence of copy number increase in these driver mutations and represented the likely presence of cancer cells.

Preliminary western blot analysis suggested an adaptation of cells towards the mesenchymal phenotype. Further investigation with RNA FISH Affymetrix probes concludes that the genomic and proteomic expression of EMT markers were heterogeneous. This heterogeneity is validated by both pooled sample analysis with qRT-PCR and single cell characterization of EMT proteins with immunostaining.

Immunostaining of embryonic stem cell markers demonstrated the expression of Rex1 in the cultured samples, which suggest the presence of CSCs in these cultures. Under the absence of either microwells or hypoxia, relative proportion of CD44+/CD24- (phenotype of breast CSCs) was reduced as compared to cells cultured under normoxia or in non-tapered microwells.

The pathways influencing proliferation of CTCs have not been investigated. qRT-PCR analysis of cultured CTCs suggested the role of the Notch pathway, due to increased

HIF-1 α and SNAIL-1 expressions. SNAIL-1 is also termed as the ‘survival factor’ that leads to protective traits and induce partial G1/S cell-cycle arrest (Barrallo-Gimeno and Nieto 2005). Cell cycle arrest in Day 14 cultured samples were confirmed with PI staining under flow cytometry analysis.

Despite undergoing cell cycle arrest, some samples could be induced to form spheroids after being transferred to fresh Geltrex® or non-adherent dishes.

Chapter 5 Clinical Utility of CTC cultures

5.1 Sample cohort

CTC counts have been reported to correlate negatively with patient survival (Cristofanilli et al. 2005, de Bono et al. 2008). Having optimized the culture conditions, it was determined if the presence of clusters is predictive of a patient's survival or response to treatment. To date, 173 blood samples of 10 ml each from a total of 60 patients with clinically measurable tumors, classified under locally advanced (P2A/B and PCL cohorts) or metastatic (CTB cohort) breast cancer, were screened for this study. These samples were obtained at different time points (pre or post onset) of the current treatment regime. The demographic details of these patients are summarized in **Table 5.1**. Correlations between cluster formation and the respective demographic details were inconclusive due to the low sample size.

Table 5.1 Demographic details of patients (n=60) with locally advanced or metastatic breast cancer. ILC = Invasive Lobular Carcinoma; IDC = Invasive Ductal Carcinoma; AJCC = American Joint Committee on Cancer; ER = Oestrogen receptor; PR = Progesterone receptor; HER2 = Human Epidermal Growth Factor Receptor 2; AC = Doxorubicin /Cyclophosphamide.

| Age (years) | | |
|----------------------------------|-------|-------|
| Median | 47.5 | |
| Range | 33-78 | |
| Race | | |
| Chinese | 38 | 63.3% |
| Indian | 5 | 8.3% |
| Malay | 11 | 18.3% |
| Others | 6 | 10% |
| Histology | | |
| IDC | 49 | 81.7% |
| ILC or IDC with lobular features | 5 | 8.3% |
| Others | 6 | 10% |
| tumor grade | | |
| 1 | 3 | 5% |
| 2 | 18 | 30% |
| 3 | 35 | 58.3% |
| Not specified | 4 | 6.7% |
| Metastatic disease | | |
| Yes | 25 | 41.7% |
| No | 35 | 58.3% |
| AJCC stage | | |
| I | 0 | 0% |
| II | 16 | 26.7% |
| III | 19 | 31.7% |
| IV | 25 | 41.7% |
| ER status | | |
| Negative | 21 | 35% |
| Positive | 39 | 65% |
| PR status | | |
| Negative | 18 | 30% |
| Positive | 42 | 70% |
| HER2 status | | |
| Negative | 47 | 78.3% |
| Positive | 13 | 21.7% |
| Treatment regimen | | |
| AC | 15 | 25% |
| AC+Sunitinib | 16 | 26.7% |
| Paclitaxel/carboplatin/lapatinib | 7 | 11.7% |
| Others | 22 | 36.7% |

5.2 Evaluation and tabulating of results

To examine possible correlations between cluster formation and patient prognosis, details of each individual sample were mapped and contrasted to the presence of cluster after 2 weeks culture (see **Appendix Tables A1.1-1.4**). Positive samples were marked as Y, while negative samples were marked N.

5.2.1 Metastatic cohort (CTB)

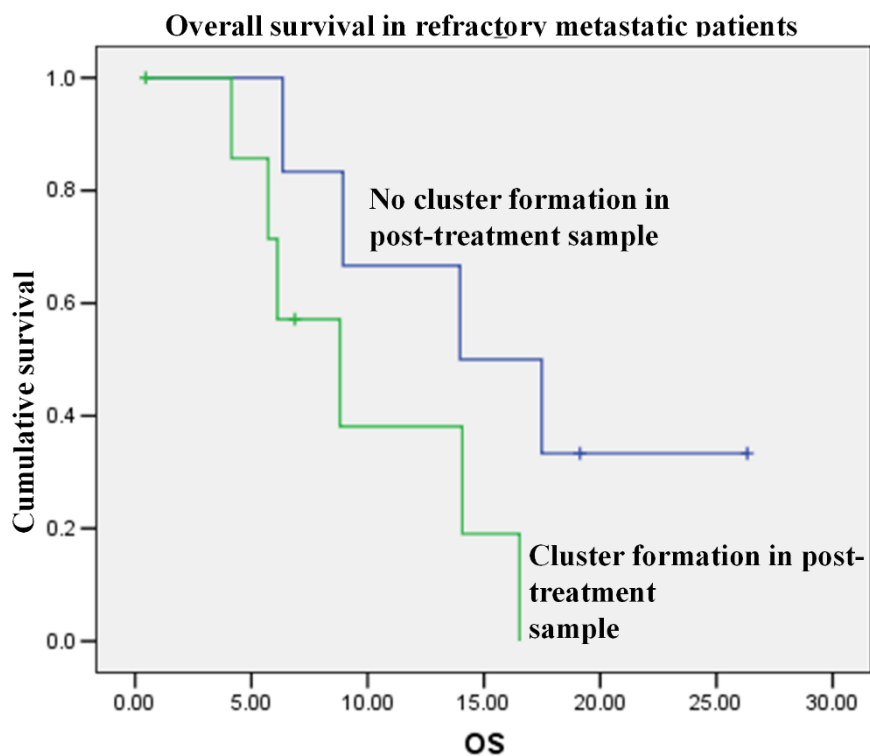
The refractory metastatic cohort consisted of 30 samples from 22 patients enrolled when they presented with progressive disease after their last treatment regimen, but before commencing with a new treatment regimen (chemotherapy, endocrine therapy or radiotherapy) (see **Appendix Table A1.1**). Of which, 73.3% of all samples formed clusters in culture, and more than half came from pre-treatment samples (14/22, 63.6% of samples). Of the 8 patients with samples provided at both pre-treatment and post-treatment time points, 6 patients had positive pre-treatment samples, and 33.3% (2/6) of them had a negative post-treatment sample. These 2 patients either had radiological responsive or stable disease ($p=0.308$). For the other 4 patients, 50% (2/4) had early radiological progressive disease while one was not accessed. These suggest that cluster formation may correlate with poorer prognosis.

To further verify this, a Kaplan–Meier survival analysis was performed on the 14 samples obtained at post-treatment time points (**Table 5.2**).

Table 5.2 List of 14 post-treatment samples from patients with refractory cancer computed for survival statistics in Figure 5B.

| Sample | ID | Survived | With early radiological progressive disease (within 3 months) | OS (months) | Cluster |
|--------|---------|----------|---|-------------|---------|
| 1 | CTB 002 | Y | Y | 28.41 | N |
| 2 | CTB 004 | N | Y | 13.98 | N |
| 3 | CTB 005 | N | Y | 8.81 | Y |
| 4 | CTB 006 | N | N | 5.72 | Y |
| 5 | CTB 007 | N | Y | 4.14 | Y |
| 6 | CTB 009 | N | Y | 6.12 | Y |
| 7 | CTB 012 | N | Y | 8.94 | N |
| 8 | CTB 014 | N | NA | 16.54 | Y |
| 9 | CTB 015 | N | Radiological response after 2 months | 6.35 | N |
| 10 | CTB 016 | Y | N | 16.97 | N |
| 11 | CTB 017 | Y | N | 21.21 | N |
| 12 | CTB 019 | N | N | 14.21 | Y |
| 13 | CTB 026 | Y | N | 8.22 | Y |
| 14 | CTB 029 | Y | NA | 5.56 | Y |

Graphical representation of the data confirmed that cluster formation correlated with shorter overall survival in patients (**Figure 5.1**). Patients providing samples that led to clusters experienced a mean survival period of 9.8 months (95% confidence interval (CI), 5.9-13.7), while patients who provided samples that did not lead to clusters had a longer mean survival period of 16.6 months (95% CI, 10.4-22.8; log rank p-value, 0.087). Further Cox regression (investigation of multiple variables) or adjusted analyses (to other variables) were not carried out due to the small sample size. Although the results were not statistically significant (due to small sample size), these findings nevertheless provided intriguing clinical utility for CTC cultures.



| Months | 0 | 5 | 10 | 15 | 20 | 25 |
|----------------------|----|----|----|----|----|----|
| Number at risk | 14 | 12 | 6 | 4 | 2 | 1 |
| No cluster formation | 6 | 6 | 4 | 3 | 2 | 1 |
| Cluster formation | 8 | 6 | 2 | 1 | 0 | 0 |

Figure 5.1 Graphical representation of the Kaplan–Meier survival analysis. Comparison of overall (cumulative) survival in refractory metastatic patients (CTB cohort) who provided samples at post treatment time points against cluster formation (n=14). Data is summarized in separated table (below).

5.2.2 Locally advanced patients (PCL and P2A/B cohorts)

The locally advanced cohort consisted of samples from two treatment regimes. In the PCL (Paclitaxel+carboplatin+lapatinib) treated cohort, 7 patients were enrolled and 28 samples were obtained at either single or multiple time points (see **Appendix Table A1.2**). Of which, 78.6% of all samples formed clusters in culture, and cluster formation was also progressively reduced in samples obtained at later treatment time points (Pre-treatment and <3 weeks post-treatment: 100% (n=8); 6-9 weeks post-

treatment: 75% (n=8); pre- or post- surgery: 63.6% (n=11); $p<0.001$).

In the P2A/B cohorts (AC with or without intermittent sunitinib (sutent)), 31 patients were recruited and 115 samples were obtained at either single or multiple time points (see **Appendix Table A1.3**). Of which, 63.6% of all P2A samples and 61.7% of all P2B samples formed clusters in culture, and cluster formation was similarly reduced in samples of later treatment time points (**Figure 5.2**) (P2A: Pre-treatment – 90.9% (n=11); 2-3 weeks post-treatment: 80% (n=20); 6-11 weeks post-treatment: 47.1% (n=17); pre- or post- surgery: 0% (n=6); $p<0.001$ and P2B: Pre-treatment and post sutent pre AC – 83.3% (n=24); 2-3 weeks post-treatment: 72.2% (n=18); 6-11 weeks post-treatment: 28.6% (n=14); pre- or post- surgery: 0% (n=4); $p<0.001$). These findings further support the possibility that the potential of CTC cluster formation could be used as an early predictor of treatment response.

Intriguingly, for the P2A cohort, 66.6% pre-treatment samples (n=3) which did not yield clusters came from patients with invasive lobular carcinoma (ILC). The other P2A/B samples (n=3; 2 from 2-3 weeks post-treatment, 1 from post-surgery) from patients with ILC also did not form clusters, with the exception of one post-treatment sample from the P2A cohort. These suggest that the current CTC culture conditions might not be able to promote growth of certain cancer subtypes.

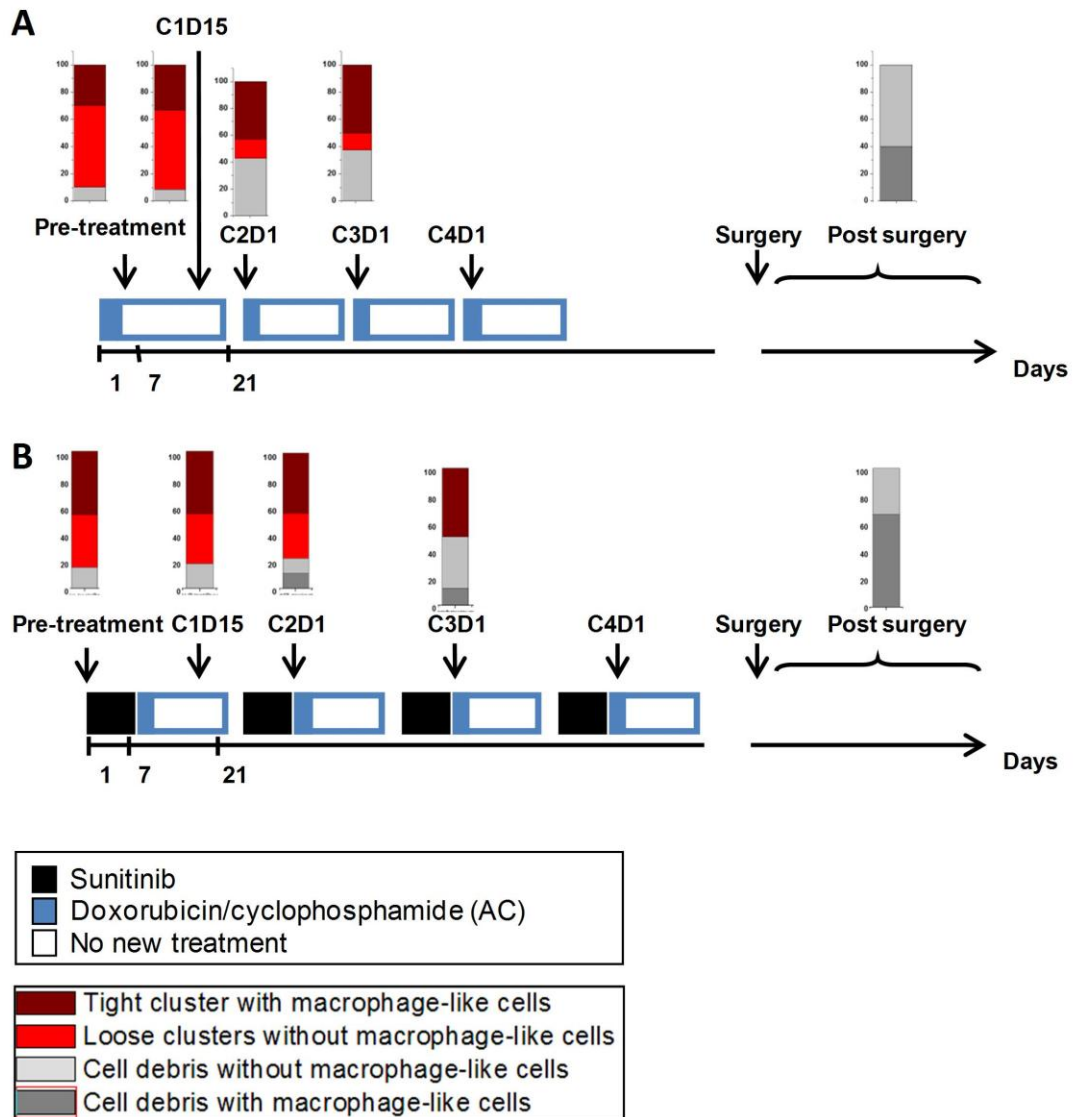


Figure 5.2 Clinical correlation of cluster formation with patient survival. Treatment schedule for the patients (n=31) receiving Doxorubicin/cyclophosphamide (AC) (A) without or (B) with Sunitinib. Cluster formation is reduced during therapy cycles, reflecting response to chemotherapy for treatment efficacy.

5.2.3 Cluster formation in early-stage cancer samples (CES cohort)

From the metastatic and locally advanced cohorts, the overall cluster formation frequency was 66.5% (n=173). This is significantly higher than previously reported CTC culture techniques (**Table 1.3**). In fact, the culture protocol was able to identify putative CK+ CTCs (cluster formation) from samples with initial negligible amount of CK+ CTCs (**Table 5.3**).

Table 5.3 CK+ CTC cell count ml⁻¹ of blood

| Sample no | CK+ cell count ml ⁻¹ of blood | | Amplification (fold change) |
|-----------|--|--------|-----------------------------|
| | Day 0 | Day 14 | |
| 1 | 220 | 6912 | 31.4 |
| 2 | 165 | 6451 | 39 |
| 3 | 154 | 1578 | 10.2 |
| 4 | 120 | 1901 | 15.8 |
| 5 | 104 | 4506 | 43.6 |
| 6 | 103 | 512 | 5 |
| 7 | 77 | 666 | 8.6 |
| 8 | 51 | 307 | 6 |
| 9 | 0 | 1741 | NA |
| 10 | 0 | 614 | NA |

Since the relapse of early stage breast cancer is prevalent in this country (Saxena et al. 2012), blood samples from patients with stage IA–IIIC cancer were obtained subsequently to evaluate the ability to detect cancer in the early onset. 53 samples were obtained from 32 patients (with no clinically measurable tumor) after surgery (see **Appendix Table A1.4**). 43.4% of all samples generated clusters, an observation more prevalent in patients with pathological involvement of 4 or more lymph nodes (9/16 (56%)) compared with those with 0–3 lymph nodes (14/37 (38%); $p=0.214$). The metastasis to lymph nodes has been shown to predict prognosis and survival of patients (Trojani et al. 1987). Hence, it will be interesting to expand this study to obtain more statistically significant results.

Attempts to correlate cluster formation from cultured CTCs with time since surgery suggest that 10/20 (50%) of the samples taken shortly after surgery, but before adjuvant chemotherapy, formed clusters. For samples taken shortly after 3-6 months of adjuvant chemotherapy, cluster formation reduced to just 26% (6/23) but this rebounded to 70% (7/10) ($p=0.049$) for samples obtained 1 year post-adjuvant

chemotherapy. This suggests a potential risk of relapse in patients after chemotherapy. Among these ten samples (taken shortly after surgery but before adjuvant chemotherapy), cluster formation occurred in 2/4 (50%) of patients with pT1N0M0 disease as compared to 5/6 (83%) patients with higher pathological stage of the disease ($p=0.260$), which reflects the correlation between the cluster formation with disease stage.

5.3 Chapter Summary

173 blood samples of 10 ml each from a total of 60 patients with clinically measurable tumors were screened for this study. Overall cluster formation frequency was 66.5% ($n=173$). Putative CK+ CTCs could also be detected in cultured samples with initial negligible amount of CK+ CTCs. Cluster formation was reduced in samples of later treatment time points, which supports the possibility of monitoring CTC cluster formation as an early predictor of treatment response. Correlations between cluster formation and the respective demographic details (e.g. lymph node involvement) were inconclusive due to the low sample size.

For larger sample sets, verification was done with a two-way analysis of variance (ANOVA) (Finak et al.) for the two independent variables (culture positivity and patient survival status). 95% confidence intervals were determined. Patients providing samples that led to clusters experienced a mean survival period of 9.8 months (95% confidence interval (CI), 5.9-13.7), while patients who provided samples that did not lead to clusters had a longer mean survival period of 16.6 months (95% CI, 10.4-22.8; log rank p -value, 0.087). A Kaplan–Meier survival analysis was performed on the 14 samples obtained at post-treatment time points (**Table 5.2**). Graphical representation

of the data confirmed that cluster formation correlated with shorter overall survival in patients (**Figure 5.1**). Multivariate analysis of covariance (MANCOVA) for continuous independent variables requires large sample sizes and was not utilized in this study.

Samples taken from patients shortly after 3-6 months of adjuvant chemotherapy with early stage cancer demonstrated a reduction in cluster formation to 26% (6/23) but rebounded to 70% (7/10) ($p=0.049$) for samples obtained 1 year post-adjuvant chemotherapy. This suggests a potential risk of relapse in patients after chemotherapy. Cluster formation also occurred in a higher proportion (50%, $n=4$) of patients with pT1N0M0 disease as compared to (83%, $n=6$) patients with higher pathological stage of the disease ($p=0.260$), which reflects the correlation between the cluster formation with disease stage.

Although the results were not statistically significant (due to small sample size), these findings nevertheless provided intriguing clinical utility for CTC cultures.

Chapter 6: Conclusions and Future Work

6.1 Conclusions

Cancer metastasis often leads to mortality, and CTCs isolated from liquid biopsies may serve to illuminate our understanding of mechanisms underlying the spread of cancer. Evolving techniques for CTC culture could overcome limitations imposed by low sample sizes, thus presenting an unprecedented opportunity to carry out a wider range of downstream analysis that can eventually translate into utility for clinical or biological aspects.

The current study describes a novel method for the *in vitro* expansion of CTCs from patients with early stage, locally advanced or metastatic breast cancers. RBC-lysed blood samples were seeded into non-coated dishes patterned with tapered microwells (**Figures 2.2**) and maintained under hypoxic conditions. Within each microwell, cell clusters were observed for the positive samples by Day 14 of culture (**Figure 3.7**). These cultures could be harvested for characterization (**Figure 3.9**) or passage into 3D gel or non-adherent substrates for further proliferation into spheroids (**Figure 4.9**).

Resultant clusters cultured were heterogeneous in diameter and composition, comprising Small putative CTCs ($\leq 25 \mu\text{m}$; high N/C ratio; CD45⁻) and larger blood cells ($> 25 \mu\text{m}$; low N/C ratio; CD68⁺ or CD56⁺). The proportion of proliferating cells (Ki67⁺) and putative CTC counts (CK⁺) peaked in most samples at Day 14 of culture (**Figure 3.4**). A proportion of Small cells were detected with copy number increase in common breast cancer genes (attributing to ~44% of all subtypes) (Davies et al. 2002, Magbanua et al. 2012). Cultured CTCs also vary in terms of EMT status (**Figures 4.4, 4.6**), with a portion shifting towards the mesenchymal subtype under hypoxia and microwell conditions. This shift in EMT phenotype is likely to be

triggered by hypoxia, which induces EMT via up-regulation of HIF1- α (**Figure 4.10**).

Blood cells were known to be present as part of the tumor stroma, and play a role in promoting tumor growth (Cortez-Retamozo, 2012 #272). In these cultures, some residual blood cells, mainly macrophages or NK cells, were indeed detected as minority sub-populations (**Figures 3.13-3.17**). Although a correlation of blood cells with patient outcome was not established at this point of time, it is possible that the blood cells could serve as an alternative prognostic factor due to their link to inflammation and tumor progression, as reported in previous reports (Finak et al. 2008, Gajewski et al. 2013). The blood cells could have also acted as ‘nursing’ cells to provide the microenvironment (e.g. cytokine secretion) required to trigger the initial CTC proliferation.

Few techniques have reported the enrichment of viable CTCs. Previous culture methods focus on promoting proliferation via growth factor supplements and depend on spontaneous immortalization to yield robust cell lines (**Table 1.3**) (He et al. 2007, Gao et al. 2014, Yu et al. 2014) (He et al. 2007, Gao et al. 2014, Yu et al. 2014) (He et al. 2007, Gao et al. 2014, Yu et al. 2014) (He et al. 2007, Gao et al. 2014, Yu et al. 2014) (He et al. 2007, Gao et al. 2014, Yu et al. 2014) (He et al. 2007, Gao et al. 2014, Yu et al. 2014) (He et al. 2007, Gao et al. 2014, Yu et al. 2014) (He et al. 2007, Gao et al. 2014, Yu et al. 2014) (He et al. 2007, Gao et al. 2014, Yu et al. 2014) (He et al. 2007, Gao et al. 2014, Yu et al. 2014) . These methods are relatively costly, and unreliable for clinical evaluation due to their low culture efficiency. The development of a novel and sensitive enrichment technique is imperative for complete downstream profiling and utility of CTCs. Recent methods for the expansion of CTCs have been reported (**Table 1.3**); however these methods still exhibit low efficiency and often require generation of cell lines before utility can be achieved. The culture protocol described in this study allowed the characterization

of putative primary CTCs after 14 days in culture. Cluster formation correlated negatively with patient survival, suggesting its clinical relevance in cancer prognosis (**Figure 5.2**).

In this study, the proposed CTC culture method is unique in terms of the combinational use of tapered microwells and hypoxia, allowing consistent and rapid phenotyping (cluster or no cluster) after 2 weeks in culture. Tapered microwells provided a topography which shields cells from fluid shear forces, concentrating cellular secretions (which may provide a biochemical niche) and prevent accidental disturbance to cells during handling. The shape of the wells (unlike flat microwells) promotes cell clustering, further providing resemblance to its microenvironment niche. Minimal starting material (petri dishes, 2.5 ml blood sample per 60 mm dish) provides a cost effective method of CTC expansion and enrichment (with removal of most blood cells). Overall, absence of external factors, which may manipulate cells chemically and genetically, reduces the phenotypic changes incurred from *in vitro* maintenance of primary cells.

The short-term nature of this assay favors rapid phenotyping of cultures, enabling analysis of serial samples at real-time. Further simplification of the protocol will render the assay relevant to clinicians, who can monitor patient response with ease. It is possible that cluster size may also correlate with patient prognosis, and this parameter will be explored in future studies with a larger sample cohort. Characterization of primary cells in a short-term culture is also more advantageous than using cell lines, since prolonged culture and passaging often introduce dramatic changes in the cells' epigenetics and gene expression (Lacroix and Leclercq 2004, van

Staveren et al. 2009).

The culture assay led to two interesting findings. Firstly, CSC-like cells (CD44+/CD24- cells or Rex1+ cells) were detected in the cultures (**Figures 4.7-4.8**), and some cells were likely to be highly invasive (**Figure 4.11**). Secondly, cluster formation was reduced when a patient underwent certain drug regimens, which suggested the potential of this assay to reflect treatment efficacy (**Figure 5.2**). In addition, samples obtained from patients with early-stage cancer also led to clusters at a higher frequency than existing techniques for early stage cancer detection, thus hinting at the potential as a diagnostic technique for predicting relapse (see **Appendix Table 1.4**).

In summary, the CTC culture assay provides a unique and unbiased opportunity to expand and enrich rare cancer cells associated with unique parameters (e.g. stemness, tumorigenicity, resistance) of the metastatic cascade.

6.2 Future Work

Moving forward, the assay is currently in the process of evaluation with a larger breast sample cohort, as well as samples from other cancer types (e.g. non-small cell lung cancer, prostate, spinal and head and neck cancer), so as to validate clinical utility and flexibility of the protocol for use in other cancer types. Experiments from these trials are still ongoing and hence not mentioned in this study. It is anticipated that the use of the CTC culture assay will be focused on short-term evaluation purposes, as the current phenotypic changes in CTCs under prolonged culture *in vitro* have yet to be profiled.

6.2.1 Bench to bedside applications

Extensive research on CTCs has now fully demonstrated its independent prognostic relevance on patient survival in metastatic breast cancers (Bidard et al. 2014). Past attempts to alter treatment strategies to improve patient prognosis had been unsuccessful (Smerage et al. 2014), thus heightening the pressing need to develop novel therapeutic strategies.

EMT and CSCs are now explored to more clearly define their involvement in cancer progression and metastasis, as well as in the case of drug resistance and relapses after treatment (Tan et al. 2014). Components of EMT and CSC formation process may be investigated for use as novel drug targets. The next application of the CTC culture assay is to promote personalized treatment, via monitoring clinical treatment efficacy and to carry out drug screening of the CTC clusters obtained from respective patients *in vitro*. Future studies can be aimed to establish multivariate correlations of cluster or spheroid formation with cancer stage and treatment time-points. Finally, cultures can also be profiled to identify key EMT signatures via transcriptomics or genomics, which could open doors for the generation of novel diagnostic devices or therapeutic targets.

6.2.2 Insights on metastatic cascade

Our knowledge of the dynamics of CTCs and their colonization pattern in humans is still fragmentary (Pantel and Alix-Panabieres 2007). To facilitate understanding of these mechanisms, spheroids obtained from this study may be stained with fluorescence dyes and injected into humanized murine mouse models or zebrafish models of metastasis for real-time monitoring of their interaction with epithelial or blood cells, and transit (persist/becomes trapped or extravasate) in blood vessels.

Alternatively, the cultures can also be seeded into disease-on-a-chip devices for the investigation of intravasation or extravasation processes *in vitro* (Aref et al. 2013).

6.2.3 CTC profiling

It is now widely accepted that CTCs exhibit strong heterogeneity including different morphologies and distinct genomic alterations. Differences are also noted in terms of epigenetics and proteomics. However, due to challenges for culturing CTCs, there are currently only a few studies concerning point mutations in cultured CTCs. Of which, these studies either report the presence of heterogeneity (Zhang et al. 2013, Gao et al. 2014) and/or low frequency (Yu et al. 2014) of the mutations detected.

A preliminary screen with three of the cultured samples using the Cytoscan HD analysis revealed a list of major genome-wide alterations (data not shown). Plans are currently being made to increase the number of samples and improve the signal versus noise ratio by lowering DNA contamination (removal of residual blood cells via negative selection with FACS). High resolution sequencing will also be attempted to detect single nucleotide polymorphism (SNP) markers, so that samples with contaminating (and usually degraded) DNA may also be processed.

Clearly there is an urgent need to further improve phenotyping and genotyping of CTCs in relation to prognosis and adaptive treatment. In addition CTCs can also be used to evaluate their physical properties such as measurement of membrane elasticity using micropipette aspiration or AFM techniques. These additional studies can provide further understanding on how CTCs can evade arrest in capillaries, persist in circulation and eventually localize to specific organs.

References

- Aceto, N., A. Bardia, D. T. Miyamoto, M. C. Donaldson, B. S. Wittner, J. A. Spencer, M. Yu, A. Pely, A. Engstrom, H. Zhu, B. W. Brannigan, R. Kapur, S. L. Stott, T. Shioda, S. Ramaswamy, D. T. Ting, C. P. Lin, M. Toner, D. A. Haber and S. Maheswaran (2014). "Circulating tumor cell clusters are oligoclonal precursors of breast cancer metastasis." Cell **158**(5): 1110-1122.
- Adams, D. L., S. S. Martin, R. K. Alpaugh, M. Charpentier, S. Tsai, R. C. Bergan, I. M. Ogden, W. Catalona, S. Chumsri, C. M. Tang and M. Cristofanilli (2014). "Circulating giant macrophages as a potential biomarker of solid tumors." Proc Natl Acad Sci U S A **111**(9): 3514-3519.
- Aguirre-Ghiso, J. A. (2007). "Models, mechanisms and clinical evidence for cancer dormancy." Nat Rev Cancer **7**(11): 834-846.
- Akalay, I., B. Janji, M. Hasmim, M. Z. Noman, F. Andre, P. De Cremoux, P. Bertheau, C. Badoual, P. Vielh, A. K. Larsen, M. Sabbah, T. Z. Tan, J. H. Keira, N. T. Hung, J. P. Thiery, F. Mami-Chouaib and S. Chouaib (2013). "Epithelial-to-mesenchymal transition and autophagy induction in breast carcinoma promote escape from T-cell-mediated lysis." Cancer Res **73**(8): 2418-2427.
- Al-Hajj, M., M. S. Wicha, A. Benito-Hernandez, S. J. Morrison and M. F. Clarke (2003). "Prospective identification of tumorigenic breast cancer cells." Proc Natl Acad Sci U S A **100**(7): 3983-3988.
- Alix-Panabieres, C. and K. Pantel (2014). "Technologies for detection of circulating tumor cells: facts and vision." Lab Chip **14**(1): 57-62.
- Alix-Panabieres, C., J. P. Vendrell, O. Pelle, X. Rebillard, S. Riethdorf, V. Muller, M. Fabbro and K. Pantel (2007). "Detection and characterization of putative metastatic precursor cells in cancer patients." Clin Chem **53**(3): 537-539.
- Allan, A. L., S. A. Vantghem, A. B. Tuck, A. F. Chambers, I. H. Chin-Yee and M. Keeney (2005). "Detection and quantification of circulating tumor cells in mouse models of human breast cancer using immunomagnetic enrichment and multiparameter flow cytometry." Cytometry A **65**(1): 4-14.
- Allard, W. J., J. Matera, M. C. Miller, M. Repollet, M. C. Connelly, C. Rao, A. G. Tibbe, J. W. Uhr and L. W. Terstappen (2004). "Tumor cells circulate in the peripheral blood of all major carcinomas but not in healthy subjects or patients with nonmalignant diseases." Clin Cancer Res **10**(20): 6897-6904.
- Alunni-Fabroni, M. and M. T. Sandri (2010). "Circulating tumour cells in clinical practice: Methods of detection and possible characterization." Methods **50**(4): 289-297.
- Andreopoulou, E., L. Y. Yang, K. M. Rangel, J. M. Reuben, L. Hsu, S. Krishnamurthy, V. Valero, H. A. Fritsche and M. Cristofanilli (2012). "Comparison of assay methods for detection of circulating tumor cells in metastatic breast cancer: AdnaGen AdnaTest

BreastCancer Select/Detect versus Veridex CellSearch system." Int J Cancer **130**(7): 1590-1597.

Ansieau, S., J. Bastid, A. Doreau, A. P. Morel, B. P. Bouchet, C. Thomas, F. Fauvet, I. Puisieux, C. Doglioni, S. Piccinin, R. Maestro, T. Voeltzel, A. Selmi, S. Valsesia-Wittmann, C. Caron de Fromental and A. Puisieux (2008). "Induction of EMT by twist proteins as a collateral effect of tumor-promoting inactivation of premature senescence." Cancer Cell **14**(1): 79-89.

Anthea, M., R. L. J. Hopkins, C. W. McLaughlin, S. Johnson, M. Q. Warner, D. LaHart and J. D. Wright (1993). *Human Biology and Health*. Englewood Cliffs, New Jersey, USA, Prentice Hall.

Aref, A. R., R. Y. Huang, W. Yu, K. N. Chua, W. Sun, T. Y. Tu, J. Bai, W. J. Sim, I. K. Zervantonakis, J. P. Thiery and R. D. Kamm (2013). "Screening therapeutic EMT blocking agents in a three-dimensional microenvironment." Integr Biol (Camb) **5**(2): 381-389.

Armstrong, A. J., M. S. Marengo, S. Oltean, G. Kemeny, R. L. Bitting, J. D. Turnbull, C. I. Herold, P. K. Marcom, D. J. George and M. A. Garcia-Blanco (2011). "Circulating tumor cells from patients with advanced prostate and breast cancer display both epithelial and mesenchymal markers." Mol Cancer Res **9**(8): 997-1007.

Ashworth, T. R. (1869). "A case of cancer in which cells similar to those in the tumours were seen in the blood after death." Aust Med J : **14**: 146-149.

Bacelli, I., A. Schneeweiss, S. Riethdorf, A. Stenzinger, A. Schillert, V. Vogel, C. Klein, M. Saini, T. Bauerle, M. Wallwiener, T. Holland-Letz, T. Hofner, M. Sprick, M. Scharpf, F. Marme, H. P. Sinn, K. Pantel, W. Weichert and A. Trumpp (2013). "Identification of a population of blood circulating tumor cells from breast cancer patients that initiates metastasis in a xenograft assay." Nat Biotechnol **31**(6): 539-544.

Balasubramanian, P., J. C. Lang, K. R. Jatana, B. Miller, E. Ozer, M. Old, D. E. Schuller, A. Agrawal, T. N. Teknos, T. A. Summers, Jr., M. B. Lustberg, M. Zborowski and J. J. Chalmers (2012). "Multiparameter analysis, including EMT markers, on negatively enriched blood samples from patients with squamous cell carcinoma of the head and neck." PLoS One **7**(7): e42048.

Barcellos-Hoff, M. H., D. Lyden and T. C. Wang (2013). "The evolution of the cancer niche during multistage carcinogenesis." Nat Rev Cancer **13**(7): 511-518.

Barrallo-Gimeno, A. and M. A. Nieto (2005). "The Snail genes as inducers of cell movement and survival: implications in development and cancer." Development **132**(14): 3151-3161.

Bashir, R. (2004). "BioMEMS: state-of-the-art in detection, opportunities and prospects." Adv Drug Deliv Rev **56**(11): 1565-1586.

Bhagat, A. A., H. Bow, H. W. Hou, S. J. Tan, J. Han and C. T. Lim (2010). "Microfluidics for cell separation." Med Biol Eng Comput **48**(10): 999-1014.

Bidard, F. C., D. J. Peeters, T. Fehm, F. Nole, R. Gisbert-Criado, D. Mavroudis, S. Grisanti, D. Generali, J. A. Garcia-Saenz, J. Stebbing, C. Caldas, P. Gazzaniga, L. Manso, R. Zamarchi, A. F. de Lascoiti, L. De Mattos-Arruda, M. Ignatiadis, R. Lebofsky, S. J. van Laere, F. Meier-Stiegen, M. T. Sandri, J. Vidal-Martinez, E. Politaki, F. Consoli, A. Bottini, E. Diaz-Rubio, J. Krell, S. J. Dawson, C. Raimondi, A. Rutten, W. Janni, E. Munzone, V. Caranana, S. Agelaki, C. Almici, L. Dirix, E. F. Solomayer, L. Zorzino, H. Johannes, J. S. Reis-Filho, K. Pantel, J. Y. Pierga and S. Michiels (2014). "Clinical validity of circulating tumour cells in patients with metastatic breast cancer: a pooled analysis of individual patient data." Lancet Oncol **15**(4): 406-414.

Biggs, M. J., R. G. Richards and M. J. Dalby (2010). "Nanotopographical modification: a regulator of cellular function through focal adhesions." Nanomedicine **6**(5): 619-633.

Borgen, E., B. Naume, J. M. Nesland, G. Kvalheim, K. Beiske, O. Fodstad, I. Diel, E. F. Solomayer, P. Theocharous, R. C. Coombes, B. M. Smith, E. Wunder, J. P. Marolleau, J. Garcia and K. Pantel (1999). "Standardization of the immunocytochemical detection of cancer cells in BM and blood: I. establishment of objective criteria for the evaluation of immunostained cells." Cytotherapy **1**(5): 377-388.

Brabletz, T. (2012). "EMT and MET in metastasis: where are the cancer stem cells?" Cancer Cell **22**(6): 699-701.

Braun, S., F. D. Vogl, B. Naume, W. Janni, M. P. Osborne, R. C. Coombes, G. Schlimok, I. J. Diel, B. Gerber, G. Gebauer, J. Y. Pierga, C. Marth, D. Oruzio, G. Wiedswang, E. F. Solomayer, G. Kundt, B. Strobl, T. Fehm, G. Y. Wong, J. Bliss, A. Vincent-Salomon and K. Pantel (2005). "A pooled analysis of bone marrow micrometastasis in breast cancer." N Engl J Med **353**(8): 793-802.

Brodland, D. G. and J. A. Zitelli (1992). "Mechanisms of metastasis." J Am Acad Dermatol **27**(1): 1-8.

Budd, G. T., M. Cristofanilli, M. J. Ellis, A. Stopeck, E. Borden, M. C. Miller, J. Matera, M. Repollet, G. V. Doyle, L. W. Terstappen and D. F. Hayes (2006). "Circulating tumor cells versus imaging--predicting overall survival in metastatic breast cancer." Clin Cancer Res **12**(21): 6403-6409.

Bui, M. and R. E. Reiter (1998). "Stem cell genes in androgen-independent prostate cancer." Cancer Metastasis Rev **17**(4): 391-399.

Butler, T. P. and P. M. Gullino (1975). "Quantitation of cell shedding into efferent blood of mammary adenocarcinoma." Cancer Res **35**(3): 512-516.

Carmeliet, P. and R. K. Jain (2011). "Molecular mechanisms and clinical applications of angiogenesis." Nature **473**(7347): 298-307.

Casazza, A., G. Di Conza, M. Wenes, V. Finisguerra, S. Deschoemaeker and M.

- Mazzone (2014). "Tumor stroma: a complexity dictated by the hypoxic tumor microenvironment." Oncogene **33**(14): 1743-1754.
- Chaffer, C. L. and R. A. Weinberg (2011). "A perspective on cancer cell metastasis." Science **331**(6024): 1559-1564.
- Chambers, A. F., A. C. Groom and I. C. MacDonald (2002). "Dissemination and growth of cancer cells in metastatic sites." Nat Rev Cancer **2**(8): 563-572.
- Chen, C. L., D. Mahalingam, P. Osmulski, R. R. Jadhav, C. M. Wang, R. J. Leach, T. C. Chang, S. D. Weitman, A. P. Kumar, L. Sun, M. E. Gaczynska, I. M. Thompson and T. H. Huang (2013). "Single-cell analysis of circulating tumor cells identifies cumulative expression patterns of EMT-related genes in metastatic prostate cancer." Prostate **73**(8): 813-826.
- Chen, J., N. Imanaka, J. Chen and J. D. Griffin (2010). "Hypoxia potentiates Notch signaling in breast cancer leading to decreased E-cadherin expression and increased cell migration and invasion." Br J Cancer **102**(2): 351-360.
- Cho, E. H., M. Wendel, M. Lutgen, C. Yoshioka, D. Marrinucci, D. Lazar, E. Schram, J. Nieva, L. Bazhenova, A. Morgan, A. H. Ko, W. M. Korn, A. Kolatkar, K. Bethel and P. Kuhn (2012). "Characterization of circulating tumor cell aggregates identified in patients with epithelial tumors." Phys Biol **9**(1): 016001.
- Christofori, G. (2006). "New signals from the invasive front." Nature **441**(7092): 444-450.
- Clevers, H. (2011). "The cancer stem cell: premises, promises and challenges." Nat Med **17**(3): 313-319.
- Coen, J. J., A. L. Zietman, H. Thakral and W. U. Shipley (2002). "Radical radiation for localized prostate cancer: local persistence of disease results in a late wave of metastases." J Clin Oncol **20**(15): 3199-3205.
- Cohen, S. J., C. J. Punt, N. Iannotti, B. H. Saidman, K. D. Sabbath, N. Y. Gabrail, J. Picus, M. Morse, E. Mitchell, M. C. Miller, G. V. Doyle, H. Tissing, L. W. Terstappen and N. J. Meropol (2008). "Relationship of circulating tumor cells to tumor response, progression-free survival, and overall survival in patients with metastatic colorectal cancer." J Clin Oncol **26**(19): 3213-3221.
- Coumans, F. A., S. Siesling and L. W. Terstappen (2013). "Detection of cancer before distant metastasis." BMC Cancer **13**: 283.
- Cristofanilli, M., G. T. Budd, M. J. Ellis, A. Stopeck, J. Matera, M. C. Miller, J. M. Reuben, G. V. Doyle, W. J. Allard, L. W. Terstappen and D. F. Hayes (2004). "Circulating tumor cells, disease progression, and survival in metastatic breast cancer." N Engl J Med **351**(8): 781-791.
- Cristofanilli, M., D. F. Hayes, G. T. Budd, M. J. Ellis, A. Stopeck, J. M. Reuben, G. V. Doyle, J. Matera, W. J. Allard, M. C. Miller, H. A. Fritsche, G. N. Hortobagyi and L.

W. Terstappen (2005). "Circulating tumor cells: a novel prognostic factor for newly diagnosed metastatic breast cancer." J Clin Oncol **23**(7): 1420-1430.

Curcio, E., S. Salerno, G. Barbieri, L. De Bartolo, E. Drioli and A. Bader (2007). "Mass transfer and metabolic reactions in hepatocyte spheroids cultured in rotating wall gas-permeable membrane system." Biomaterials **28**(36): 5487-5497.

Davidson, B., C. G. Trope and R. Reich (2012). "Epithelial-mesenchymal transition in ovarian carcinoma." Front Oncol **2**: 33.

Davies, H., G. R. Bignell, C. Cox, P. Stephens, S. Edkins, S. Clegg, J. Teague, H. Woffendin, M. J. Garnett, W. Bottomley, N. Davis, E. Dicks, R. Ewing, Y. Floyd, K. Gray, S. Hall, R. Hawes, J. Hughes, V. Kosmidou, A. Menzies, C. Mould, A. Parker, C. Stevens, S. Watt, S. Hooper, R. Wilson, H. Jayatilake, B. A. Gusterson, C. Cooper, J. Shipley, D. Hargrave, K. Pritchard-Jones, N. Maitland, G. Chenevix-Trench, G. J. Riggins, D. D. Bigner, G. Palmieri, A. Cossu, A. Flanagan, A. Nicholson, J. W. Ho, S. Y. Leung, S. T. Yuen, B. L. Weber, H. F. Seigler, T. L. Darrow, H. Paterson, R. Marais, C. J. Marshall, R. Wooster, M. R. Stratton and P. A. Futreal (2002). "Mutations of the BRAF gene in human cancer." Nature **417**(6892): 949-954.

de Bono, J. S., H. I. Scher, R. B. Montgomery, C. Parker, M. C. Miller, H. Tissing, G. V. Doyle, L. W. Terstappen, K. J. Pienta and D. Raghavan (2008). "Circulating tumor cells predict survival benefit from treatment in metastatic castration-resistant prostate cancer." Clin Cancer Res **14**(19): 6302-6309.

Deng, G., M. Herrler, D. Burgess, E. Manna, D. Krag and J. F. Burke (2008). "Enrichment with anti-cytokeratin alone or combined with anti-EpCAM antibodies significantly increases the sensitivity for circulating tumor cell detection in metastatic breast cancer patients." Breast Cancer Res **10**(4): R69.

Di Carlo, D., D. Irimia, R. G. Tompkins and M. Toner (2007). "Continuous inertial focusing, ordering, and separation of particles in microchannels." Proc Natl Acad Sci U S A **104**(48): 18892-18897.

Du, Z., K. H. Cheng, M. W. Vaughn, N. L. Collie and L. S. Gollahon (2007). "Recognition and capture of breast cancer cells using an antibody-based platform in a microelectromechanical systems device." Biomed Microdevices **9**(1): 35-42.

Eramo, A., F. Lotti, G. Sette, E. Piloizzi, M. Biffoni, A. Di Virgilio, C. Conticello, L. Ruco, C. Peschle and R. De Maria (2008). "Identification and expansion of the tumorigenic lung cancer stem cell population." Cell Death Differ **15**(3): 504-514.

Erten, A., D. Hall, C. Hoh, H. S. Tran Cao, S. Kaushal, S. Esener, R. M. Hoffman, M. Bouvet, J. Chen, S. Kesari and M. Makale (2010). "Enhancing magnetic resonance imaging tumor detection with fluorescence intensity and lifetime imaging." J Biomed Opt **15**(6): 066012.

Eyler, C. E. and J. N. Rich (2008). "Survival of the fittest: cancer stem cells in therapeutic resistance and angiogenesis." J Clin Oncol **26**(17): 2839-2845.

Farace, F., C. Massard, N. Vimond, F. Drusch, N. Jacques, F. Billiot, A. Laplanche, A. Chauchereau, L. Lacroix, D. Planchard, S. Le Moulec, F. Andre, K. Fizazi, J. C. Soria and P. Vielh (2011). "A direct comparison of CellSearch and ISET for circulating tumour-cell detection in patients with metastatic carcinomas." Br J Cancer **105**(6): 847-853.

Fehm, T., A. Sagalowsky, E. Clifford, P. Beitsch, H. Saboorian, D. Euhus, S. Meng, L. Morrison, T. Tucker, N. Lane, B. M. Ghadimi, K. Heselmeyer-Haddad, T. Ried, C. Rao and J. Uhr (2002). "Cytogenetic evidence that circulating epithelial cells in patients with carcinoma are malignant." Clin Cancer Res **8**(7): 2073-2084.

Fehm, T., E. F. Solomayer, S. Meng, T. Tucker, N. Lane, J. Wang and G. Gebauer (2005). "Methods for isolating circulating epithelial cells and criteria for their classification as carcinoma cells." Cytotherapy **7**(2): 171-185.

Fidler, I. J. (1970). "Metastasis: quantitative analysis of distribution and fate of tumor embolilabeled with 125 I-5-iodo-2'-deoxyuridine." J Natl Cancer Inst **45**(4): 773-782.

Finak, G., N. Bertos, F. Pepin, S. Sadekova, M. Souleimanova, H. Zhao, H. Chen, G. Omeroglu, S. Meterissian, A. Omeroglu, M. Hallett and M. Park (2008). "Stromal gene expression predicts clinical outcome in breast cancer." Nat Med **14**(5): 518-527.

Fortier, A. M., E. Asselin and M. Cadrin (2013). "Keratin 8 and 18 loss in epithelial cancer cells increases collective cell migration and cisplatin sensitivity through claudin1 up-regulation." J Biol Chem **288**(16): 11555-11571.

Foulkes, W. D., M. J. Grainge, E. A. Rakha, A. R. Green and I. O. Ellis (2009). "Tumor size is an unreliable predictor of prognosis in basal-like breast cancers and does not correlate closely with lymph node status." Breast Cancer Res Treat **117**(1): 199-204.

Friedl, P. and D. Gilmour (2009). "Collective cell migration in morphogenesis, regeneration and cancer." Nat Rev Mol Cell Biol **10**(7): 445-457.

Friedl, P. and K. Wolf (2003). "Tumour-cell invasion and migration: diversity and escape mechanisms." Nat Rev Cancer **3**(5): 362-374.

Gadd, S. J. and L. K. Ashman (1983). "Binding of mouse monoclonal antibodies to human leukaemic cells via the Fc receptor: a possible source of 'false positive' reactions in specificity screening." Clin Exp Immunol **54**(3): 811-818.

Gajewski, T. F., H. Schreiber and Y. X. Fu (2013). "Innate and adaptive immune cells in the tumor microenvironment." Nat Immunol **14**(10): 1014-1022.

Gao, D., I. Vela, A. Sboner, P. J. Iaquinta, W. R. Karthaus, A. Gopalan, C. Dowling, J. N. Wanjala, E. A. Undvall, V. K. Arora, J. Wongvipat, M. Kossai, S. Ramazanoglu, L. P. Barboza, W. Di, Z. Cao, Q. F. Zhang, I. Sirota, L. Ran, T. Y. MacDonald, H. Beltran, J. M. Mosquera, K. A. Touijer, P. T. Scardino, V. P. Laudone, K. R. Curtis, D. E. Rathkopf, M. J. Morris, D. C. Danila, S. F. Slovin, S. B. Solomon, J. A. Eastham, P. Chi, B. Carver, M. A. Rubin, H. I. Scher, H. Clevers, C. L. Sawyers and Y. Chen

(2014). "Organoid cultures derived from patients with advanced prostate cancer." Cell **159**(1): 176-187.

Gascoyne, P. R., J. Noshari, T. J. Anderson and F. F. Becker (2009). "Isolation of rare cells from cell mixtures by dielectrophoresis." Electrophoresis **30**(8): 1388-1398.

Gerlinger, M., A. J. Rowan, S. Horswell, J. Larkin, D. Endesfelder, E. Gronroos, P. Martinez, N. Matthews, A. Stewart, P. Tarpey, I. Varela, B. Phillimore, S. Begum, N. Q. McDonald, A. Butler, D. Jones, K. Raine, C. Latimer, C. R. Santos, M. Nohadani, A. C. Eklund, B. Spencer-Dene, G. Clark, L. Pickering, G. Stamp, M. Gore, Z. Szallasi, J. Downward, P. A. Futreal and C. Swanton (2012). "Intratumor heterogeneity and branched evolution revealed by multiregion sequencing." N Engl J Med **366**(10): 883-892.

Gertler, R., R. Rosenberg, K. Fuehrer, M. Dahm, H. Nekarda and J. R. Siewert (2003). "Detection of circulating tumor cells in blood using an optimized density gradient centrifugation." Recent Results Cancer Res **162**: 149-155.

Gleghorn, J. P., E. D. Pratt, D. Denning, H. Liu, N. H. Bander, S. T. Tagawa, D. M. Nanus, P. A. Giannakakou and B. J. Kirby (2010). "Capture of circulating tumor cells from whole blood of prostate cancer patients using geometrically enhanced differential immunocapture (GEDI) and a prostate-specific antibody." Lab Chip **10**(1): 27-29.

Glinsky, V. V., G. V. Glinsky, O. V. Glinskii, V. H. Huxley, J. R. Turk, V. V. Mossine, S. L. Deutscher, K. J. Pienta and T. P. Quinn (2003). "Intravascular metastatic cancer cell homotypic aggregation at the sites of primary attachment to the endothelium." Cancer Res **63**(13): 3805-3811.

Goeminne, J. C., T. Guillaume and M. Symann (2000). "Pitfalls in the detection of disseminated non-hematological tumor cells." Ann Oncol **11**(7): 785-792.

Gupta, G. P. and J. Massague (2006). "Cancer metastasis: building a framework." Cell **127**(4): 679-695.

Gupta, V., I. Jafferji, M. Garza, V. O. Melnikova, D. K. Hasegawa, R. Pethig and D. W. Davis (2012). "ApoStream(), a new dielectrophoretic device for antibody independent isolation and recovery of viable cancer cells from blood." Biomicrofluidics **6**(2): 24133.

Hao, L., J. Lawrence, Y. F. Phua, K. S. Chian, G. C. Lim and H. Y. Zheng (2005). "Enhanced human osteoblast cell adhesion and proliferation on 316 LS stainless steel by means of CO2 laser surface treatment." J Biomed Mater Res B Appl Biomater **73**(1): 148-156.

Hautkappe, A. L., M. Lu, H. Mueller, A. Bex, A. Harstrick, M. Roggendorf and H. Ruebben (2000). "Detection of germ-cell tumor cells in the peripheral blood by nested reverse transcription-polymerase chain reaction for alpha-fetoprotein-messenger RNA and beta human chorionic gonadotropin-messenger RNA." Cancer Res **60**(12): 3170-3174.

Hayes, D. F., M. Cristofanilli, G. T. Budd, M. J. Ellis, A. Stopeck, M. C. Miller, J. Matera, W. J. Allard, G. V. Doyle and L. W. Terstappen (2006). "Circulating tumor cells at each follow-up time point during therapy of metastatic breast cancer patients predict progression-free and overall survival." Clin Cancer Res **12**(14 Pt 1): 4218-4224.

He, W., H. Wang, L. C. Hartmann, J. X. Cheng and P. S. Low (2007). "In vivo quantitation of rare circulating tumor cells by multiphoton intravital flow cytometry." Proc Natl Acad Sci U S A **104**(28): 11760-11765.

Heddleston, J. M., Z. Li, R. E. McLendon, A. B. Hjelmeland and J. N. Rich (2009). "The hypoxic microenvironment maintains glioblastoma stem cells and promotes reprogramming towards a cancer stem cell phenotype." Cell Cycle **8**(20): 3274-3284.

Herlyn, M., Z. Steplewski, D. Herlyn and H. Koprowski (1979). "Colorectal carcinoma-specific antigen: detection by means of monoclonal antibodies." Proc Natl Acad Sci U S A **76**(3): 1438-1442.

Hirschhaeuser, F., H. Menne, C. Dittfeld, J. West, W. Mueller-Klieser and L. A. Kunz-Schughart (2010). "Multicellular tumor spheroids: an underestimated tool is catching up again." J Biotechnol **148**(1): 3-15.

Ho, M. M., A. V. Ng, S. Lam and J. Y. Hung (2007). "Side population in human lung cancer cell lines and tumors is enriched with stem-like cancer cells." Cancer Res **67**(10): 4827-4833.

Hosler, B. A., M. B. Rogers, C. A. Kozak and L. J. Gudas (1993). "An octamer motif contributes to the expression of the retinoic acid-regulated zinc finger gene Rex-1 (Zfp-42) in F9 teratocarcinoma cells." Mol Cell Biol **13**(5): 2919-2928.

Hosokawa, M., H. Kenmotsu, Y. Koh, T. Yoshino, T. Yoshikawa, T. Naito, T. Takahashi, H. Murakami, Y. Nakamura, A. Tsuya, T. Shukuya, A. Ono, H. Akamatsu, R. Watanabe, S. Ono, K. Mori, H. Kanbara, K. Yamaguchi, T. Tanaka, T. Matsunaga and N. Yamamoto (2013). "Size-based isolation of circulating tumor cells in lung cancer patients using a microcavity array system." PLoS One **8**(6): e67466.

Hou, H. W., M. E. Warkiani, B. L. Khoo, Z. R. Li, R. A. Soo, D. S. Tan, W. T. Lim, J. Han, A. A. Bhagat and C. T. Lim (2013). "Isolation and retrieval of circulating tumor cells using centrifugal forces." Sci Rep **3**: 1259.

Howard, E. W., S. C. Leung, H. F. Yuen, C. W. Chua, D. T. Lee, K. W. Chan, X. Wang and Y. C. Wong (2008). "Decreased adhesiveness, resistance to anoikis and suppression of GRP94 are integral to the survival of circulating tumor cells in prostate cancer." Clin Exp Metastasis **25**(5): 497-508.

Huang, R. Y., M. K. Wong, T. Z. Tan, K. T. Kuay, A. H. Ng, V. Y. Chung, Y. S. Chu, N. Matsumura, H. C. Lai, Y. F. Lee, W. J. Sim, C. Chai, E. Pietschmann, S. Mori, J. J. Low, M. Choolani and J. P. Thiery (2013). "An EMT spectrum defines an anoikis-resistant and spheroidogenic intermediate mesenchymal state that is sensitive to e-

cadherin restoration by a src-kinase inhibitor, saracatinib (AZD0530)." Cell Death Dis **4**: e915.

Hur, S. C., N. K. Henderson-MacLennan, E. R. McCabe and D. Di Carlo (2011). "Deformability-based cell classification and enrichment using inertial microfluidics." Lab Chip **11**(5): 912-920.

Husemann, Y., J. B. Geigl, F. Schubert, P. Musiani, M. Meyer, E. Burghart, G. Forni, R. Eils, T. Fehm, G. Riethmuller and C. A. Klein (2008). "Systemic spread is an early step in breast cancer." Cancer Cell **13**(1): 58-68.

Jiang, Y., B. N. Jahagirdar, R. L. Reinhardt, R. E. Schwartz, C. D. Keene, X. R. Ortiz-Gonzalez, M. Reyes, T. Lenvik, T. Lund, M. Blackstad, J. Du, S. Aldrich, A. Lisberg, W. C. Low, D. A. Largaespada and C. M. Verfaillie (2002). "Pluripotency of mesenchymal stem cells derived from adult marrow." Nature **418**(6893): 41-49.

Jordan, N. V., G. L. Johnson and A. N. Abell (2011). "Tracking the intermediate stages of epithelial-mesenchymal transition in epithelial stem cells and cancer." Cell Cycle **10**(17): 2865-2873.

Jung, U., K. E. Norman, K. Scharffetter-Kochanek, A. L. Beaudet and K. Ley (1998). "Transit time of leukocytes rolling through venules controls cytokine-induced inflammatory cell recruitment in vivo." J Clin Invest **102**(8): 1526-1533.

Kaganoi, J., Y. Shimada, M. Kano, T. Okumura, G. Watanabe and M. Imamura (2004). "Detection of circulating oesophageal squamous cancer cells in peripheral blood and its impact on prognosis." Br J Surg **91**(8): 1055-1060.

Kallergi, G., M. A. Papadaki, E. Politaki, D. Mavroudis, V. Georgoulas and S. Agelaki (2011). "Epithelial to mesenchymal transition markers expressed in circulating tumour cells of early and metastatic breast cancer patients." Breast Cancer Res **13**(3): R59.

Kalluri, R. and R. A. Weinberg (2009). "The basics of epithelial-mesenchymal transition." J Clin Invest **119**(6): 1420-1428.

Kang, M. K. and S. K. Kang (2007). "Tumorigenesis of chemotherapeutic drug-resistant cancer stem-like cells in brain glioma." Stem Cells Dev **16**(5): 837-847.

Kang, Y. and K. Pantel (2013). "Tumor cell dissemination: emerging biological insights from animal models and cancer patients." Cancer Cell **23**(5): 573-581.

Kang, Y., P. M. Siegel, W. Shu, M. Drobnjak, S. M. Kakonen, C. Cordon-Cardo, T. A. Guise and J. Massague (2003). "A multigenic program mediating breast cancer metastasis to bone." Cancer Cell **3**(6): 537-549.

Kasimir-Bauer, S., O. Hoffmann, D. Wallwiener, R. Kimmig and T. Fehm (2012). "Expression of stem cell and epithelial-mesenchymal transition markers in primary breast cancer patients with circulating tumor cells." Breast Cancer Res **14**(1): R15.

- Khoo, B. L., M. E. Warkiani, D. S. Tan, A. A. Bhagat, D. Irwin, D. P. Lau, A. S. Lim, K. H. Lim, S. S. Krisna, W. T. Lim, Y. S. Yap, S. C. Lee, R. A. Soo, J. Han and C. T. Lim (2014). "Clinical validation of an ultra high-throughput spiral microfluidics for the detection and enrichment of viable circulating tumor cells." PLoS One **9**(7): e99409.
- Kienast, Y., L. von Baumgarten, M. Fuhrmann, W. E. Klinkert, R. Goldbrunner, J. Herms and F. Winkler (2010). "Real-time imaging reveals the single steps of brain metastasis formation." Nat Med **16**(1): 116-122.
- Kim, J., J. Chu, X. Shen, J. Wang and S. H. Orkin (2008). "An extended transcriptional network for pluripotency of embryonic stem cells." Cell **132**(6): 1049-1061.
- Kowalewska, M., M. Chechlinska, S. Markowicz, P. Kober and R. Nowak (2006). "The relevance of RT-PCR detection of disseminated tumour cells is hampered by the expression of markers regarded as tumour-specific in activated lymphocytes." Eur J Cancer **42**(16): 2671-2674.
- Krivacic, R. T., A. Ladanyi, D. N. Curry, H. B. Hsieh, P. Kuhn, D. E. Bergsrud, J. F. Kepros, T. Barbera, M. Y. Ho, L. B. Chen, R. A. Lerner and R. H. Bruce (2004). "A rare-cell detector for cancer." Proc Natl Acad Sci U S A **101**(29): 10501-10504.
- Kruger, W. H., R. Jung, B. Detlefsen, S. Mumme, A. Badbaran, J. Brandner, H. Renges, N. Kroger and A. R. Zander (2001). "Interference of cytokeratin-20 and mammaglobin-reverse-transcriptase polymerase chain assays designed for the detection of disseminated cancer cells." Med Oncol **18**(1): 33-38.
- Kuntaegowdanahalli, S. S., A. A. Bhagat, G. Kumar and I. Papautsky (2009). "Inertial microfluidics for continuous particle separation in spiral microchannels." Lab Chip **9**(20): 2973-2980.
- Labelle, M., S. Begum and R. O. Hynes (2011). "Direct signaling between platelets and cancer cells induces an epithelial-mesenchymal-like transition and promotes metastasis." Cancer Cell **20**(5): 576-590.
- Lacroix, M. and G. Leclercq (2004). "Relevance of breast cancer cell lines as models for breast tumours: an update." Breast Cancer Res Treat **83**(3): 249-289.
- Lampin, M., C. Warocquier, C. Legris, M. Degrange and M. F. Sigot-Luizard (1997). "Correlation between substratum roughness and wettability, cell adhesion, and cell migration." J Biomed Mater Res **36**(1): 99-108.
- Lapidot, T., C. Sirard, J. Vormoor, B. Murdoch, T. Hoang, J. Caceres-Cortes, M. Minden, B. Paterson, M. A. Caligiuri and J. E. Dick (1994). "A cell initiating human acute myeloid leukaemia after transplantation into SCID mice." Nature **367**(6464): 645-648.
- Lee, A., J. Park, M. Lim, V. Sunkara, S. Y. Kim, G. H. Kim, M. H. Kim and Y. K. Cho (2014). "All-in-one centrifugal microfluidic device for size-selective circulating tumor

cell isolation with high purity." Anal Chem **86**(22): 11349-11356.

Lehmann-Che, J., F. Amira-Bouhidel, E. Turpin, M. Antoine, H. Soliman, L. Legres, C. Bocquet, R. Bernoud, E. Flandre, M. Varna, A. de Roquancourt, L. F. Plassa, S. Giacchetti, M. Espie, C. de Bazelaire, L. Cahen-Doidy, E. Bourstyn, A. Janin, H. de The and P. Bertheau (2011). "Immunohistochemical and molecular analyses of HER2 status in breast cancers are highly concordant and complementary approaches." Br J Cancer **104**(11): 1739-1746.

Li, A., T. S. Lim, H. Shi, J. Yin, S. J. Tan, Z. Li, B. C. Low, K. S. Tan and C. T. Lim (2011). "Molecular mechanistic insights into the endothelial receptor mediated cytoadherence of Plasmodium falciparum-infected erythrocytes." PLoS One **6**(3): e16929.

Li, X., M. T. Lewis, J. Huang, C. Gutierrez, C. K. Osborne, M. F. Wu, S. G. Hilsenbeck, A. Pavlick, X. Zhang, G. C. Chamness, H. Wong, J. Rosen and J. C. Chang (2008). "Intrinsic resistance of tumorigenic breast cancer cells to chemotherapy." J Natl Cancer Inst **100**(9): 672-679.

Li, Z., S. Bao, Q. Wu, H. Wang, C. Eyler, S. Sathornsumetee, Q. Shi, Y. Cao, J. Lathia, R. E. McLendon, A. B. Hjelmeland and J. N. Rich (2009). "Hypoxia-inducible factors regulate tumorigenic capacity of glioma stem cells." Cancer Cell **15**(6): 501-513.

Liotta, L. A., M. G. Saidel and J. Kleinerman (1976). "The significance of hematogenous tumor cell clumps in the metastatic process." Cancer Res **36**(3): 889-894.

Liu, J., Y. Tan, H. Zhang, Y. Zhang, P. Xu, J. Chen, Y. C. Poh, K. Tang, N. Wang and B. Huang (2012). "Soft fibrin gels promote selection and growth of tumorigenic cells." Nat Mater **11**(8): 734-741.

Loberg, R. D., Y. Fridman, B. A. Pienta, E. T. Keller, L. K. McCauley, R. S. Taichman and K. J. Pienta (2004). "Detection and isolation of circulating tumor cells in urologic cancers: a review." Neoplasia **6**(4): 302-309.

Loeb, S., A. Vellekoop, H. U. Ahmed, J. Catto, M. Emberton, R. Nam, D. J. Rosario, V. Scattoni and Y. Lotan (2013). "Systematic review of complications of prostate biopsy." Eur Urol **64**(6): 876-892.

Lu, H., K. R. Clauser, W. L. Tam, J. Frose, X. Ye, E. N. Eaton, F. Reinhardt, V. S. Donnemberg, R. Bhargava, S. A. Carr and R. A. Weinberg (2014). "A breast cancer stem cell niche supported by juxtacrine signalling from monocytes and macrophages." Nat Cell Biol **16**(11): 1105-1117.

Lu, J., T. Fan, Q. Zhao, W. Zeng, E. Zaslavsky, J. J. Chen, M. A. Frohman, M. G. Golightly, S. Madajewicz and W. T. Chen (2010). "Isolation of circulating epithelial and tumor progenitor cells with an invasive phenotype from breast cancer patients." Int J Cancer **126**(3): 669-683.

Luzzi, K. J., I. C. MacDonald, E. E. Schmidt, N. Kerkvliet, V. L. Morris, A. F.

Chambers and A. C. Groom (1998). "Multistep nature of metastatic inefficiency: dormancy of solitary cells after successful extravasation and limited survival of early micrometastases." Am J Pathol **153**(3): 865-873.

Machowska, M., K. Wachowicz, M. Sopel and R. Rzepecki (2014). "Nuclear location of tumor suppressor protein maspin inhibits proliferation of breast cancer cells without affecting proliferation of normal epithelial cells." BMC Cancer **14**: 142.

Magbana, M. J., E. V. Sosa, J. H. Scott, J. Simko, C. Collins, D. Pinkel, C. J. Ryan and J. W. Park (2012). "Isolation and genomic analysis of circulating tumor cells from castration resistant metastatic prostate cancer." BMC Cancer **12**: 78.

Mager, M. D., V. LaPointe and M. M. Stevens (2011). "Exploring and exploiting chemistry at the cell surface." Nat Chem **3**(8): 582-589.

Mani, S. A., W. Guo, M. J. Liao, E. N. Eaton, A. Ayyanan, A. Y. Zhou, M. Brooks, F. Reinhard, C. C. Zhang, M. Shipitsin, L. L. Campbell, K. Polyak, C. Brisken, J. Yang and R. A. Weinberg (2008). "The epithelial-mesenchymal transition generates cells with properties of stem cells." Cell **133**(4): 704-715.

Marrinucci, D., K. Bethel, D. Lazar, J. Fisher, E. Huynh, P. Clark, R. Bruce, J. Nieva and P. Kuhn (2010). "Cytomorphology of circulating colorectal tumor cells: a small case series." J Oncol **2010**: 861341.

Martin-Ramirez, J., M. Hofman, M. van den Biggelaar, R. P. Hebbel and J. Voorberg (2012). "Establishment of outgrowth endothelial cells from peripheral blood." Nat Protoc **7**(9): 1709-1715.

Mehes, G., A. Witt, E. Kubista and P. F. Ambros (2001). "Circulating breast cancer cells are frequently apoptotic." Am J Pathol **159**(1): 17-20.

Meng, S., D. Tripathy, E. P. Frenkel, S. Shete, E. Z. Naftalis, J. F. Huth, P. D. Beitsch, M. Leitch, S. Hoover, D. Euhus, B. Haley, L. Morrison, T. P. Fleming, D. Herlyn, L. W. Terstappen, T. Fehm, T. F. Tucker, N. Lane, J. Wang and J. W. Uhr (2004). "Circulating tumor cells in patients with breast cancer dormancy." Clin Cancer Res **10**(24): 8152-8162.

Minn, A. J., G. P. Gupta, P. M. Siegel, P. D. Bos, W. Shu, D. D. Giri, A. Viale, A. B. Olshen, W. L. Gerald and J. Massague (2005). "Genes that mediate breast cancer metastasis to lung." Nature **436**(7050): 518-524.

Mittal, S., I. Y. Wong, W. M. Deen and M. Toner (2012). "Antibody-functionalized fluid-permeable surfaces for rolling cell capture at high flow rates." Biophys J **102**(4): 721-730.

Moeller, H. C., M. K. Mian, S. Shrivastava, B. G. Chung and A. Khademhosseini (2008). "A microwell array system for stem cell culture." Biomaterials **29**(6): 752-763.

Molloy, T. J., A. J. Bosma and L. J. van't Veer (2008). "Towards an optimized platform for the detection, enrichment, and semi-quantitation circulating tumor cells."

Breast Cancer Res Treat **112**(2): 297-307.

Muller, V., N. Stahmann, S. Riethdorf, T. Rau, T. Zabel, A. Goetz, F. Janicke and K. Pantel (2005). "Circulating tumor cells in breast cancer: correlation to bone marrow micrometastases, heterogeneous response to systemic therapy and low proliferative activity." Clin Cancer Res **11**(10): 3678-3685.

Munz, M., C. Kieu, B. Mack, B. Schmitt, R. Zeidler and O. Gires (2004). "The carcinoma-associated antigen EpCAM upregulates c-myc and induces cell proliferation." Oncogene **23**(34): 5748-5758.

Nagao, K., J. Zhu, M. B. Heneghan, J. C. Hanson, M. I. Morasso, L. Tessarollo, S. Mackem and M. C. Udey (2009). "Abnormal placental development and early embryonic lethality in EpCAM-null mice." PLoS One **4**(12): e8543.

Nagrath, S., L. V. Sequist, S. Maheswaran, D. W. Bell, D. Irimia, L. Ulkus, M. R. Smith, E. L. Kwak, S. Digumarthy, A. Muzikansky, P. Ryan, U. J. Balis, R. G. Tompkins, D. A. Haber and M. Toner (2007). "Isolation of rare circulating tumour cells in cancer patients by microchip technology." Nature **450**(7173): 1235-1239.

Navin, N., J. Kendall, J. Troge, P. Andrews, L. Rodgers, J. McIndoo, K. Cook, A. Stepansky, D. Levy, D. Esposito, L. Muthuswamy, A. Krasnitz, W. R. McCombie, J. Hicks and M. Wigler (2011). "Tumour evolution inferred by single-cell sequencing." Nature **472**(7341): 90-94.

Nguyen, D. X., P. D. Bos and J. Massague (2009). "Metastasis: from dissemination to organ-specific colonization." Nat Rev Cancer **9**(4): 274-284.

Nikkhah, M., F. Edalat, S. Manoucheri and A. Khademhosseini (2012). "Engineering microscale topographies to control the cell-substrate interface." Biomaterials **33**(21): 5230-5246.

Nima, Z. A., M. Mahmood, Y. Xu, T. Mustafa, F. Watanabe, D. A. Nedosekin, M. A. Juratli, T. Fahmi, E. I. Galanzha, J. P. Nolan, A. G. Basnakian, V. P. Zharov and A. S. Biris (2014). "Circulating tumor cell identification by functionalized silver-gold nanorods with multicolor, super-enhanced SERS and photothermal resonances." Sci Rep **4**: 4752.

Nole, F., E. Munzone, L. Zorzino, I. Minchella, M. Salvatici, E. Botteri, M. Medici, E. Verri, L. Adamoli, N. Rotmensz, A. Goldhirsch and M. T. Sandri (2008). "Variation of circulating tumor cell levels during treatment of metastatic breast cancer: prognostic and therapeutic implications." Ann Oncol **19**(5): 891-897.

Onder, T. T., P. B. Gupta, S. A. Mani, J. Yang, E. S. Lander and R. A. Weinberg (2008). "Loss of E-cadherin promotes metastasis via multiple downstream transcriptional pathways." Cancer Res **68**(10): 3645-3654.

Ozkumur, E., A. M. Shah, J. C. Ciciliano, B. L. Emmink, D. T. Miyamoto, E. Brachtel, M. Yu, P. I. Chen, B. Morgan, J. Trautwein, A. Kimura, S. Sengupta, S. L. Stott, N. M. Karabacak, T. A. Barber, J. R. Walsh, K. Smith, P. S. Spuhler, J. P. Sullivan, R. J. Lee,

- D. T. Ting, X. Luo, A. T. Shaw, A. Bardia, L. V. Sequist, D. N. Louis, S. Maheswaran, R. Kapur, D. A. Haber and M. Toner (2013). "Inertial focusing for tumor antigen-dependent and -independent sorting of rare circulating tumor cells." Sci Transl Med **5**(179): 179ra147.
- Paget, S. (1989). "The distribution of secondary growths in cancer of the breast. 1889." Cancer Metastasis Rev **8**(2): 98-101.
- Pantel, K. and C. Alix-Panabieres (2007). "The clinical significance of circulating tumor cells." Nat Clin Pract Oncol **4**(2): 62-63.
- Pantel, K. and R. H. Brakenhoff (2004). "Dissecting the metastatic cascade." Nat Rev Cancer **4**(6): 448-456.
- Pantel, K., R. H. Brakenhoff and B. Brandt (2008). "Detection, clinical relevance and specific biological properties of disseminating tumour cells." Nat Rev Cancer **8**(5): 329-340.
- Pantel, K., R. J. Cote and O. Fodstad (1999). "Detection and clinical importance of micrometastatic disease." J Natl Cancer Inst **91**(13): 1113-1124.
- Pantel, K. and U. Woelfle (2005). "Detection and molecular characterisation of disseminated tumour cells: implications for anti-cancer therapy." Biochim Biophys Acta **1756**(1): 53-64.
- Peduzzi, P., J. Concato, A. R. Feinstein and T. R. Holford (1995). "Importance of events per independent variable in proportional hazards regression analysis. II. Accuracy and precision of regression estimates." J Clin Epidemiol **48**(12): 1503-1510.
- Polyak, K. (2011). "Heterogeneity in breast cancer." J Clin Invest **121**(10): 3786-3788.
- Racila, E., D. Euhus, A. J. Weiss, C. Rao, J. McConnell, L. W. Terstappen and J. W. Uhr (1998). "Detection and characterization of carcinoma cells in the blood." Proc Natl Acad Sci U S A **95**(8): 4589-4594.
- Rack, B., U. Andergassen, J. Neugebauer, J. Salmen, P. Hepp, H. Sommer, W. Lichtenegger, K. Friese, M. W. Beckmann, D. Hauner, H. Hauner and W. Janni (2010). "The German SUCCESS C Study - The First European Lifestyle Study on Breast Cancer." Breast Care (Basel) **5**(6): 395-400.
- Reuben, J. M., S. Krishnamurthy, W. Woodward and M. Cristofanilli (2008). "The role of circulating tumor cells in breast cancer diagnosis and prediction of therapy response." Expert Opin Med Diagn **2**(4): 339-348.
- Rhodes, L. V., J. W. Antoon, S. E. Muir, S. Elliott, B. S. Beckman and M. E. Burow (2010). "Effects of human mesenchymal stem cells on ER-positive human breast carcinoma cells mediated through ER-SDF-1/CXCR4 crosstalk." Mol Cancer **9**: 295.
- Riethdorf, S., H. Fritsche, V. Müller, T. Rau and B. R. Christian Schindlbeck⁶, Wolfgang Janni⁶, Cornelia Coith¹, Katrin Beck³, Fritz Jänicke³, Summer Jackson⁴,

- Terrie Gornet⁴, Massimo Cristofanilli⁵ and Klaus Pantel¹ (2007). "Detection of Circulating Tumor Cells in Peripheral Blood of Patients with Metastatic Breast Cancer: A Validation Study of the CellSearch System." Clin Cancer Res **13**: 920.
- Riethdorf, S., V. Muller, L. Zhang, T. Rau, S. Loibl, M. Komor, M. Roller, J. Huober, T. Fehm, I. Schrader, J. Hilfrich, F. Holms, H. Tesch, H. Eidtmann, M. Untch, G. von Minckwitz and K. Pantel (2010). "Detection and HER2 expression of circulating tumor cells: prospective monitoring in breast cancer patients treated in the neoadjuvant GeparQuattro trial." Clin Cancer Res **16**(9): 2634-2645.
- Riethdorf, S. and K. Pantel (2009). "Clinical relevance and current challenges of research on disseminating tumor cells in cancer patients." Breast Cancer Res **11 Suppl 3**: S10.
- Riethdorf, S., H. Wikman and K. Pantel (2008). "Review: Biological relevance of disseminated tumor cells in cancer patients." Int J Cancer **123**(9): 1991-2006.
- Ring, A. E., L. Zabaglo, M. G. Ormerod, I. E. Smith and M. Dowsett (2005). "Detection of circulating epithelial cells in the blood of patients with breast cancer: comparison of three techniques." Br J Cancer **92**(5): 906-912.
- Rosenblum, M. D. and R. R. Shivers (2000). "'Rings' of F-actin form around the nucleus in cultured human MCF7 adenocarcinoma cells upon exposure to both taxol and taxotere." Comp Biochem Physiol C Toxicol Pharmacol **125**(1): 121-131.
- Sahlgren, C., M. V. Gustafsson, S. Jin, L. Poellinger and U. Lendahl (2008). "Notch signaling mediates hypoxia-induced tumor cell migration and invasion." Proc Natl Acad Sci U S A **105**(17): 6392-6397.
- Saliba, A. E., L. Saias, E. Psychari, N. Minc, D. Simon, F. C. Bidard, C. Mathiot, J. Y. Pierga, V. Fraissier, J. Salamero, V. Saada, F. Farace, P. Vielh, L. Malaquin and J. L. Viovy (2010). "Microfluidic sorting and multimodal typing of cancer cells in self-assembled magnetic arrays." Proc Natl Acad Sci U S A **107**(33): 14524-14529.
- Saxena, N., M. Hartman, N. Bhoo-Pathy, J. N. Lim, T. C. Aw, P. Iau, N. A. Taib, S. C. Lee, C. H. Yip and H. M. Verkooijen (2012). "Breast cancer in South East Asia: comparison of presentation and outcome between a middle income and a high income country." World J Surg **36**(12): 2838-2846.
- Schilling, D., T. Todenhofer, J. Hennenlotter, C. Schwentner, T. Fehm and A. Stenzl (2012). "Isolated, disseminated and circulating tumour cells in prostate cancer." Nat Rev Urol **9**(8): 448-463.
- Shao, N., E. Wickstrom and B. Panchapakesan (2008). "Nanotube-antibody biosensor arrays for the detection of circulating breast cancer cells." Nanotechnology **19**(46): 465101.
- Sharma, S. V., D. Y. Lee, B. Li, M. P. Quinlan, F. Takahashi, S. Maheswaran, U. McDermott, N. Azizian, L. Zou, M. A. Fischbach, K. K. Wong, K. Brandstetter, B. Wittner, S. Ramaswamy, M. Classon and J. Settleman (2010). "A chromatin-mediated

- reversible drug-tolerant state in cancer cell subpopulations." Cell **141**(1): 69-80.
- Siewerts, A. M., J. Kraan, J. Bolt, P. van der Spoel, F. Elstrodt, M. Schutte, J. W. Martens, J. W. Gratama, S. Sleijfer and J. A. Foekens (2009). "Anti-epithelial cell adhesion molecule antibodies and the detection of circulating normal-like breast tumor cells." J Natl Cancer Inst **101**(1): 61-66.
- Singh, A. and J. Settleman (2010). "EMT, cancer stem cells and drug resistance: an emerging axis of evil in the war on cancer." Oncogene **29**(34): 4741-4751.
- Singh, S. K., I. D. Clarke, M. Terasaki, V. E. Bonn, C. Hawkins, J. Squire and P. B. Dirks (2003). "Identification of a cancer stem cell in human brain tumors." Cancer Res **63**(18): 5821-5828.
- Smerage, J. B., W. E. Barlow, G. N. Hortobagyi, E. P. Winer, B. Leyland-Jones, G. Srkalovic, S. Tejwani, A. F. Schott, M. A. O'Rourke, D. L. Lew, G. V. Doyle, J. R. Gralow, R. B. Livingston and D. F. Hayes (2014). "Circulating tumor cells and response to chemotherapy in metastatic breast cancer: SWOG S0500." J Clin Oncol **32**(31): 3483-3489.
- Snapper, S. B., F. Takeshima, I. Anton, C. H. Liu, S. M. Thomas, D. Nguyen, D. Dudley, H. Fraser, D. Purich, M. Lopez-Ilasaca, C. Klein, L. Davidson, R. Bronson, R. C. Mulligan, F. Southwick, R. Geha, M. B. Goldberg, F. S. Rosen, J. H. Hartwig and F. W. Alt (2001). "N-WASP deficiency reveals distinct pathways for cell surface projections and microbial actin-based motility." Nat Cell Biol **3**(10): 897-904.
- Soeda, A., M. Park, D. Lee, A. Mintz, A. Androutsellis-Theotokis, R. D. McKay, J. Engh, T. Iwama, T. Kunisada, A. B. Kassam, I. F. Pollack and D. M. Park (2009). "Hypoxia promotes expansion of the CD133-positive glioma stem cells through activation of HIF-1alpha." Oncogene **28**(45): 3949-3959.
- Solakoglu, O., C. Maierhofer, G. Lahr, E. Breit, P. Scheunemann, I. Heumos, U. Pichlmeier, G. Schlimok, R. Oberneder, M. W. Kollermann, J. Kollermann, M. R. Speicher and K. Pantel (2002). "Heterogeneous proliferative potential of occult metastatic cells in bone marrow of patients with solid epithelial tumors." Proc Natl Acad Sci U S A **99**(4): 2246-2251.
- Sollier, E., D. E. Go, J. Che, D. R. Gossett, S. O'Byrne, W. M. Weaver, N. Kummer, M. Rettig, J. Goldman, N. Nickols, S. McCloskey, R. P. Kulkarni and D. D. Carlo (2014). "Size-selective collection of circulating tumor cells using Vortex technology." Lab Chip **14**: 63-77.
- Spinney, L. (2006). "Cancer: caught in time." Nature **442**(7104): 736-738.
- Stegg, P. S. (2006). "Tumor metastasis: mechanistic insights and clinical challenges." Nat Med **12**(8): 895-904.
- Stevens, L. C. (1964). "Experimental Production of Testicular Teratomas in Mice." Proc Natl Acad Sci U S A **52**: 654-661.

Stewart, B. and C. P. Wild (2014). World Cancer Report 2014

Stott, S. L., C. H. Hsu, D. I. Tsukrov, M. Yu, D. T. Miyamoto, B. A. Waltman, S. M. Rothenberg, A. M. Shah, M. E. Smas, G. K. Korir, F. P. Floyd, Jr., A. J. Gilman, J. B. Lord, D. Winokur, S. Springer, D. Irimia, S. Nagrath, L. V. Sequist, R. J. Lee, K. J. Isselbacher, S. Maheswaran, D. A. Haber and M. Toner (2010). "Isolation of circulating tumor cells using a microvortex-generating herringbone-chip." Proc Natl Acad Sci U S A **107**(43): 18392-18397.

Stott, S. L., R. J. Lee, S. Nagrath, M. Yu, D. T. Miyamoto, L. Ulkus, E. J. Inserra, M. Ulman, S. Springer, Z. Nakamura, A. L. Moore, D. I. Tsukrov, M. E. Kempner, D. M. Dahl, C. L. Wu, A. J. Iafrate, M. R. Smith, R. G. Tompkins, L. V. Sequist, M. Toner, D. A. Haber and S. Maheswaran (2010). "Isolation and characterization of circulating tumor cells from patients with localized and metastatic prostate cancer." Sci Transl Med **2**(25): 25ra23.

Stratton, M. R., P. J. Campbell and P. A. Futreal (2009). "The cancer genome." Nature **458**(7239): 719-724.

Sugarbaker, P. H. (1996). "Observations concerning cancer spread within the peritoneal cavity and concepts supporting an ordered pathophysiology." Cancer Treat Res **82**: 79-100.

Sun, Y. F., X. R. Yang, J. Zhou, S. J. Qiu, J. Fan and Y. Xu (2011). "Circulating tumor cells: advances in detection methods, biological issues, and clinical relevance." J Cancer Res Clin Oncol **137**(8): 1151-1173.

Talasaz, A. H., A. A. Powell, D. E. Huber, J. G. Berbee, K. H. Roh, W. Yu, W. Xiao, M. M. Davis, R. F. Pease, M. N. Mindrinos, S. S. Jeffrey and R. W. Davis (2009). "Isolating highly enriched populations of circulating epithelial cells and other rare cells from blood using a magnetic sweeper device." Proc Natl Acad Sci U S A **106**(10): 3970-3975.

Talmadge, J. E. and I. J. Fidler (2010). "AACR centennial series: the biology of cancer metastasis: historical perspective." Cancer Res **70**(14): 5649-5669.

Tam, W. L. and R. A. Weinberg (2013). "The epigenetics of epithelial-mesenchymal plasticity in cancer." Nat Med **19**(11): 1438-1449.

Tan, S. J., R. L. Lakshmi, P. Chen, W. T. Lim, L. Yobas and C. T. Lim (2010). "Versatile label free biochip for the detection of circulating tumor cells from peripheral blood in cancer patients." Biosens Bioelectron **26**(4): 1701-1705.

Tan, T. Z., Q. H. Miow, Y. Miki, T. Noda, S. Mori, R. Y. Huang and J. P. Thiery (2014). "Epithelial-mesenchymal transition spectrum quantification and its efficacy in deciphering survival and drug responses of cancer patients." EMBO Mol Med **6**(10): 1279-1293.

Therasse, P., S. G. Arbuck, E. A. Eisenhauer, J. Wanders, R. S. Kaplan, L. Rubinstein, J. Verweij, M. Van Glabbeke, A. T. van Oosterom, M. C. Christian and S. G. Gwyther

(2000). "New guidelines to evaluate the response to treatment in solid tumors. European Organization for Research and Treatment of Cancer, National Cancer Institute of the United States, National Cancer Institute of Canada." J Natl Cancer Inst **92**(3): 205-216.

Thiery, J. P. (2002). "Epithelial-mesenchymal transitions in tumour progression." Nat Rev Cancer **2**(6): 442-454.

Thiery, J. P. and C. T. Lim (2013). "Tumor dissemination: an EMT affair." Cancer Cell **23**(3): 272-273.

Thiery, J. P. and J. P. Sleeman (2006). "Complex networks orchestrate epithelial-mesenchymal transitions." Nat Rev Mol Cell Biol **7**(2): 131-142.

Toner, M. and D. Irimia (2005). "Blood-on-a-chip." Annu Rev Biomed Eng **7**: 77-103.

Tosoni, D., P. P. Di Fiore and S. Pece (2012). "Functional purification of human and mouse mammary stem cells." Methods Mol Biol **916**: 59-79.

Trojani, M., I. de Mascarel, J. M. Coindre and F. Bonichon (1987). "Micrometastases to axillary lymph nodes from invasive lobular carcinoma of breast: detection by immunohistochemistry and prognostic significance." Br J Cancer **56**(6): 838-839.

Urruticoechea, A., I. E. Smith and M. Dowsett (2005). "Proliferation marker Ki-67 in early breast cancer." J Clin Oncol **23**(28): 7212-7220.

van Oudenaarden, A. and J. A. Theriot (1999). "Cooperative symmetry-breaking by actin polymerization in a model for cell motility." Nat Cell Biol **1**(8): 493-499.

van Staveren, W. C., D. Y. Solis, A. Hebrant, V. Detours, J. E. Dumont and C. Maenhaut (2009). "Human cancer cell lines: Experimental models for cancer cells in situ? For cancer stem cells?" Biochim Biophys Acta **1795**(2): 92-103.

Van Vliet, K. J. and G. Bao (2003). "The biomechanics toolbox: experimental approaches for living cells and biomolecules." Acta Materialia **51** (19): 5881-5905.

Visvader, J. E. (2011). "Cells of origin in cancer." Nature **469**(7330): 314-322.

Vona, G., L. Estepa, C. Beroud, D. Damotte, F. Capron, B. Nalpas, A. Mineur, D. Franco, B. Lacour, S. Pol, C. Brechot and P. Paterlini-Brechot (2004). "Impact of cytomorphological detection of circulating tumor cells in patients with liver cancer." Hepatology **39**(3): 792-797.

Vona, G., A. Sabile, M. Louha, V. Sitruk, S. Romana, K. Schutze, F. Capron, D. Franco, M. Pazzagli, M. Vekemans, B. Lacour, C. Brechot and P. Paterlini-Brechot (2000). "Isolation by size of epithelial tumor cells : a new method for the immunomorphological and molecular characterization of circulating tumor cells." Am J Pathol **156**(1): 57-63.

Wang, L., S. K. Murthy, W. H. Fowle, G. A. Barabino and R. L. Carrier (2009).

"Influence of micro-well biomimetic topography on intestinal epithelial Caco-2 cell phenotype." Biomaterials **30**(36): 6825-6834.

Wang, S., K. Liu, J. Liu, Z. T. Yu, X. Xu, L. Zhao, T. Lee, E. K. Lee, J. Reiss, Y. K. Lee, L. W. Chung, J. Huang, M. Rettig, D. Seligson, K. N. Duraiswamy, C. K. Shen and H. R. Tseng (2011). "Highly efficient capture of circulating tumor cells by using nanostructured silicon substrates with integrated chaotic micromixers." Angew Chem Int Ed Engl **50**(13): 3084-3088.

Warkiani, M. E., G. Guan, K. B. Luan, W. C. Lee, A. A. Bhagat, P. K. Chaudhuri, D. S. Tan, W. T. Lim, S. C. Lee, P. C. Chen, C. T. Lim and J. Han (2014a). "Slanted spiral microfluidics for the ultra-fast, label-free isolation of circulating tumor cells." Lab Chip **14**(1): 128-137.

Warkiani, M. E., B. L. Khoo, D. S. Tan, A. A. Bhagat, W. T. Lim, Y. S. Yap, S. C. Lee, R. A. Soo, J. Han and C. T. Lim (2014). "An ultra-high-throughput spiral microfluidic biochip for the enrichment of circulating tumor cells." Analyst **139**(13): 3245-3255.

Wei, Z., X. Li, D. Zhao, H. Yan, Z. Hu, Z. Liang and Z. Li (2014b). "Flow-through cell electroporation microchip integrating dielectrophoretic viable cell sorting." Anal Chem **86**(20): 10215-10222.

Weiss, L. (1990). "Metastatic inefficiency." Adv Cancer Res **54**: 159-211.

Weissleder, R. (2002). "Scaling down imaging: molecular mapping of cancer in mice." Nat Rev Cancer **2**(1): 11-18.

Went, P. T., A. Lugli, S. Meier, M. Bundi, M. Mirlacher, G. Sauter and S. Dirnhofer (2004). "Frequent EpCam protein expression in human carcinomas." Hum Pathol **35**(1): 122-128.

Whitesides, G. M. (2006). "The origins and the future of microfluidics." Nature **442**(7101): 368-373.

Wicha, M. S. (2014). "Targeting self-renewal, an Achilles' heel of cancer stem cells." Nat Med **20**(1): 14-15.

Willipinski-Stapelfeldt, B., S. Riethdorf, V. Assmann, U. Woelfle, T. Rau, G. Sauter, J. Heukeshoven and K. Pantel (2005). "Changes in cytoskeletal protein composition indicative of an epithelial-mesenchymal transition in human micrometastatic and primary breast carcinoma cells." Clin Cancer Res **11**(22): 8006-8014.

Wittekind, C. and M. Neid (2005). "Cancer invasion and metastasis." Oncology **69 Suppl 1**: 14-16.

Wu, C. H., S. R. Lin, J. S. Hsieh, F. M. Chen, C. Y. Lu, F. J. Yu, T. L. Cheng, T. J. Huang, S. Y. Huang and J. Y. Wang (2006). "Molecular detection of disseminated tumor cells in the peripheral blood of patients with gastric cancer: evaluation of their prognostic significance." Dis Markers **22**(3): 103-109.

Wu, Y. L., C. Dudognon, E. Nguyen, J. Hillion, F. Pendino, I. Tarkanyi, J. Aradi, M. Lanotte, J. H. Tong, G. Q. Chen and E. Segal-Bendirdjian (2006). "Immunodetection of human telomerase reverse-transcriptase (hTERT) re-appraised: nucleolin and telomerase cross paths." *J Cell Sci* **119**(Pt 13): 2797-2806.

Xu, T., B. Lu, Y. C. Tai and A. Goldkorn (2010). "A cancer detection platform which measures telomerase activity from live circulating tumor cells captured on a microfilter." *Cancer Res* **70**(16): 6420-6426.

Yu, M., A. Bardia, N. Aceto, F. Bersani, M. W. Madden, M. C. Donaldson, R. Desai, H. Zhu, V. Comaills, Z. Zheng, B. S. Wittner, P. Stojanov, E. Brachtel, D. Sgroi, R. Kapur, T. Shioda, D. T. Ting, S. Ramaswamy, G. Getz, A. J. Iafrate, C. Benes, M. Toner, S. Maheswaran and D. A. Haber (2014). "Cancer therapy. Ex vivo culture of circulating breast tumor cells for individualized testing of drug susceptibility." *Science* **345**(6193): 216-220.

Yu, M., A. Bardia, B. S. Wittner, S. L. Stott, M. E. Smas, D. T. Ting, S. J. Isakoff, J. C. Ciciliano, M. N. Wells, A. M. Shah, K. F. Concannon, M. C. Donaldson, L. V. Sequist, E. Brachtel, D. Sgroi, J. Baselga, S. Ramaswamy, M. Toner, D. A. Haber and S. Maheswaran (2013). "Circulating breast tumor cells exhibit dynamic changes in epithelial and mesenchymal composition." *Science* **339**(6119): 580-584.

Yu, M., S. Stott, M. Toner, S. Maheswaran and D. A. Haber (2011). "Circulating tumor cells: approaches to isolation and characterization." *J Cell Biol* **192**(3): 373-382.

Yu, M., D. T. Ting, S. L. Stott, B. S. Wittner, F. Oszolak, S. Paul, J. C. Ciciliano, M. E. Smas, D. Winokur, A. J. Gilman, M. J. Ulman, K. Xega, G. Contino, B. Alagesan, B. W. Brannigan, P. M. Milos, D. P. Ryan, L. V. Sequist, N. Bardeesy, S. Ramaswamy, M. Toner, S. Maheswaran and D. A. Haber (2012). "RNA sequencing of pancreatic circulating tumour cells implicates WNT signalling in metastasis." *Nature* **487**(7408): 510-513.

Zabaglo, L., M. G. Ormerod and M. Dowsett (2003). "Measurement of proliferation marker Ki67 in breast tumour FNAs using laser scanning cytometry in comparison to conventional immunocytochemistry." *Cytometry B Clin Cytom* **56**(1): 55-61.

Zhang, L., L. D. Ridgway, M. D. Wetzel, J. Ngo, W. Yin, D. Kumar, J. C. Goodman, M. D. Groves and D. Marchetti (2013). "The identification and characterization of breast cancer CTCs competent for brain metastasis." *Sci Transl Med* **5**(180): 180ra148.

Zheng, S., H. K. Lin, B. Lu, A. Williams, R. Datar, R. J. Cote and Y. C. Tai (2011). "3D microfilter device for viable circulating tumor cell (CTC) enrichment from blood." *Biomed Microdevices* **13**(1): 203-213.

Zhou, M. D., S. Hao, A. J. Williams, R. A. Harouaka, B. Schrand, S. Rawal, Z. Ao, R. Brennaman, E. Gilboa, B. Lu, S. Wang, J. Zhu, R. Datar, R. Cote, Y. C. Tai and S. Y. Zheng (2014). "Separable Bilayer Microfiltration Device for Viable Label-free Enrichment of Circulating Tumour Cells." *Sci Rep* **4**: 7392.

Zieglschmid, V., C. Hollmann and O. Bocher (2005). "Detection of disseminated

tumor cells in peripheral blood." Crit Rev Clin Lab Sci **42**(2): 155-196.

Zlotnik, A., A. M. Burkhardt and B. Homey (2011). "Homeostatic chemokine receptors and organ-specific metastasis." Nat Rev Immunol **11**(9): 597-606.

Appendices

List of Tables

Table A1.1 Clinicopathological characteristics of breast cancer patients with refractory metastatic disease under the CTB clinical trial.

Table A1.2 Clinicopathological characteristics of breast cancer patients under the PCL clinical trial.

Table A1.3 Clinicopathological characteristics of newly diagnosed breast cancer patients from P2A/P2B (doxorubicin/cyclophosphamide (AC) with or without Sunitinib) clinical trial.

Table A1.4 Clinicopathological characteristics of breast cancer patients under the CES (early-stage cancer, no metastatic sites) clinical trial.

Table A1.1 Clinicopathological characteristics of breast cancer patients with refractory metastatic disease under the CTB clinical trial. C = Chinese; M = Malay; I = Indian; O = Others; IDC = invasive ductal carcinoma; ER = oestrogen receptor; PR = progesterone receptor; FAC = 5-fluouracil/ doxorubicin/cyclophosphamide; Post-Sutent pre-AC are considered as ≤ 3 weeks after treatment; pre-surgery were considered as 3-5 weeks after treatment; post-surgery were considered as >5 weeks after surgery. Y = samples with clusters (positive). N = samples without clusters (negative).

| Sample | ID | Time-point | Race | Age | Histology | Grade | Stage | ER/PR/HER2 | Metastatic site | Treatment | Treatment response | Cluster |
|--------|---------|---------------------------|------|-----|---------------------------|-------|-------|------------|-----------------------------------|------------------------------|---|---------|
| 1 | CTB 002 | Pre-treatment | C | 44 | IDC | 2 | IV | PPN | LN, small liver met | Docetaxel | | Y |
| 2 | CTB 002 | 3 weeks post treatment | C | 44 | IDC | 2 | IV | PPN | LN, small liver met | Docetaxel | Radiological response after 2 months | N |
| 3 | CTB 003 | Pre-treatment | C | 64 | IDC | 2 | IV | NNP | LN, small lung, brain | AC | | Y |
| 4 | CTB 004 | 3 weeks post treatment | C | 57 | IDC | 3 | IV | PPP | Lung, pleura, liver, bone, breast | Vinorelbine and Afatinib | Radiological stable disease after 2 months | N |
| 5 | CTB 005 | Pre-treatment | I | 48 | IDC with lobular features | 2 | IV | PPN | LN, small lung, bone, brain | Capecitabine | | N |
| 6 | CTB 005 | 5 weeks post treatment | I | 48 | IDC with lobular features | 2 | IV | PPN | LN, small lung, bone, brain | Capecitabine | Radiologically stable disease after 2 months | Y |
| 7 | CTB 006 | Pre-treatment | C | 50 | IDC | 2 | IV | PPN | Bone, liver | Fulvestrant | | N |
| 8 | CTB 006 | >5 weeks post treatment | C | 50 | IDC | 2 | IV | PPN | Bone, liver | Fulvestrant | Radiologically progressive disease after 3 months | Y |
| 9 | CTB 007 | Pre-treatment | C | 53 | Metaplastic SCC | 3 | IV | NPN | LN, lung | Vinorelbine and Capecitabine | | Y |

| | | | | | | | | | | | | |
|----|---------|------------------------|---|----|-----------------|---|----|-----|--|---|---|---|
| 10 | CTB 007 | 3 weeks post treatment | C | 53 | Metaplastic SCC | 3 | IV | NPN | LN, lung | Vinorelbine and Capecitabine | Radiologically progressive disease after 2 months | Y |
| 11 | CTB 008 | Pre-treatment | M | 71 | IDC | 3 | IV | PPP | LN, lung, bone | No treatment | | Y |
| 12 | CTB 009 | Pre-treatment | C | 33 | IDC | 3 | IV | PPN | LN, lung, pleura, liver, adrenal, bone | Fulvestrant | | Y |
| 13 | CTB 009 | 3 weeks post treatment | C | 33 | IDC | 3 | IV | PPN | LN, lung, pleura, liver, adrenal, bone | Fulvestrant | Radiologically progressive disease after 1 month | Y |
| 14 | CTB 010 | Pre-treatment | C | 39 | IDC | 2 | IV | PPN | LN, pleural, local invasion | Taxol | | Y |
| 15 | CTB 011 | Pre-treatment | M | 40 | IDC | 3 | IV | PPN | LN, lung, bone | Radiotherapy | | Y |
| 16 | CTB 012 | Pre-treatment | C | 54 | IDC | 3 | IV | NNN | Bone | Radiotherapy, 5 fluorouracil, doxorubicin, cyclophosphamide | | Y |
| 17 | CTB 012 | 3 weeks post treatment | C | 54 | IDC | 3 | IV | NNN | Bone | Radiotherapy, 5 fluorouracil, doxorubicin, cyclophosphamide | No documented progression within 3 months | N |
| 18 | CTB 013 | Pre-treatment | I | 64 | IDC | 3 | IV | PPN | LN, lung | Docetaxel | | Y |
| 19 | CTB 014 | Pre-treatment | C | 57 | IDC | 3 | IV | NNN | LN, lung | PI3K inhibitor/Placebo + Paclitaxel | | Y |
| 20 | CTB 014 | 3 weeks post treatment | C | 57 | IDC | 3 | IV | NNN | LN, lung | PI3K inhibitor/Placebo + Paclitaxel | No documented progression within 3 months | Y |
| 21 | CTB | 3 weeks | C | 44 | IDC | 3 | IV | NNN | LN, lung | Gemcitabine+Carboplatin | Radiological | N |

| | | | | | | | | | | | | |
|----|--------|------------------------|---|----|-----|---|----|-----|--------------------------------|-------------------------|---|---|
| | 015 | post treatment | | | | | | | | | response after 2 months | |
| 22 | CTB016 | 3 weeks post treatment | C | 41 | IDC | 2 | IV | PPN | Bone, breast | Capecitabine | Radiologically progressive disease after 3 months | N |
| 23 | CTB017 | 4 weeks post treatment | O | 35 | IDC | . | IV | PPN | Pleura, peritoneum, small bone | Letrozole | Radiologically stable disease after 3 months | N |
| 24 | CTB018 | Pre-treatment | C | 44 | IDC | 2 | IV | PPN | Lung | Letrozole | | Y |
| 25 | CTB019 | Post treatment | C | 40 | IDC | 3 | IV | NNN | LN, pleural effusion, sternum | Gemcitabine+Carboplatin | Radiological response after 6 weeks | Y |
| 26 | CTB026 | Post treatment | M | 54 | IDC | 2 | IV | PPN | Lung, pleural effusion | Exemestane | Radiological stable disease after 6 weeks | Y |
| 27 | CTB028 | Pre-treatment | C | 65 | IDC | 2 | IV | NNP | Liver, bone | Vinorelbine+herceptin | | Y |
| 28 | CTB029 | Pre-treatment | C | 49 | IDC | | IV | PPN | Lung, pleural effusion, bone | Paclitaxel | | Y |
| 29 | CTB029 | 3 weeks post treatment | C | 49 | IDC | | IV | PPN | Lung, pleural effusion, bone | Paclitaxel | Not yet assessed | Y |
| 30 | CTB021 | Pre-treatment | O | 38 | IDC | 3 | IV | PPN | Lung, bone, liver | Eribulin | | Y |

Table A1.2 Clinicopathological characteristics of breast cancer patients under the PCL clinical trial. C = Chinese; M = Malay; I = Indian; O = Others; IDC = invasive ductal carcinoma; ER = oestrogen receptor; PR = progesterone receptor; P: Positive. N: Negative. Post-Sutent pre-AC are considered as ≤ 3 weeks after treatment; pre-surgery were considered as 3-5 weeks after treatment; post-surgery were considered as >5 weeks after surgery. Y = samples with clusters (positive). N = samples without clusters (negative).

| Sample | ID | Time-point | Race | Age | Histology | Grade | Stage | ER/PR/HER2 | Diagnosis | Treatment | Treatment response | Cluster |
|--------|--------|----------------------------------|------|-----|---|-------|-------|------------|-------------------------------|----------------------------------|--------------------|---------|
| 1 | PCL027 | Pre-surgery | C | 37 | ILC | 3 | IIIB | NNP | Refractory metastatic disease | Paclitaxel+carboplatin+lapatinib | no pCR | Y |
| 2 | PCL028 | Post surgery | O | 35 | IDC | 3 | IIIA | PPP | Refractory metastatic disease | Paclitaxel+carboplatin+lapatinib | no pCR | Y |
| 3 | PCL030 | 3 weeks and 1 day post treatment | M | 78 | Invasive ca with squamous differentiation | 3 | IIIB | NPP | Newly diagnosed | Paclitaxel+carboplatin+lapatinib | no pCR | Y |
| 4 | PCL030 | Pre-surgery | M | 78 | Invasive ca with squamous differentiation | 3 | IIIB | NPP | Newly diagnosed | Paclitaxel+carboplatin+lapatinib | no pCR | Y |
| 5 | PCL030 | Post-surgery | M | 78 | Invasive ca with squamous differentiation | 3 | IIIB | NPP | Newly diagnosed | Paclitaxel+carboplatin+lapatinib | no pCR | Y |
| 6 | PCL031 | Pre-treatment | C | 55 | IDC | 2 | IIIA | PPP | Newly diagnosed | Paclitaxel+carboplatin+lapatinib | no pCR | Y |

| | | | | | | | | | | | | |
|----|------------|---|---|----|-----|---|------|-----|--------------------|----------------------------------|--------|---|
| 7 | PCL0 31 | 3 weeks and 1 day post treatment | C | 55 | IDC | 2 | IIIA | PPP | Newly diagnosed | Paclitaxel+carboplatin+lapatinib | no pCR | Y |
| 8 | PCL0 31 | 6 weeks and 1 day post treatment | C | 55 | IDC | 2 | IIIA | PPP | Newly diagnosed | Paclitaxel+carboplatin+lapatinib | no pCR | N |
| 9 | PCL0 31 | 9 weeks and 1 day post treatment | C | 55 | IDC | 2 | IIIA | PPP | Newly diagnosed | Paclitaxel+carboplatin+lapatinib | no pCR | N |
| 10 | PCL0 31 | Pre- surgery | C | 55 | IDC | 2 | IIIA | PPP | Newly diagnosed | Paclitaxel+carboplatin+lapatinib | no pCR | N |
| 11 | PCL0 31 | Post- surgery | C | 55 | IDC | 2 | IIIA | PPP | Newly diagnosed | Paclitaxel+carboplatin+lapatinib | no pCR | N |
| 12 | PCL0 32 | Pre- treatment | M | 51 | IDC | 3 | IIIB | PPP | Newly diagnosed | Paclitaxel+carboplatin+lapatinib | no pCR | Y |
| 13 | PCL0 32 | 3 weeks and 1 day post treatment | M | 51 | IDC | 3 | IIIB | PPP | Newly diagnosed | Paclitaxel+carboplatin+lapatinib | no pCR | Y |
| 14 | PCL0 32 | 6 weeks and 1 day post treatment | M | 51 | IDC | 3 | IIIB | PPP | Newly diagnosed | Paclitaxel+carboplatin+lapatinib | no pCR | Y |
| 15 | PCL0 32 | 9 weeks and 1 day post treatment | M | 51 | IDC | 3 | IIIB | PPP | Newly diagnosed | Paclitaxel+carboplatin+lapatinib | no pCR | Y |

| | | | | | | | | | | | | |
|----|------------|---|---|----|-----|---|------|-----|--------------------|----------------------------------|--------|---|
| 16 | PCL0 32 | Pre- surgery | M | 51 | IDC | 3 | IIIB | PPP | Newly diagnosed | Paclitaxel+carboplatin+lapatinib | no pCR | N |
| 17 | PCL0 32 | Post- surgery | M | 51 | IDC | 3 | IIIB | PPP | Newly diagnosed | Paclitaxel+carboplatin+lapatinib | no pCR | N |
| 18 | PCL0 37 | Pre- treatment | C | 38 | ILC | 2 | IIA | PPP | Newly diagnosed | Paclitaxel+carboplatin+lapatinib | no pCR | Y |
| 19 | PCL0 37 | 3 weeks and 1 day post treatment | C | 38 | ILC | 2 | IIA | PPP | Newly diagnosed | Paclitaxel+carboplatin+lapatinib | no pCR | Y |
| 20 | PCL0 37 | 6 weeks and 1 day post treatment | C | 38 | ILC | 2 | IIA | PPP | Newly diagnosed | Paclitaxel+carboplatin+lapatinib | no pCR | Y |
| 21 | PCL0 37 | 9 weeks and 1 day post treatment | C | 38 | ILC | 2 | IIA | PPP | Newly diagnosed | Paclitaxel+carboplatin+lapatinib | no pCR | Y |
| 22 | PCL0 37 | Pre- surgery | C | 38 | ILC | 2 | IIA | PPP | Newly diagnosed | Paclitaxel+carboplatin+lapatinib | no pCR | Y |
| 23 | PCL0 37 | Post- surgery | C | 38 | ILC | 2 | IIA | PPP | Newly diagnosed | Paclitaxel+carboplatin+lapatinib | no pCR | Y |
| 24 | PCL0 38 | Pre- treatment | C | 61 | IDC | 3 | IIIA | NNP | Newly diagnosed | Paclitaxel+carboplatin+lapatinib | no pCR | Y |
| 25 | PCL0 38 | 3 weeks and 1 day post treatment | C | 61 | IDC | 3 | IIIA | NNP | Newly diagnosed | Paclitaxel+carboplatin+lapatinib | no pCR | Y |

| | | | | | | | | | | | | |
|----|------------|---|---|----|-----|---|------|-----|--------------------|----------------------------------|--------|---|
| 26 | PCL0 38 | 6 weeks and 1 day post treatment | C | 61 | IDC | 3 | IIIA | NNP | Newly diagnosed | Paclitaxel+carboplatin+lapatinib | no pCR | Y |
| 27 | PCL0 38 | 9 weeks and 1 day post treatment | C | 61 | IDC | 3 | IIIA | NNP | Newly diagnosed | Paclitaxel+carboplatin+lapatinib | no pCR | Y |
| 28 | PCL0 38 | Pre- surgery | C | 61 | IDC | 3 | IIIA | NNP | Newly diagnosed | Paclitaxel+carboplatin+lapatinib | no pCR | Y |

Table A1.3 Clinicopathological characteristics of newly diagnosed breast cancer patients from P2A/P2B (doxorubicin/cyclophosphamide (AC) with or without Sunitinib) clinical trial.

C = Chinese; M = Malay; I = Indian; O = Others; IDC = invasive ductal carcinoma; ER = oestrogen; PR = progesterone; FAC = 5-fluouracil/doxorubicin/cyclophosphamide; Post-Sunitinib pre-AC are considered as ≤ 3 weeks after treatment; pre-surgery and post-surgery are considered as >5 weeks after treatment. Y = samples with clusters (positive). N = samples without clusters (negative).

| Sample | Patient | ID | Time-point | Race | Age | Histology | Grade | Stage | ER/PR/HER2 | Metastatic site | Treatment | Treatment response | Cluster |
|--------|---------|-------|----------------------------------|------|-----|----------------------------------|-------|-------|------------|-----------------|-----------|--|---------|
| 1 | 1 | P2A13 | 2 weeks and 1 day post treatment | C | 64 | IDC | 3 | IIIB | NNN | | AC | no pCR | Y |
| 2 | 2 | P2A14 | Pre-treatment | C | 53 | IDC | 1 | IIIA | PPN | | AC | | Y |
| 3 | 3 | P2A15 | Post surgery | C | 47 | invasive micropapillary ca | 2 | IIIA | PPN | | AC | no pCR; chest wall recurrence while on adjuvant RT | N |
| 4 | 4 | P2A16 | 2 weeks and 1 day post treatment | C | 47 | IDC with micropapillary features | 3 | IIIB | PPN | | AC | no pCR | Y |
| 5 | 4 | P2A16 | 3 weeks and 1 day post treatment | C | 47 | IDC with micropapillary features | 3 | IIIB | PPN | | AC | no pCR | Y |
| 6 | 4 | P2A16 | 6 weeks and 1 day post treatment | C | 47 | IDC with micropapillary features | 3 | IIIB | PPN | | AC | no pCR | Y |
| 7 | 4 | P2A16 | 9 weeks and 1 day post treatment | C | 47 | IDC with micropapillary features | 3 | IIIB | PPN | | AC | no pCR | Y |

| | | | | | | | | | | | | | |
|----|---|-------|------------------------------------|---|----|-----|---|-----|-----|--|----|----------------|---|
| 8 | 5 | P2A17 | Pre-treatment | C | 60 | IDC | 3 | IIB | PPN | | AC | | Y |
| 9 | 5 | P2A17 | 2 weeks and 1 day post treatment | C | 60 | IDC | 3 | IIB | PPN | | AC | no pCR | Y |
| 10 | 5 | P2A17 | 3 weeks and 1 day post treatment | C | 60 | IDC | 3 | IIB | PPN | | AC | no pCR | Y |
| 11 | 5 | P2A17 | 6 weeks and 1 day post treatment | C | 60 | IDC | 3 | IIB | PPN | | AC | no pCR | Y |
| 12 | 5 | P2A17 | 11 weeks and 1 days post treatment | C | 60 | IDC | 3 | IIB | PPN | | AC | no pCR | N |
| 13 | 6 | P2A18 | Pre-treatment | O | 47 | IDC | 3 | IIB | NPN | | AC | | Y |
| 14 | 6 | P2A18 | 2 weeks and 1 day post treatment | O | 47 | IDC | 3 | IIB | NPN | | AC | no pCR | Y |
| 15 | 6 | P2A18 | 9 weeks and 1 day post treatment | O | 47 | IDC | 3 | IIB | NPN | | AC | no pCR | N |
| 16 | 6 | P2A18 | Post surgery | O | 47 | IDC | 3 | IIB | NPN | | AC | no pCR | N |
| 17 | 7 | P2A19 | Pre-treatment | O | 46 | ILC | . | IIA | PNN | | AC | | N |
| 18 | 7 | P2A19 | 2 weeks and 1 day post | O | 46 | ILC | . | IIA | PNN | | AC | no surgery yet | N |

| | | | | | | | | | | | | | |
|----|---|-------|------------------------------------|---|----|-----|---|-----|-----|------|----|----------------|---|
| | | | treatment | | | | | | | | | | |
| 19 | 7 | P2A19 | 3 weeks and 1 day post treatment | O | 46 | ILC | . | IIA | PNN | | AC | no surgery yet | N |
| 20 | 7 | P2A19 | 6 weeks and 1 day post treatment | O | 46 | ILC | . | IIA | PNN | | AC | no surgery yet | N |
| 21 | 7 | P2A19 | 9 weeks and 1 day post treatment | O | 46 | ILC | . | IIA | PNN | | AC | no surgery yet | N |
| 22 | 7 | P2A19 | 11 weeks and 1 days post treatment | O | 46 | ILC | . | IIA | PNN | | AC | no surgery yet | Y |
| 23 | 7 | P2A19 | Post-surgery | O | 48 | IDC | 4 | IIB | NPN | | AC | no pCR | N |
| 24 | 8 | P2A20 | Pre-treatment | M | 45 | IDC | 3 | IV | NNN | Bone | AC | | Y |
| 25 | 8 | P2A20 | 2 weeks and 1 day post treatment | M | 46 | IDC | 3 | IV | NNN | Bone | AC | | Y |
| 26 | 8 | P2A20 | 3 weeks and 1 day post treatment | M | 47 | IDC | 3 | IV | NNN | Bone | AC | | N |
| 27 | 8 | P2A20 | 6 weeks and 1 day post treatment | M | 48 | IDC | 3 | IV | NNN | Bone | AC | | N |

| | | | | | | | | | | | | | |
|----|----|-------|----------------------------------|---|----|-----|---|------|-----|------|----|----------------|---|
| 28 | 8 | P2A20 | Post-surgery | M | 48 | IDC | 3 | IV | NNN | Bone | AC | | N |
| 29 | 9 | P2A21 | Pre-treatment | C | 38 | IDC | . | IIB | PPN | | AC | | Y |
| 30 | 9 | P2A21 | 2 weeks and 1 day post treatment | C | 38 | IDC | . | IIB | PPN | | AC | no surgery yet | Y |
| 31 | 9 | P2A21 | 3 weeks and 1 day post treatment | C | 38 | IDC | . | IIB | PPN | | AC | no surgery yet | N |
| 32 | 9 | P2A21 | 6 weeks and 1 day post treatment | C | 38 | IDC | . | IIB | PPN | | AC | no surgery yet | N |
| 33 | 9 | P2A21 | 9 weeks and 1 day post treatment | C | 38 | IDC | . | IIB | PPN | | AC | no surgery yet | N |
| 34 | 10 | P2A22 | Pre-treatment | C | 68 | IDC | 2 | IIIB | PPN | | AC | | Y |
| 35 | 10 | P2A22 | 2 weeks and 1 day post treatment | C | 68 | IDC | 2 | IIIB | PPN | | AC | no surgery yet | Y |
| 36 | 10 | P2A22 | 6 weeks and 1 day post treatment | C | 68 | IDC | 2 | IIIB | PPN | | AC | no surgery yet | Y |
| 37 | 11 | P2A23 | Pre-treatment | C | 35 | IDC | 3 | IIA | NNN | | AC | | Y |
| 38 | 11 | P2A23 | 2 weeks and 1 day post | C | 35 | IDC | 3 | IIA | NNN | | AC | no surgery yet | Y |

| | | | | | | | | | | | | | |
|----|----|-------|----------------------------------|---|----|-----|---|-----|-----|--|----|----------------|---|
| | | | treatment | | | | | | | | | | |
| 39 | 11 | P2A23 | 9 weeks and 1 day post treatment | C | 35 | IDC | 3 | IIA | NNN | | AC | no surgery yet | N |
| 40 | 12 | P2A24 | Post-surgery | C | 33 | | 2 | IIB | NPP | | AC | no surgery yet | N |
| 41 | 13 | P2A25 | Pre-treatment | C | 46 | IDC | 2 | IIA | NPP | | AC | no surgery yet | Y |
| 42 | 13 | P2A25 | 2 weeks and 1 day post treatment | C | 46 | IDC | 2 | IIA | NPP | | AC | no surgery yet | Y |
| 43 | 13 | P2A25 | 3 weeks and 1 day post treatment | C | 46 | IDC | 2 | IIA | NPP | | AC | no surgery yet | Y |
| 44 | 13 | P2A25 | 6 weeks and 1 day post treatment | C | 46 | IDC | 2 | IIA | NPP | | AC | no surgery yet | Y |
| 45 | 13 | P2A25 | 9 weeks and 1 day post treatment | C | 46 | IDC | 2 | IIA | NPP | | AC | no surgery yet | Y |
| 46 | 14 | P2A26 | Pre-treatment | I | 56 | IDC | 1 | IV | NPP | | AC | no surgery yet | Y |
| 47 | 14 | P2A26 | 2 weeks and 1 day post treatment | I | 56 | IDC | 1 | IV | NPP | | AC | no surgery yet | Y |

| | | | | | | | | | | | | | |
|----|----|-------|----------------------------------|---|----|-----|---|------|-----|--|--------------|----------------|---|
| 48 | 14 | P2A26 | 3 weeks and 1 day post treatment | I | 56 | IDC | 1 | IV | NPP | | AC | no surgery yet | Y |
| 49 | 14 | P2A26 | 6 weeks and 1 day post treatment | I | 56 | IDC | 1 | IV | NPP | | AC | no surgery yet | Y |
| 50 | 14 | P2A26 | 9 weeks and 1 day post treatment | I | 56 | IDC | 1 | IV | NPP | | AC | no surgery yet | N |
| 51 | 14 | P2A26 | Post-surgery | I | 56 | IDC | 1 | IV | NPP | | AC | | N |
| 52 | 15 | P2A27 | Pre-treatment | C | 61 | IDC | 3 | IIB | NPP | | AC | no surgery yet | Y |
| 53 | 15 | P2A27 | 2 weeks and 1 day post treatment | C | 61 | IDC | 3 | IIB | NPP | | AC | no surgery yet | Y |
| 54 | 15 | P2A27 | 3 weeks and 1 day post treatment | C | 61 | IDC | 3 | IIB | NPP | | AC | no surgery yet | Y |
| 55 | 15 | P2A27 | 6 weeks and 1 day post treatment | C | 61 | IDC | 3 | IIB | NPP | | AC | no surgery yet | Y |
| 56 | 16 | P2B08 | Pre-treatment | C | 37 | IDC | 3 | IIIA | PPN | | AC+Sunitinib | | Y |
| 57 | 16 | P2B08 | 2 weeks and 1 day post treatment | C | 37 | IDC | 3 | IIIA | PPN | | AC+Sunitinib | no pCR | Y |

| | | | | | | | | | | | | | |
|----|----|-------|----------------------------------|---|----|-----|---|------|-----|------------------|--------------|--------|---|
| 58 | 17 | P2B09 | Pre-treatment | M | 57 | IDC | 3 | IIIA | NNN | | AC+Sunitinib | | Y |
| 59 | 17 | P2B09 | Post Sutant Preuten | M | 57 | IDC | 3 | IIIA | NNN | | AC+Sunitinib | no pCR | Y |
| 60 | 18 | P2B10 | Pre-treatment | C | 50 | IDC | 3 | IIIB | PPN | | AC+Sunitinib | | Y |
| 61 | 18 | P2B10 | Post Sutant Pre AC | C | 50 | IDC | 3 | IIIB | PPN | | AC+Sunitinib | no pCR | Y |
| 62 | 18 | P2B10 | 2 weeks and 1 day post treatment | C | 50 | IDC | 3 | IIIB | PPN | | AC+Sunitinib | no pCR | Y |
| 63 | 18 | P2B10 | 9 weeks and 1 day post treatment | C | 50 | IDC | 3 | IIIB | PPN | | AC+Sunitinib | no pCR | N |
| 64 | 19 | P2B11 | Pre-treatment | C | 45 | IDC | 3 | IIA | NNN | | AC+Sunitinib | | Y |
| 65 | 19 | P2B11 | Post Sutant Pre AC | C | 45 | IDC | 3 | IIA | NNN | | AC+Sunitinib | pCR | Y |
| 66 | 19 | P2B11 | 2 weeks and 1 day post treatment | C | 45 | IDC | 3 | IIA | NNN | | AC+Sunitinib | pCR | N |
| 67 | 19 | P2B11 | 9 weeks and 1 day post treatment | C | 45 | IDC | 3 | IIA | NNN | | AC+Sunitinib | pCR | N |
| 68 | 20 | P2B12 | Pre-treatment | C | 54 | IDC | 2 | IV | NNN | LN, lung, pleura | AC+Sunitinib | | Y |

| | | | | | | | | | | | | | |
|----|----|-------|---|---|----|-----|---|------|-----|----------------------|--------------|------------|---|
| 69 | 20 | P2B12 | Post Sutent Pre AC | C | 54 | IDC | 2 | IV | NNN | LN, lung, pleura | AC+Sunitinib | no surgery | Y |
| 70 | 20 | P2B12 | 3 weeks and 1 day post treatment | C | 54 | IDC | 2 | IV | NNN | LN, lung, pleura | AC+Sunitinib | no surgery | N |
| 71 | 20 | P2B12 | 6 weeks and 1 day post treatment | C | 54 | IDC | 2 | IV | NNN | LN, lungs, pleura | AC+Sunitinib | no surgery | N |
| 72 | 21 | P2B13 | Pre- treatment | C | 46 | IDC | 2 | IIB | PPN | | AC+Sunitinib | | Y |
| 73 | 21 | P2B13 | Post Sutent Pre AC | C | 46 | IDC | 2 | IIB | PPN | | AC+Sunitinib | no surgery | Y |
| 74 | 21 | P2B13 | 2 weeks and 1 day post treatment | C | 46 | IDC | 2 | IIB | PPN | | AC+Sunitinib | no surgery | Y |
| 75 | 21 | P2B13 | 3 weeks and 1 day post treatment | C | 46 | IDC | 2 | IIB | PPN | | AC+Sunitinib | no surgery | Y |
| 76 | 21 | P2B13 | 6 weeks and 1 day post treatment | C | 46 | IDC | 2 | IIB | PPN | | AC+Sunitinib | no surgery | Y |
| 77 | 21 | P2B13 | 9 weeks and 1 day post treatment | C | 46 | IDC | 2 | IIB | PPN | | AC+Sunitinib | no surgery | Y |
| 78 | 22 | P2B14 | Pre- treatment | I | 41 | IDC | 3 | IIIA | NPN | | AC+Sunitinib | | Y |

| | | | | | | | | | | | | | |
|----|----|-------|----------------------------------|---|----|---------------|---|------|-----|--|--------------|---------------------------------------|---|
| 79 | 22 | P2B14 | Post Sunitinib Pre AC | I | 41 | IDC | 3 | IIIA | NPN | | AC+Sunitinib | no pCR | Y |
| 80 | 22 | P2B14 | 2 weeks and 1 day post treatment | I | 41 | IDC | 3 | IIIA | NPN | | AC+Sunitinib | no pCR | Y |
| 81 | 22 | P2B14 | 3 weeks and 1 day post treatment | I | 41 | IDC | 3 | IIIA | NPN | | AC+Sunitinib | no pCR | Y |
| 82 | 22 | P2B14 | 6 weeks and 1 day post treatment | I | 41 | IDC | 3 | IIIA | NPN | | AC+Sunitinib | no pCR | Y |
| 83 | 22 | P2B14 | 9 weeks and 1 day post treatment | I | 41 | IDC | 3 | IIIA | NPN | | AC+Sunitinib | no pCR | Y |
| 84 | 23 | P2B15 | Pre-treatment | C | 45 | IDC | 3 | IIIC | NNN | | AC+Sunitinib | | Y |
| 85 | 23 | P2B15 | Post Sunitinib Pre AC | C | 45 | IDC | 3 | IIIC | NNN | | AC+Sunitinib | no pCR | Y |
| 86 | 23 | P2B15 | 2 weeks and 1 day post treatment | C | 45 | IDC | 3 | IIIC | NNN | | AC+Sunitinib | no pCR | Y |
| 87 | 23 | P2B15 | 3 weeks and 1 day post treatment | C | 45 | IDC | 3 | IIIC | NNN | | AC+Sunitinib | no pCR; surgery mixed IDC/metaplastic | Y |
| 88 | 24 | P2B16 | Pre-treatment | O | 49 | Mixed IDC/ILC | 2 | IIB | PPN | | AC+Sunitinib | | Y |

| | | | | | | | | | | | | | |
|----|----|-------|---|---|----|------------------|---|------|-----|--|--------------|----------------|---|
| 89 | 24 | P2B16 | Post Sutent Pre AC | O | 49 | Mixed IDC/ILC | 2 | IIB | PPN | | AC+Sunitinib | no pCR | Y |
| 90 | 24 | P2B16 | 2 weeks and 1 day post treatment | O | 49 | Mixed IDC/ILC | 2 | IIB | PPN | | AC+Sunitinib | no pCR | Y |
| 91 | 24 | P2B16 | 3 weeks and 1 day post treatment | O | 49 | Mixed IDC/ILC | 2 | IIB | PPN | | AC+Sunitinib | no pCR | Y |
| 92 | 24 | P2B16 | 6 weeks and 1 day post treatment | O | 49 | Mixed IDC/ILC | 2 | IIB | PPN | | AC+Sunitinib | no pCR | N |
| 93 | 24 | P2B16 | Post- surgery | O | 49 | Mixed IDC/ILC | 2 | IIB | PPN | | AC+Sunitinib | no pCR | N |
| 94 | 25 | P2B17 | 6 weeks and 1 day post treatment | C | 48 | IDC | 3 | IIIA | NNN | | AC+Sunitinib | no pCR | N |
| 95 | 25 | P2B17 | 9 weeks and 1 day post treatment | C | 48 | IDC | 3 | IIIA | NNN | | AC+Sunitinib | no pCR | N |
| 96 | 26 | P2B19 | Pre- treatment | M | 37 | IDC | 1 | IIA | PPN | | AC+Sunitinib | no pCR | Y |
| 97 | 26 | P2B19 | Post Sutent Pre AC | M | 37 | IDC | 1 | IIA | PPN | | AC+Sunitinib | no surgery yet | Y |
| 98 | 26 | P2B19 | 2 weeks and 1 day post treatment | M | 37 | IDC | 1 | IIA | PPN | | AC+Sunitinib | no surgery yet | Y |

| | | | | | | | | | | | | | |
|-----|----|-------|----------------------------------|---|----|-----|---|------|-----|--|--------------|----------------|---|
| 99 | 26 | P2B19 | 3 weeks and 1 day post treatment | M | 37 | IDC | 1 | IIA | PPN | | AC+Sunitinib | no surgery yet | Y |
| 100 | 27 | P2B21 | Pre-treatment | M | 48 | IDC | 3 | IIB | PPP | | AC+Sunitinib | no pCR | Y |
| 101 | 27 | P2B21 | Post Sutent Pre AC | M | 48 | IDC | 3 | IIB | PPP | | AC+Sunitinib | no pCR | N |
| 102 | 27 | P2B21 | Post-surgery | M | 48 | IDC | 3 | IIB | PPP | | AC+Sunitinib | no pCR | N |
| 103 | 28 | P2B22 | 3 weeks and 1 day post treatment | I | 54 | IDC | 3 | IIA | NNN | | AC+Sunitinib | no pCR | Y |
| 104 | 29 | P2B23 | 3 weeks and 1 day post treatment | M | 44 | IDC | 3 | IIIA | PPP | | AC+Sunitinib | no pCR | N |
| 105 | 29 | P2B23 | 6 weeks and 1 day post treatment | M | 44 | IDC | 3 | IIIA | PPP | | AC+Sunitinib | no pCR | N |
| 106 | 29 | P2B23 | 9 weeks and 1 day post treatment | M | 44 | IDC | 3 | IIIA | PPP | | AC+Sunitinib | no pCR | N |
| 107 | 29 | P2B23 | Post-surgery | M | 44 | IDC | 3 | IIIA | PPP | | AC+Sunitinib | no pCR | N |
| 108 | 30 | P2B24 | Pre-treatment | C | 47 | IDC | 3 | IIB | PPN | | AC+Sunitinib | no surgery yet | N |
| 109 | 30 | P2B24 | Post Sutent Pre AC | C | 47 | IDC | 3 | IIB | PPN | | AC+Sunitinib | no surgery yet | N |

| | | | | | | | | | | | | | |
|-----|----|-------|----------------------------------|---|----|--------------------|---|------|-----|--|--------------|----------------|---|
| 110 | 30 | P2B24 | 2 weeks and 1 day post treatment | C | 47 | IDC | 3 | IIB | PPN | | AC+Sunitinib | no surgery yet | N |
| 111 | 30 | P2B24 | 3 weeks and 1 day post treatment | C | 47 | IDC | 3 | IIB | PPN | | AC+Sunitinib | no surgery yet | N |
| 112 | 30 | P2B24 | 6 weeks and 1 day post treatment | C | 47 | IDC | 3 | IIB | PPN | | AC+Sunitinib | no surgery yet | N |
| 113 | 30 | P2B24 | 9 weeks and 1 day post treatment | C | 47 | IDC | 3 | IIB | PPN | | AC+Sunitinib | no surgery yet | N |
| 114 | 30 | P2B24 | Post-surgery | C | 47 | IDC | 3 | IIB | PPN | | AC+Sunitinib | | N |
| 115 | 31 | P2B25 | Pre-treatment | M | 57 | invasive carcinoma | 3 | IIIB | PPN | | AC+Sunitinib | defaulted | N |

Table A1.4 Clinicopathological characteristics of breast cancer patients under the CES (early-stage cancer, no metastatic sites) clinical trial. C = Chinese; M = Malay; I = Indian; O = Others; IDC = invasive ductal carcinoma; ER = oestrogen receptor; PR = progesterone receptor; FAC = 5-fluouracil/ doxorubicin/cyclophosphamide; TCH = post adjuvant Herceptin+Docetaxel+Carboplatin; FEC = Fluorouracil, Epirubicin, and Cyclophosphamide; Post-Sutent pre-AC are considered as ≤ 3 weeks after treatment; pre-surgery were considered as 3-5 weeks after treatment; post-surgery were considered as >5 weeks after surgery. Y = samples with clusters (positive). N = samples without clusters (negative). TNM = Tumor/Nodes/Metastasis.

| Sample | Patient ID | ID | Time point | Race | Age | Histology | Grade | TNM | ER/PR/HER2 | Treatment | Cluster |
|--------|------------|---------|----------------------------|------|-----|-----------|-------|--------|------------|-----------|---------|
| 1 | 1 | CES 001 | Post-surgery | C | 59 | IDC | 1 | T1N1M0 | PPN | FAC | Y |
| 2 | | CES 001 | Post adjuvant chemotherapy | C | 59 | IDC | 1 | T1N1M0 | PPN | FAC | Y |
| 3 | | CES 001 | 1 year post FAC | C | 59 | IDC | 1 | T1N1M0 | PPN | FAC | Y |
| 4 | 2 | CES 002 | Post-surgery | C | 67 | IDC | 2 | T2N0M0 | PPN | FAC | Y |
| 5 | | CES 002 | Post FAC | C | 67 | IDC | 2 | T2N0M0 | PPN | FAC | N |
| 6 | 3 | CES 003 | Post-surgery | C | 60 | IDC | 3 | T3N3M0 | PPN | AC | Y |
| 7 | | CES 003 | 1 year post taxol | C | 60 | IDC | 3 | T3N3M0 | PPN | AC | Y |
| 8 | 4 | CES 004 | Post-surgery | C | 57 | IDC | 3 | T1N0M0 | PPP | AC | Y |

| | | | | | | | | | | | |
|----|----|--------|--|---|----|-----|---|----------------------|-----|--|---|
| 9 | | CES004 | 1 year after surgery and adjuvant chemotherapy | C | 57 | IDC | 3 | T1N0M0 | PPP | AC | N |
| 10 | 5 | CES005 | Post-surgery | C | 50 | IDC | 2 | T1N0M0 | PPN | AC | N |
| 11 | | CES005 | 1 year post AC | C | 50 | IDC | 2 | T1N0M0 | PPN | AC | Y |
| 12 | 6 | CES006 | Post adjuvant AC | M | 49 | IDC | 3 | T3N1M0 | PPN | AC | N |
| 13 | | CES006 | 1 year after surgery and adjuvant chemotherapy | M | 49 | IDC | 3 | T3N1M0 | PPN | AC | N |
| 14 | | CES006 | Post paclitaxel | M | 49 | IDC | 3 | T3N1M0 | PPN | AC | N |
| 15 | 7 | CES008 | Post adjuvant paclitaxel | C | 44 | IDC | 3 | cT2N1M0, ypT1N0M0 | PPP | AC (neoadjuvant) followed by surgery and adjuvant paclitaxel | Y |
| 16 | | CES008 | 1 year after surgery and adjuvant chemotherapy | C | 44 | IDC | 3 | cT2N1M0, ypT1N0M0 | PPP | AC (neoadjuvant) followed by surgery and adjuvant paclitaxel | N |
| 17 | 8 | CES010 | Post TCH | C | 51 | IDC | 3 | T2N1M0 | PPP | Herceptin+Docetaxel+Carboplatin | N |
| 18 | 9 | CES011 | Post-surgery | C | 45 | IDC | 3 | T1N0M0 | PPN | AC | Y |
| 19 | 10 | CES012 | Post FAC | O | 35 | IDC | 3 | T2N3M0 | NNN | FAC | N |

| | | | | | | | | | | | |
|----|----|--------|--|---|----|-----|---|-----------------------------|-----|--|---|
| 20 | 11 | CES013 | Post paclitaxel | C | 49 | IDC | 2 | T2N0M0 | PPN | AC followed by paclitaxel | N |
| 21 | 12 | CES014 | Post paclitaxel | I | 58 | IDC | 3 | T2N0M0 | NNN | AC followed by paclitaxel | N |
| 22 | 13 | CES015 | Post-surgery | C | 62 | IDC | 2 | T2N2M0 | PNN | AC followed by paclitaxel | N |
| 23 | | CES015 | Post paclitaxel | C | 62 | IDC | 2 | T2N2M0 | PNN | AC followed by paclitaxel | Y |
| 24 | 14 | CES016 | Post-surgery | C | 61 | IDC | 3 | T1N1M0 | NNN | AC followed by paclitaxel | N |
| 25 | | | Post paclitaxel | C | 61 | IDC | 3 | T1N1M0 | NNN | AC followed by paclitaxel | N |
| 26 | 15 | CES017 | Post adjuvant paclitaxel | C | 38 | IDC | 1 | cT2N0M0, ypT1N1mi cM0 | PPN | Neoadjuvant AC followed by adjuvant paclitaxel | N |
| 27 | 16 | CES018 | Post adjuvant paclitaxel | C | 33 | IDC | 2 | T2N2M0 | PPN | AC followed by paclitaxel | Y |
| 28 | | CES018 | 1 year after surgery and adjuvant chemotherapy | C | 33 | IDC | 2 | T2N2M0 | PPN | AC followed by paclitaxel | Y |
| 29 | 17 | CES021 | Post adjuvant docetaxel | O | 37 | IDC | 3 | T2N2M0 | NNN | FEC followed by docetaxel | Y |
| 30 | | CES021 | Post FEC | O | 37 | IDC | 3 | T2N2M0 | NNN | FEC followed by docetaxel | N |
| 31 | | CES021 | 1 year after surgery and adjuvant chemotherapy | O | 37 | IDC | 3 | T2N2M0 | NNN | FEC followed by docetaxel | Y |
| 32 | 18 | CES022 | 1 year after surgery and adjuvant chemotherapy | C | 46 | IDC | 3 | T2N0M0 | NNN | AC followed by paclitaxel | Y |

| | | | | | | | | | | | |
|----|----|------------|--|---|----|-----|---|----------------------|-----|--|---|
| 33 | 19 | CES0 23 | Post-surgery | I | 35 | IDC | 3 | T2N1M0 | PPN | AC followed by paclitaxel | Y |
| 34 | 20 | CES0 24 | Post-surgery | O | 44 | IDC | 2 | T2N0M0 | PPN | FEC followed by docetaxel | N |
| 35 | | CES0 24 | Post adjuvant chemotherapy | O | 44 | IDC | 2 | T2N0M0 | PPN | FEC followed by docetaxel | N |
| 36 | 21 | CES0 25 | Post-surgery | M | 50 | IDC | 1 | T2N1M0 | PPN | AC followed by paclitaxel | N |
| 37 | | CES0 25 | 1 year after surgery and adjuvant chemotherapy | M | 50 | IDC | 1 | T2N1M0 | PPN | AC followed by paclitaxel | Y |
| 38 | 22 | CES0 26 | Post-surgery | M | 49 | IDC | 3 | T1N0M0 | NNP | AC followed by herceptin | Y |
| 39 | 23 | CES0 27 | Post-surgery | M | 45 | IDC | 2 | T2N2M0 | PPN | AC followed by paclitaxel | Y |
| 40 | | CES0 27 | Post AC | M | 45 | IDC | 2 | T2N2M0 | PPN | AC followed by paclitaxel | N |
| 41 | | CES0 27 | Post paclitaxel | M | 45 | IDC | 2 | T2N2M0 | PPN | AC followed by paclitaxel | N |
| 42 | 24 | CES0 28 | Post paclitaxel | C | 44 | IDC | 2 | cT2N0M0, ypT1N2M0 | PPN | Neoadjuvant AC followed by adjuvant paclitaxel | N |
| 43 | 25 | CES0 29 | Post-surgery | C | 46 | IDC | 3 | T1N0M0 | NNN | TC | N |
| 44 | | CES0 29 | Post TC | C | 46 | IDC | 3 | T1N0M0 | NNN | TC | N |
| 45 | 26 | CES0 30 | Post-surgery | C | 67 | IDC | 2 | T3N2M0 | PPN | AC followed by paclitaxel | Y |
| 46 | | CES0 30 | Post adjuvant chemotherapy | C | 67 | IDC | 2 | T3N2M0 | PPN | AC followed by paclitaxel | N |

| | | | | | | | | | | | |
|----|----|------------|--------------|---|----|-----|---|----------------------|-----|--|---|
| 47 | 27 | CES0 31 | Post-surgery | C | 41 | IDC | 2 | T1N1M0 | PPP | TC | N |
| 48 | | CES0 31 | Post-TCH | C | 41 | IDC | 2 | T1N1M0 | PPP | TC | Y |
| 49 | 28 | CES0 33 | Post-surgery | M | 56 | IDC | 2 | T1N1M0 | PPN | AC followed by paclitaxel | N |
| 50 | 29 | CES0 34 | Post-surgery | C | 51 | IDC | 2 | T1N0M0 | PPN | AC followed by paclitaxel | Y |
| 51 | 30 | CES0 35 | Post AC | C | 38 | IDC | 3 | cT2N0M0, ypT0N0M0 | NNP | AC | N |
| 52 | 31 | CES0 36 | Post-surgery | C | 35 | IDC | 3 | T1N1M0 | PPN | Neoadjuvant AC followed by adjuvant paclitaxel | N |
| 53 | 32 | CES0 37 | Post-surgery | C | 44 | IDC | 2 | T1N0M0 | PPN | TC | N |